QUILL Quarterly Report

August - October 2018

Name:	**Marian Borucki**
Supervisor(s):	Dr Peter Nockemann, Dr Stephen Glover & Dr Małgorzata Swadźba-Kwaśny
Position:	PGR Student
Start date:	01.2018
Anticipated end date:	
Funding body:	Bryden Centre, Horiba Mira

Lithium ion batteries degradation study using spectroscopy techniques

Background

Lithium ion batteries (LIB) are a secondary (rechargeable) batteries that are currently the main energy storage device. LIB are applied in various applications as in portable devices, grid energy storage, grid current regulation as well as in hybrid- and electric vehicles. Energy harvested by the renewable energies is often environmental dependent, what results in discontinuous energy supply. In order to store energy that have been over generated during less energy consuming times of a day, energy storage stations based on LIB are used. The other, yet not less important, application is one where LIB are replacing the fossil fuel by storing the energy for transport sector, namely in hybrid (HEV) and electric vehicles (EV). The trend of replacing the fossil fuels both in energy sector by supplementing them with renewable energy power plants as well as by supporting the market of HEV, EV and fuel-cell vehicles (FCEV) is growing. New policies of EV30@30 and New Policy Scenario are the programmes that are aimed in expanding the market of HEV, EV and FCEV, thus the supply for lithium ion batteries will grow. Yet, for the market to growth the research, ones that solve current issues, are needed. Automotive council UK in their roadmap report for the lithium ion batteries have gathered up the issues that are needed to be addressed if the automotive of EV, HEV and FCEV is to grow. Such an issues are based on the need of improving the safety of battery usage, lowering the costs of the batteries, researching a new materials for the batteries that will allow to store more energy and provide more power, thus be fast chargeable, issues concerning the battery pack and modules combination, one that will allow to minimalize the losses related to cell joining, as well as their thermal management, increasing the lifespan of the batteries as well as increase their recyclability, eventually the research on the next gen batteries is needed.

In order to meet all the requirements a thrill study of the current batteries as well as the development of a new chemistries is needed. Lifespan as well as the safety of the battery is nowadays ones of the most important factor when it comes to the battery application in the transportation market. Battery life is limited by the degradation mechanism, ones that occur inside the cell. Currently there are known number of such mechanism occurring, even though the proper investigating technique allowing *in operando* study have not been developed yet. Moreover, the degradation is highly chemistry dependent so whenever the new chemistry is tested for the battery the new degradation mechanism could occur. On the other hand the safety of the battery is limited by the usage of the organic based electrolyte, which is highly flammable and might lead to battery explosion. Proper electrolyte, non-toxic, environmental friendly, non-flammable as well as of high performance should be developed. With developing the new electrolyte, often the development of the electrodes is needed as the electrolyte stability as well as the energy density of the battery highly depends on them.

Objective of this work

The aim of the PhD programme is to develop an experimental method basing on the analytic spectroscopic techniques, which will allow to observe and measure changes that occur inside the lithium ion battery in cell chemistry *in operando*. Additional analytical data acquired from the various degradation monitoring techniques will be processed to obtain a state of battery degradation based only on spectroscopic data. Eventually, battery of different cell chemistries will be investigated.

Progress to date

Laboratory preparation with new equipment and its installation was needed in order to initiate the study. Equipment as glove box, coin cell crimping machine, electrode punching machine as well as battery testers were bought and prepared for the functioning. Graphite and NMC based electrodes as well as commercial organic based electrolyte solution were obtained. Meanwhile the literature research as well as workshops participation was the main responsibility of mine. Initial studies of the coin lithium ion cells have been undertaken.

Conclusions and future work

CR2032 coin cell batteries based on the graphite and NMC electrodes as well as organic electrolyte are in preparation. Ageing tests of the manufactured batteries will be undertaken for the duration of up to 11 months in order of determining the degradation mechanism occurring. During the ageing study part of the cycled batteries will be disassembled depending on the charge-discharge cycles number. *Ex situ* microscopic, crystallographic as well as spectroscopic studies will be performed in favour of obtaining the information about the severity of each degradation mechanism. Meanwhile the methodology of *in situ* spectroscopic study of the cell will be developed. Data gathered through *ex situ* studies will be used to determine the level of degradation for the lithium ion cells monitored through *in situ in operando* technique.

Moreover the electrochemical systems of different electrolytes and electrodes setups will be assembles and further studied according to the previous mentioned methodology.

QUILL Quarterly Report

May - July 2018

Name:	**Robert Boyd**		
Supervisor(s):	Peter Nockemann, Martin Atkins		
Position:	PhD student		
Start date:	October 2016	Anticipated end date:	October 2019
Funding body:	DEL		

Organic Redox Flow Electrolytes

Background

Cheap, safe and efficient energy storage is essential in developing practical and sustainable energy strategies necessary for maintaining a balanced, efficient and reliable electric grid system based on both conventional electricity generation industries and the integration of intermittent renewable energy sources.

Batteries for large-scale grid storage must satisfy a different set of variables compared to many conventional rechargeable batteries. Such batteries must be; durable, maintain efficiency over a large number of charge/discharge cycles, have high round-trip efficiency, able to respond instantly to changes in load or input, and have reasonable capital costs[2]. Redox flow batteries are able to meet much of this criterion hence there has been significant interest in the optimisation of redox flow batteries for large-scale energy storage over the last few decades.

The all vanadium RFB was and remains the 'flagship' for redox flow batteries. It has a higher energy efficiency, longer operational lifetime and lower cost compared with other redox batteries (zinc bromide, sodium sulfur and lead acid)[3]. It remains the only RFB to have been sold in significant numbers due in part to being the only RFB to make use of the same metal species in both half-cells, avoiding cross-contamination issues.

Flow batteries incorporating organic molecules as the charge carriers are experiencing significant interest for large scale energy storage. Engineering the structure of organic molecules can deliver low cost redox active molecules with favourable potentials, increased solubility and greater stability. Both quinones and N-heterocycles are currently experiencing extensive investigation for application in flow batteries.

Objective of this work

Design and synthesise new flow electrolytes with superior properties compared to the all vanadium electrolyte.

Progress to date

Anthraquinone Sulfonate

Trihexyltetradecylphosphonium ($[P_{66614}]^+$), 1-ethyl-3-methylimidazolium (C_2mim]$^+$) and 1-butyl-3-methylimidazolium (C_4mim]$^+$) salts featuring the anthraquinone sulfonate anion were synthesised producing yellow salts for the imidazolium species and a viscous orange ionic liquid phosphonium derivative.

All anthraquinone salts displayed fully reversible redox behaviour in the nonaqueous acetonitrile solvent containing tetrabutylammonium tetrafluoroborate (0.1 M) supporting electrolyte, as shown in the cyclic voltammograms below.

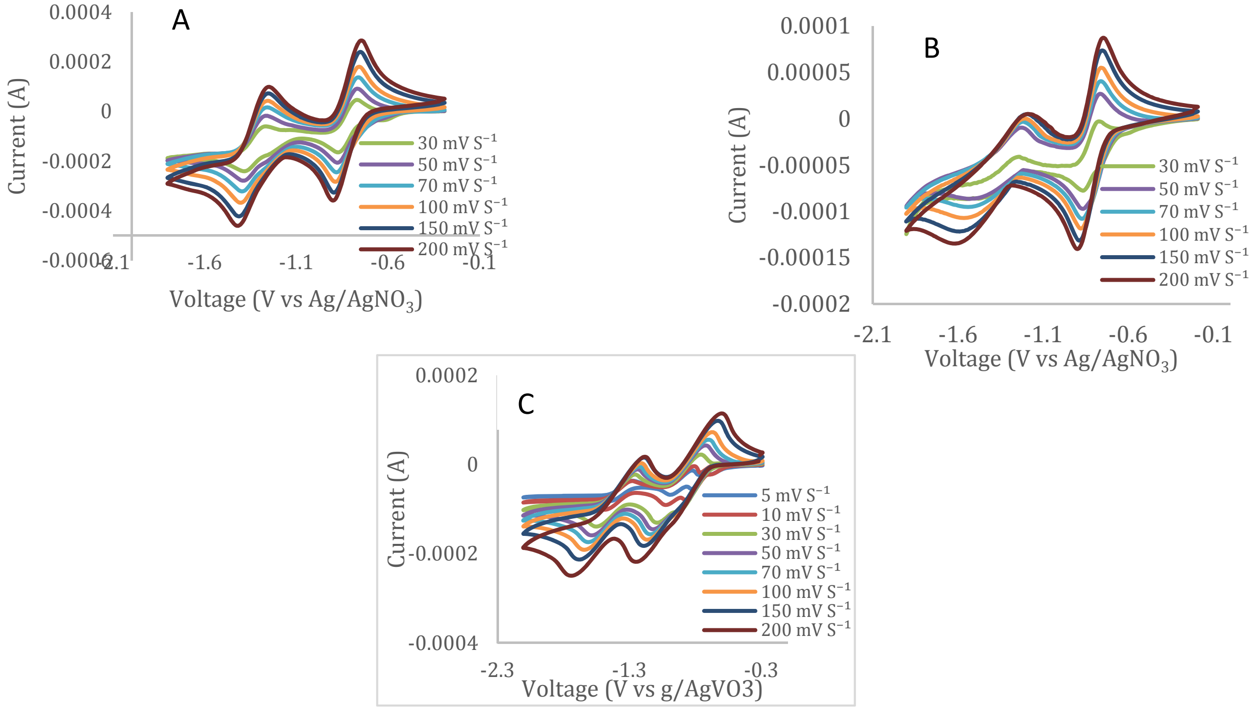

Fig. 1 (A) [P_{66614}][AQS] (0.005 M) in acetonitrile + TBATFB (0.1 M), GC(3 mm), Pt, $AgNO_3$. (B) [P_{66614}][AQS] (0.005 M) in acetonitrile + TBATFB (0.1 M), Pt, Pt, $AgNO_3$. (C) [C_2mim][AQS] (0.005 M) in acetonitrile (0.1 M TBATFB), GC (3 mm), Pt, $AgNO_3$.

In agreement with literature, two cathodic polargraphic waves were observed corresponding to $Q^{-\cdot}$ and Q^{2-} respectively.[17] Reduction potentials were observed at -0.85 V and -1.45 V (vs $AgNO_3$) for [P_{66614}][AQS] significantly lower than those associated with the sodium salt precursor which is reduced between -0.2 and -0.6 V (vs AgCl) in aqueous solvent.[18] Little change was observed on changing from glassy carbon to platinum electrode indicating the use of expensive precious metal electrodes is not required for efficient operation of a flow battery utilising anthraquinone derivatives.

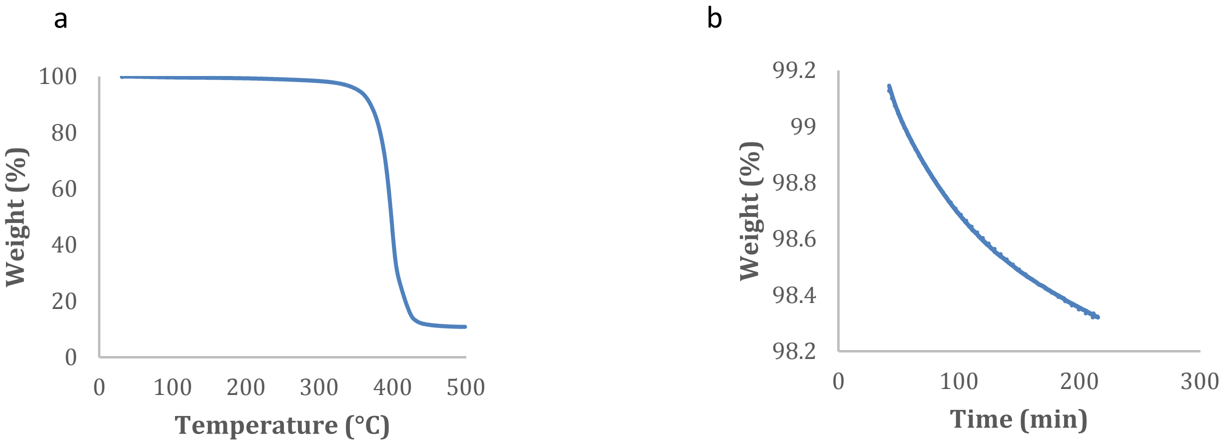

Fig. 2 Thermogravimetric (a) and isothermal (b) analysis of [P_{66614}][AQS].

Thermogravimetric analysis of [P_{66614}][AQS] indicated thermal degradation did not occur until 300 °C. Isothermal analysis, holding the temperature constant at 200 °C demonstrated the phosphonium electrolyte could reliably operate whilst being exposed to temperature spikes as under 10 % thermal degradation over a typical flow battery lifetime (30 years) was calculated from the gradient of the curve shown in figure X.

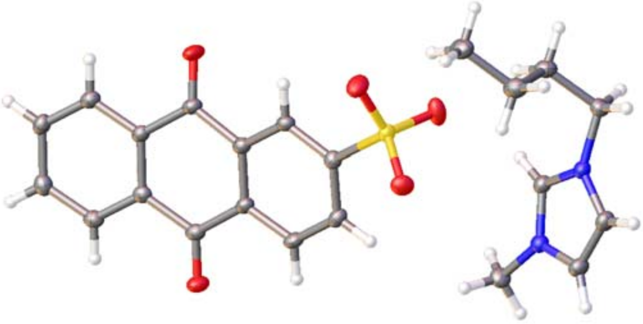

Fig. 3 Single crystal image of [C_4mim][AQS].

Single crystal analysis of [C_4mim][AQS] shows the anthraquinone anion adopts a planar geometry while the imidazolium cation takes on a distorted geometry.

Anthraquinone Cation

The anthraquinone group was incorporated into the cation in an attempt to reduce the molecular weight and improve the solubility of the quinone in organic solvent.

Anthraquinone was grafted onto an ammonium and butylimidazolium framework forming bromide salts of molecular weight 612.72 gmol^{-1} and 425.32 gmol^{-1} respectively. Both species were found to be redox-active in acetonitrile solvent, shown in the cyclic voltammogram below.

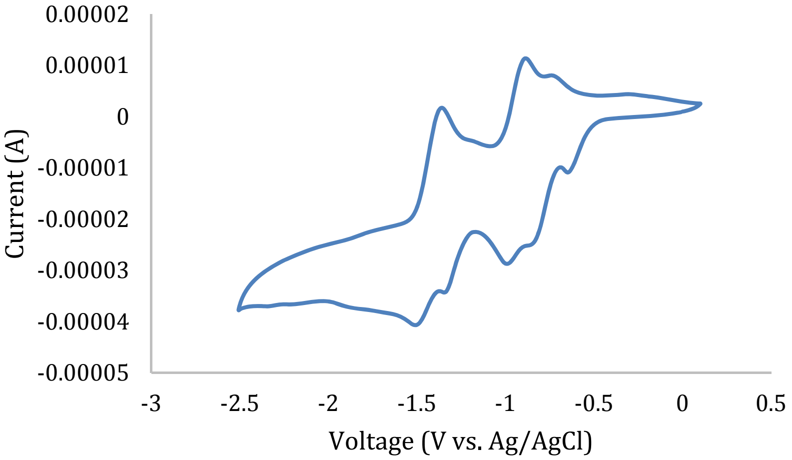

Fig. 4 Cyclic voltammogram of an ammonium anthraquinone compound featuring the bistriflimide anion.

Two reversible redox-active peaks were observed along with several other peaks. Further work is required to determine the efficiency of the quinone cation and elucidate the cause of all observable peaks.

Conclusions

All compounds synthesised displayed reversible redox behaviour and good solubility in organic electrolytes. Transferring to organic electrolytes removes the 1.4 V aqueous voltage limitation enabling greater cell potentials to be realised in order to increase the efficiency and energy density.

Future Work

Cyclic voltammetry - electrochemically analyse all anthraquinone ([Ch], [C_2mim], [C_4mim], and [P_{66614}]), hydroquinone ([Ch], [C_2mim], [C_4mim], and [P_{66614}]) and TEMPO salts synthesised under proper experimental conditions (gas purged, 3 cycles, no bubbling during measurement). H-cell – determine the charge and discharge capabilities of synthesised redox couples.

QUILL Quarterly Report

August - October 2018

Name:	Lucy Brown		
Supervisor(s):	Gosia Swadzba-Kwasny		
Position:	PhD student		
Start date:	October 2015	Anticipated end date:	April 2019
Funding body:	EPSRC		

Developing borenium ionic liquids

Background

Frustrated Lewis pairs (FLPs) are combinations of Lewis acids and Lewis bases which are unable to form adducts.[1] This is typically achieved by steric hindrance. Whilst not able to quench each other, the reactivity of the system can be utilised for the splitting of small molecules, such as H_2 and CO_2.[2] Whilst the mechanism of this is understood to be analogous to that of transition metals, FLPs offer an alternative to traditional hydrogen activation. Since the discovery in 2006 of this mechanism the wealth of reactions utilising it has grown enormously, with 1499 papers published on the topic in just 12 years. More generally work by Wagner and colleagues has demonstrated the use of an intramolecular FLP capable of trapping a huge variety of small molecules, from N_2O to CCl_4 (with cleavage of the C-Cl bond).[3] Highlights over the past year demonstrate the breadth of the reactions this approach is applied to, for example the use of gold nanoparticles which form an active FLP site on their surface in the hydrogenation of alkynes to cis-alkenes,[4] to the emergence of increasingly water tolerant systems, with Fasano *et al*. demonstrating water tolerant reductive aminations via FLPs.[5]

Borenium ionic liquids have been developed from the need for Lewis acidic ionic liquids with Lewis acidity located on the cation. Typical chlorometallate ionic liquids, which form the bulk of research on Lewis acidic ionic liquids, have their Lewis acidity on the anion, which is an electron rich species. In a sense this is surprising, but borenium ionic liquids, where the acidity is centered on a BX_2L species, have demonstrated immense acidity, with the highest Gutmann acceptor number reported in the literature. [6] Their acidity has been exploited in classic Lewis acid catalyzed reactions successfully used in both the Diels-Alder reaction and for dypnone synthesis via Aldol condensation. [7]

Objective of this work

By developing novel boron complexes and borenium ionic liquids the ambition of this work is to develop new species which may be used in frustrated Lewis pair catalysis. By including a bidentate ligand (catechol) onto the boron centre disassociate to BCl_3 can be discouraged and using non-acidic anions is anticipated to reduce the number of species with which a base can react.

Progress to date

Initial studies into the potential for using the reported borenium ionic liquids in frustrated Lewis pair chemistry has demonstrated that they are not appropriate acids for this catalysis. Owing to the equilibrium between different species in the ionic liquid and a lack of steric hindrance around the boron centre, a range of bases trialed, including triethylamine, tri-tert-butylphosphine, N,N-diisopropylethylamine formed solid adducts. This meant that they were inappropriate for FLP activity.

The first stage of this work, then, focused on developing a borenium centre with a bidentate ligand. Catechol is a ligand which has been used in the formation of borenium cations in previous work and the synthesis of B-chlorocatecholborane is readily achieved using a similar synthetic method as for the synthesis of BX_3L complexes. The catechol interacts with the boron centre through both the oxygens forming a tricoordinate boron complex. To this L-donor ligands may be added, in this work the following ligands are being explored as L-donors to the these complexes – methylimidazole, triethylamine, trioctylphosphine, tri-*tert*-butyl phosphine, shown in **Figure 1**. These ligands were selected as they include both N and P donors. It is known that N-donors can interact strongly with boron, being from the same period, in comparison to second row donors as better overlap between orbitals is achieved. [8] Furthermore an N donor is preferred to an O donor as it is capable of greater σ-bonding, this was observed in earlier work from the group that there was a greater tendency towards adduct dissociation with an O-donor compared to N-donor. The use of methylimidazole, further to this provides π-back donation from its aromatic system, this increases the donation to the boron centre and helps keep the ligand bound to the boron centre.

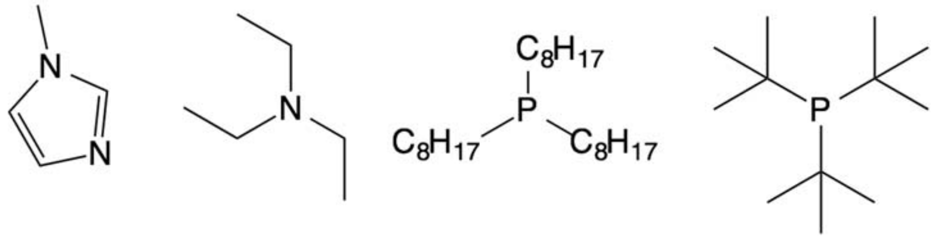

Figure 1. Ligands discussed in this work (l-r methylimidazole, triethylamine, trioctylphosphine and tri-tert-butyl phosphine)

The use of P-donors, although less basic towards BCl_3 than equivalent N-donors, comes from their ability to form incredibly basic complexes. Hence the inclusion of $(^tBu)_3P$ in this work, from Tolman parameters the ^{t}Bu ligand is known to be incredibly electron donating and therefore the basicity of the tri-substituted phosphine is high.[9] Finally the inclusion of trioctylphosphine is inspired by the opportunity for the inclusion of long alkyl chains in the liquid. Early ionic liquids research into their melting points indicated that a shorter chain length, less than 6 carbons, gave solids more prone to crystallization, while longer chains generated waxy liquids. [10] Therefore trioctylphosphine presents itself as an ideal ligand to promote the formation of a liquid, following halide abstraction.

The formation of adducts could be followed by ^{11}B NMR spectroscopy, with the B-chlorocatecholborane (BCatCl) peak emerging at ~29 ppm while tetra-coordinated adducts are found upfield. This is illustrated in **Figure 2** below. Additional peaks can be observed in the NMR spectrum of the adduct and while these need to be further investigated, the peak at 22 ppm can be identified as B_2Cat_3 which forms with loss of BCl_3.

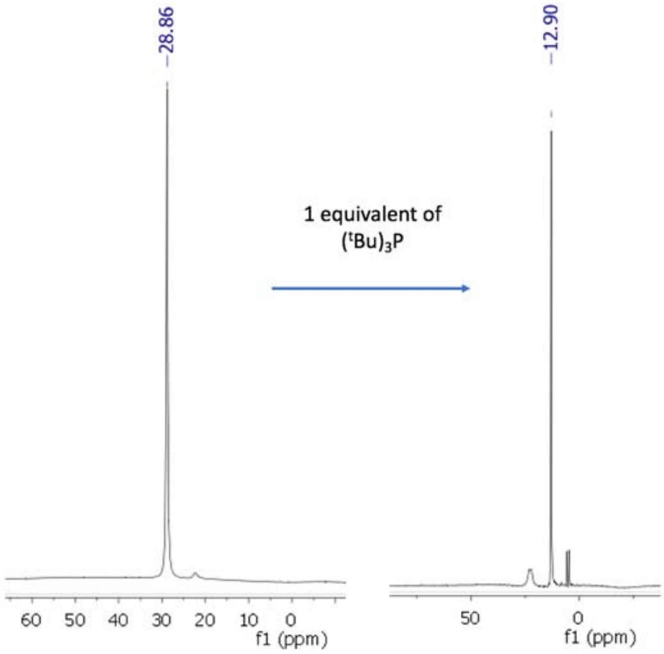

Figure 2 Two. ^{11}B NMR spectra showing the adduct formed from the combination of BCatCl with one equivalent of (^{t}Bu)$_3$P.

The reaction of BX_3L species to form ionic liquids has, until now, been exclusively performed with a chlorometallate abstracting agent. [6] This produces a dynamic equilibrium between the constituents of the ionic liquid, meaning the stability of the frustrated acid and base is compromised. As a consequence, alternative non-coordinating ligands have been explored in this work. In previous work from this group triflate was trialed as an anion with monodentate BX_3L systems, using trimethylsilyl triflate to abstract a halide. While capable of halide abstraction, the triflate centre was found to coordinate to the boron centre, resulting in a tetracoordinate species. In this work a new halide abstracting agent, methyl bistriflimide is introduced. In similar results to with the triflate species, the ^{11}B NMR spectrum suggests the product is exclusively tetracoordinate, this is shown in **Figure 3**.

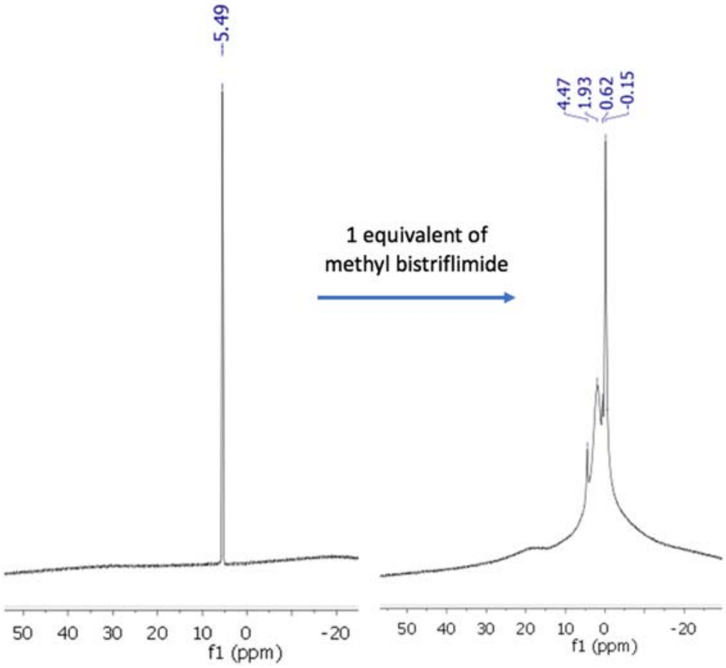

Figure 3. The introduction of methyl bistriflimide to BCl_3(mim) and formation of new tetracoordinate species illustrated in ^{11}B NMR spectroscopy.

The interaction between the bistriflimide and the boron centre is not particularly strong, with the anion dissociating in the presence of a stronger base. This means that Gutmann acceptor number data, whereby a triethyl phosphine oxide (TEPO) probe is introduced to the reactive centre and the degree of interaction between acid and base is observed by changes to the ^{31}P NMR spectrum. Due to different arrangements of the species around the boron centre, 4 different interactions between the TEPO and the boron are observed. The strongest of these interactions demonstrates this the Gutmann acceptor number of the [BCl_2(mim)][NTf_2] system is 109.2.

Synthesis of the equivalent system in with a catechol ligand, which is to say BCatCl(mim) combined with methyl bistriflimide and trimethylsilyl triflate, also showed tetra-coordinated species around the boron centre. Of the two only the system with the triflate "anion" was liquid at room temperature.

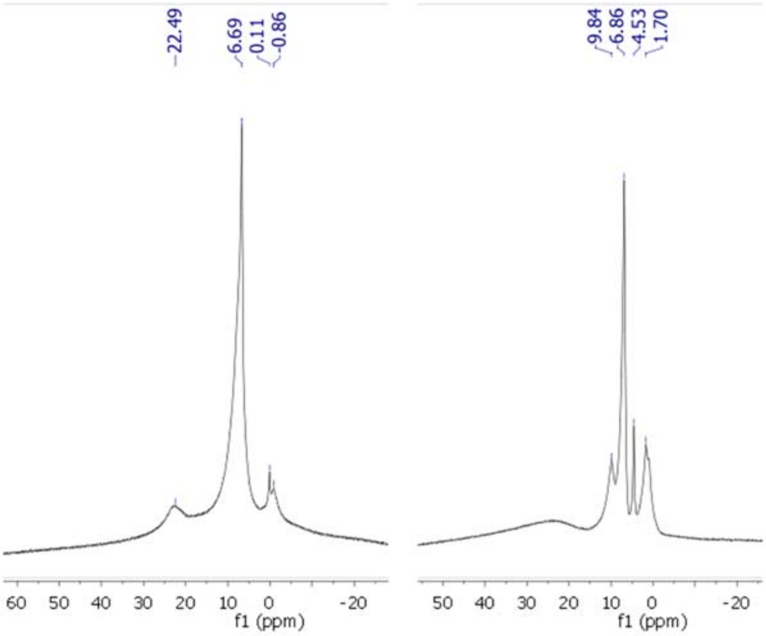

Figure 4. The introduction of trimethylsilyl triflate (L) and methyl bistriflimide (R) to BCatCl(mim) and formation of new tetracoordinate species illustrated in ^{11}B NMR spectroscopy.

Conclusions and future work

In this work expansion of the family of borenium ionic liquids is being explored. The incorporation of bidentate ligands with the aim of suppressing any dynamic equilibrium in the liquid. A variety of ligands were selected to exploit different advantages, such as encouraging good orbital overlap through the use of N-donors, using strong phosphine bases to discourage dissociation from the boron centre and finally using long alkyl chains to promote a lower melting point. The use of these ligands also allow for easy comparison with the work carried out by Swadzba-Kwasny *et al* forming [BX_2L][M_2Cl_7] systems.[6] The use of large non-coordinating anions is intended to prevent equilibria emerging between anionic and cation species which would disrupt any frustration of Lewis acidity preventing their use as FLP catalysts. There has been mixed success in this work thus far, with free borenium ions not forming but Gutmann acceptor number measurements suggesting that the interaction between bistriflimide and the boron centre is weak and that the system may be useable as a "masked" FLP.

Further work should focus on developing the boron complexes to form species capable of reacting with either methyl bistriflimide or trimethylsilyl triflate to give a free borenium cation which, as an acidic centre, may be used in FLP reactions. This work should be characterised by NMR and IR spectroscopy, in addition to thermal measurements, such as thermal gravimetric analysis (TGA) and differential scanning calorimetry (DSC).

References

1 D. W. Stephan, G. C. Welch, R. San Juan and J. D. Masuda, *Science*, 2006, **314**, 1121–1124.

2 G. C. Welch and D. W. Stephan, *J. Am. Chem. Soc.*, 2007, **129**, 1880–1881.

3 K. Samigullin, I. Georg, M. Bolte, H.-W. Lerner and M. Wagner, *Chem. Eur. J.*, 2016, **22**, 3478–3484.

4 J. L. Fiorio, N. López and L. M. Rossi, *ACS Catal.*, 2017, **7**, 2973–2980.

5 V. Fasano and M. J. Ingleson, *Chem. Eur. J.*, 2017, **23**, 2217–2224.

6 S. Coffie, J. M. Hogg, L. Cailler, A. Ferrer-Ugalde, R. W. Murphy, J. D. Holbrey, F. Coleman and M. Swadźba-Kwaśny, *Angew. Chem.*, 2015, **127**, 15183–15186.

7 K. Matuszek, S. Coffie, A. Chrobok and M. Swadźba-Kwaśny, *Catalysis Science & Technology*, 2017, **7**, 1045–1049.

8 S. Dagorne and D. A. Atwood, *Chem. Rev.*, 2008, **108**, 4037–4071.

9 C. A. Tolman, *Chem. Rev.*, 1977, **77**, 313–348.

10 I. López-Martin, E. Burello, P. N. Davey, K. R. Seddon and G. Rothenberg, *ChemPhysChem*, 2007, **8**, 690–695.

QUILL Quarterly Report

August - October 2018

Name:	**Emily Byrne**		
Supervisor(s):	Dr. Małgorzata Swadźba-Kwaśny and Dr. John Holbrey		
Position:	PhD student		
Start date:	October 2017	Anticipated end date:	October 2020
Funding body:	DfE (Department for the Economy)		

Functional liquids based on TOPO and its analogues

Background

It is proposed that deep eutectic solvents 'DES' are a chemical component mixture composed of hydrogen bond donors and acceptors which have intermolecular interactions that result in a freezing point which is lower than that of the isolated individual components of the system with no interactions between each other.[1] They are asymmetric species which, due to their orbitals' inability to overlap well and thus, pack into a regular lattice arrangement, have low lattice energy and so do not require a large amount of energy in order to exist as a liquid and as a result tend to have low melting points.

The most common and well renowned DES are those prepared with the combination of organic salts such as choline chloride, which act as a hydrogen bond acceptor and carboxylic acids or alcohols with a hydrogen bond donating role.[2–5] However, these solvents are generally miscible with water and so their application is quite limited. Therefore, work was undertaken by van Osch *et al.* which led to the publication of the first hydrophobic deep eutectic solvent using a carboxylic acid hydrogen bond donor and a long chain quaternary ammonium salt in 2015.[6] In addition to this, DES have since been formed using alcohols and fatty acid hydrogen bond donors in combination with organic salts to form deep eutectic solvents which can be used for extraction of metals[7] and natural products[8,9]. In addition to this, in an attempt to reduce the viscosity associated with these charged DES species, Ribeiro *et al.* developed DES systems using D-menthol and carboxylic acid hydrogen bond donors where the individual components used are non-ionic species.[10] More recently, DES made with the combination of trioctylphosphine oxide (TOPO) and phenol have been published and its use as a uranyl extractant shown.[11]

TOPO has a number of uses such as capping agents[12–16] in nanoparticle synthesis, metals[17,18], organic acids[19–22] and phenolics[23–26] extraction and so a number of DES will be prepared using a range of hydrogen bond donors most suited to the potential application.

Objective of this work

In this work a number of hydrogen bond donors such as catechol, resorcinol, levulinic acid, malonic acid and salicylic acid will be combined with TOPO to form a eutectic. Their physical properties will be characterised and they will be applied to an industrial application.

Progress to date

To begin this section of work, a number of hydrogen bond donors which have potential in the applications outlined above such as for nanoparticle synthesis capping agents, metal extraction and extraction of organic acids and phenolics were screened. The following hydrogen bond donors shown in Table 1. Hydrogen bond donors which form a room temperature liquid with TOPO when combined in the correct molar ratio were selected to proceed with further physical characterisation of the liquids formed. Table 1. Hydrogen bond donors which form a room temperature liquid with TOPO when combined in the correct molar ratioshows the results of the preliminary screening of chosen hydrogen bond donors.

HBD	Structure	χ_{TOPO}	RT Liquid?	Liquid in fridge?
Levulinic acid	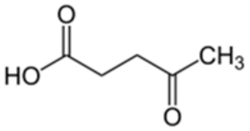	0.5	Yes. Colourless, free-flowing liquid. ✓	Yes. Colourless free-flowing liquid. ✓
Salicylic acid	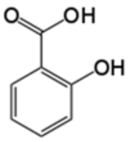	0.5	Yes. Colourless free-flowing liquid. ✓	Yes. Colourless free-flowing liquid. ✓
Resorcinol	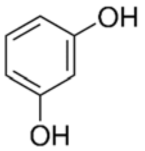	0.5	Yes. Colourless, free-flowing liquid. ✓	Yes. Colourless, free-flowing liquid. ✓
Catechol	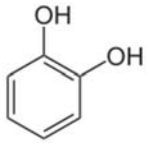	0.5	Yes. Yellow, clear, free-flowing liquid. ✓	Yes. Yellow, clear, free-flowing liquid. ✓
Malonic acid	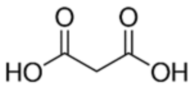	0.67	Yes. Colourless, free-flowing liquid ✓	Yes. Colourless, free-flowing liquid ✓

Table 1. Hydrogen bond donors which form a room temperature liquid with TOPO when combined in the correct molar ratio

Catechol was chosen as the hydrogen bond donor to begin studies with as comparisons could be drawn between it and the TOPO:phenol mixtures previously prepared by the group and recently published.[11] Catechol is also a reducing benzenediol, which suggests that it would have promise as a component in nanoparticle synthesis when combined with TOPO.

Initial studies of how thermal decomposition varies as a function of composition where mole ratios are in relation to TOPO (χ_{TOPO}). Mole ratios between 0.1-0.9 were prepared in increments of 0.1 and mole ratios of 0.33 and 0.67 were also prepared. Some compositions studied were omitted in Figure 1. Thermal decomposition of TOPO:catechol mixtures and individual components as a function of temperature for the purpose of clarity.

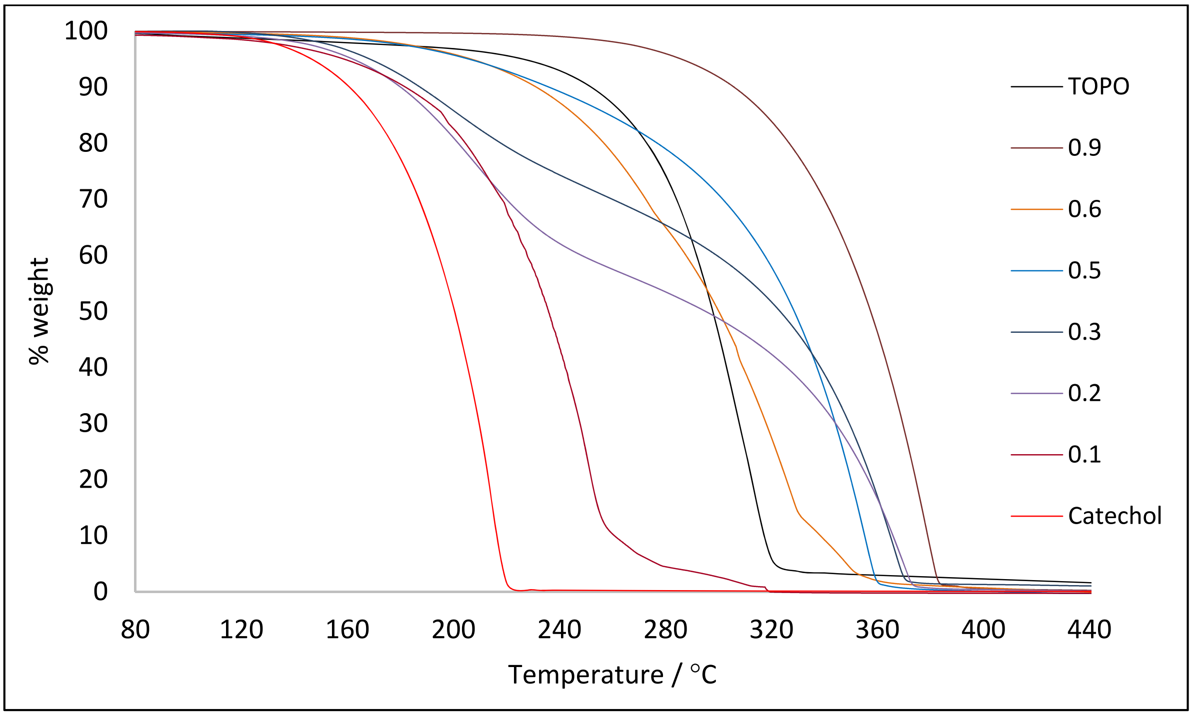

Figure 1. Thermal decomposition of TOPO:catechol mixtures and individual components as a function of temperature

Results in Figure 1. Thermal decomposition of TOPO:catechol mixtures and individual components as a function of temperature show that in all cases, the TOPO:catechol mixtures show increased stability when compared to that of pure catechol which rapidly begins to thermally decompose at 118 °C and is complete by 220 °C. Two step decomposition is observable at χ_{TOPO} values <0.8, however, above this, decomposition is observed as one step. Interestingly, χ_{TOPO} values of 0.8 and above exhibit greater thermal stability than that of pure TOPO.

Each χ_{TOPO} sample was then prepared for DSC to understand the phase behaviour of the samples at varying χ_{TOPO} values and the temperature recorded for the liquidus point and the onset of the glass transition yields a phase diagram. Glass transition temperatures and the temperature or temperatures at which melting occurs were recorded. The results of this are shown below in Figure 2. Phase behaviour of TOPO:catechol mixtures at varying χ_{TOPO} values as a function of temperature and χ_{TOPO}

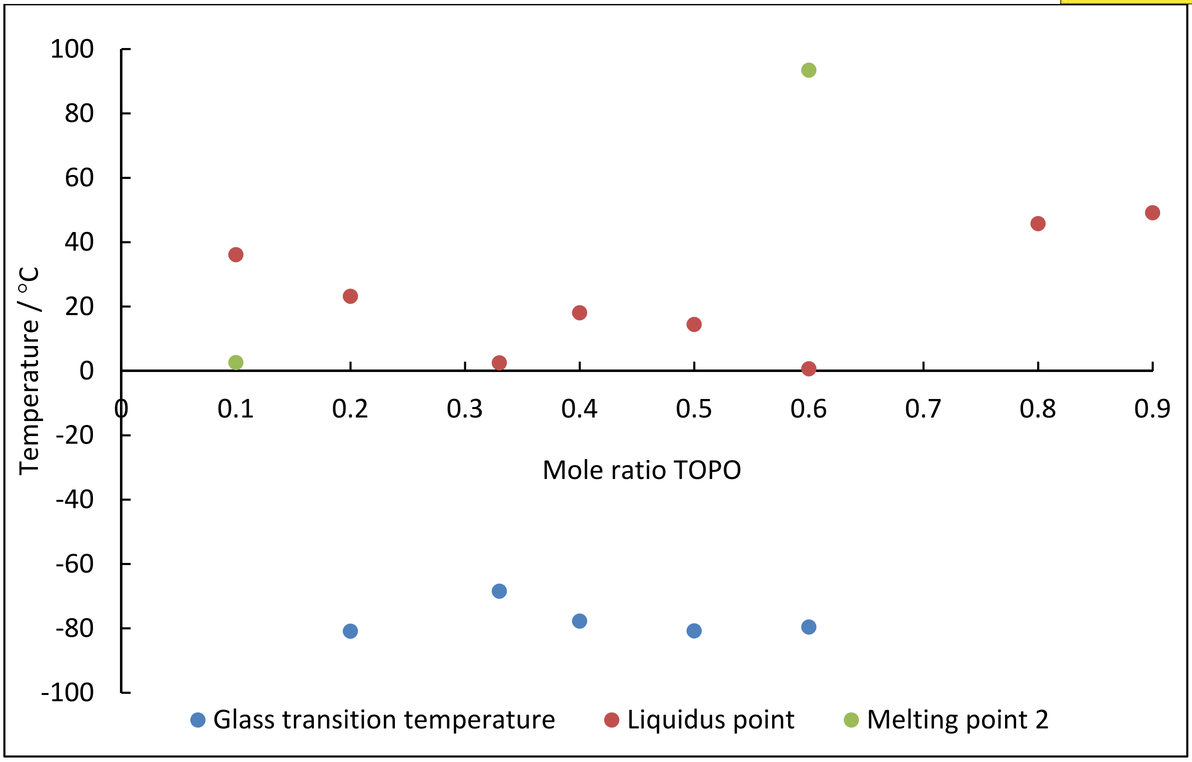

Figure 2. Phase behaviour of TOPO:catechol mixtures at varying χ_{TOPO} values as a function of temperature and χ_{TOPO}

Figure 2. Phase behaviour of TOPO:catechol mixtures at varying χ_{TOPO} values as a function of temperature and χ_{TOPO}two regions of interest, that of onset melting as represented by blue markers and the liquidus point of the sample at each χ_{TOPO} value as represented by red markers. Tracing the blue markers indicates that due to a horizonal line through the points representing the T_g for each χ_{TOPO} value, onset melting remains the same throughout the compositional range as expected. Tracing the red markers show that there are two points of depression in liquidus point along the compositional range, 0.33 and 0.6. This suggests that there are two different extents of interaction between the TOPO and catechol species which lead to packing disruption, i.e. one where two molecules of TOPO interact with one molecule of catechol (χTOPO = 0.6) and another where one molecule of TOPO interacts with two molecules of catechol (χTOPO = 0.33) suggesting two different modes of interaction between the species. It is likely that this is due to two hydrogen bond donating sites in close proximity on the ring.

Conclusions and future work

To conclude, a number of room temperature liquids were prepared with the addition of two solid, non-ionic compounds (i.e. TOPO and phenolic or organic acids) in the correct molar ratio. TOPO:catechol mixtures show an increase in thermal stability and a change in decomposition pathway with increasing χ_{TOPO} values above 0.7 from 2 step decomposition when $\chi_{TOPO} < 0.8$ and one step decomposition $\chi_{TOPO} > 0.8$. In addition to this, TOPO:catechol mixtures show two depressions in liquidus point across the compositional range from χ_{TOPO} = 0.1-0.9 suggesting that there are two different modes of interaction between TOPO and catechol molecules.

In the near future, phase diagrams will also be reported by recording the temperature at which onset melting and liquidus points occur visually using a solid-liquid cell and the results compared with DSC results. TGA, DSC and SLC of mixtures made with resorcinol, malonic acid, salicylic acid and levulinic acid. And the physical properties of these mixtures at their eutectic point will be studied. Application for these eutectics will then be applied.

1 A. P. Abbott, G. Capper, D. L. Davies, H. L. Munro, R. K. Rasheed and V. Tambyrajah, *Chem. Commun.*, 2001, 2010–2011.

2 Q. Zhang, K. De Oliveira Vigier, S. Royer and F. Jérôme, *Chem. Soc. Rev.*, 2012, **41**, 7108.

3 M. C. Kroon, M. Francisco, A. Van Den Bruinhorst and M. C. Kroon, 2013, **2012**, 3074–3085.

4 E. L. Smith, A. P. Abbott and K. S. Ryder, *Chem. Rev.*, 2014, **114**, 11060–11082.

5 A. P. Abbott, D. Boothby, G. Capper, D. L. Davies and R. K. Rasheed, *J. Am. Chem. Soc.*, 2004, **126**, 9142–9147.

6 D. J. G. P. van Osch, L. F. Zubeir, A. van den Bruinhorst, M. A. A. Rocha and M. C. Kroon, *Green Chem.*, 2015, **17**, 4518–4521.

7 D. J. G. P. van Osch, D. Parmentier, C. H. J. T. Dietz, A. van den Bruinhorst, R. Tuinier and M. C. Kroon, *Chem. Commun.*, 2016, **52**, 11987−11990.

8 J. Cao, M. Yang, F. Cao, J. Wang and E. Su, *ACS Sustain. Chem. Eng.*, 2017, **5**, 3270–3278.

9 J. . Cao, L. . Chen, M. . Li, F. . Cao, L. . Zhao and E. Su, *Green Chem.*, 2018, **20**, 1879−1886.

10 B. D. Ribeiro, C. Florindo, L. C. Iff, M. A. Z. Coelho and I. M. Marrucho, *ACS Sustain. Chem. Eng.*, 2015, **3**, 2469–2477.

11 M. Gilmore, E. N. Mccourt, F. Connolly, P. Nockemann and J. D. Holbrey, *ACS Sustain. Chem. Eng.*, 2018, (Manuscript accepted).

12 I. Mekis, D. V Talapin, A. Kornowski, M. Haase and H. Weller, *J. Phys. Chem.*, 2003, **107**, 7454–7462.

13 F. V Mikulec, M. Kuno, M. Bennati, D. A. Hall, R. G. Griffin and M. G. Bawendi, *J. Am. Chem. Soc*, 2000, **122**, 2532–2540.

14 T. Cassagneau, T. E. Mallouk and J. H. Fendler, *J. Am. Chem. Soc*, 1998, **120**, 7848–7859.

15 T. Trindade and P. O. Brien, *Chem Mater*, 1997, **9**, 523–530.

16 A. A. Guzelian, J. E. B. Katari, A. V Kadavanich, U. Banin, K. Hamad, E. Juban, A. P. Alivisatos, R. H. Wolters, C. C. Arnold and J. R. Heath, *J. Phys. Chem.*, 1996, **100**, 7212–7219.

17 T. Sato, T. Nakamura and S. Ishikawa, *Solvent Extr. Ion Exch.*, 1984, **2**, 201–212.

18 E. K. Watson and W. A. Rickelton, *Solvent Extr. Ion Exch.*, 1992, **10**, 879–889.

19 P. O. . Saboe, L. P. . Manker, W. E. . Michener, D. J. . Peterson, D. G. . Brandner, S. P. . Deutch, M. . Kumar, R. M. . Cywar, B. G. T.; and E. M. Karp, *Green Chem.*, 2018, **20**, 1791–1804.

20 T. Brouwer, M. Blahusiak, K. Babic and B. Schuur, *Sep. Purif. Technol.*, 2017, **185**, 186–195.

21 G. Kim, S. Park and B. Um, *Ind. Crop. Prod.*, 2016, **89**, 34–44.

22 S. Uenoyama, T. Hano, M. Hirata and S. Miura, *J. Chem. Technol. Biotechnol.*, 1996, **67**, 260–264.

23 P. Praveen and K. C. Loh, *Chem. Eng. J.*, 2014, **255**, 641–649.

24 P. Praveen and K. Loh, *Chemosphere*, 2016, **153**, 405–413.

25 P. Praveen and K. Loh, *J. Memb. Sci.*, 2013, **437**, 1–6.

26 P. Taylor, E. K. Watson, W. A. Rickelton, A. J. Robertson and T. J. Brown, *Solvent Extr. Ion Exch.*, 1988, **6**, 207–220.

QUILL Quarterly Report

August – October 2018

Name:	**Dr Manuela Gilea**		
Supervisor(s):			
Position:	PDRA		
Start date:	2015	Anticipated end date:	2018
Funding body:	EPSRC		

Separation of lanthanide salts by countercurrent chromatography

Background

Separation of lanthanide salts (nitrates or chlorides) became a very important industrial process due to (a) low natural abundance of lanthanides (b) geopolitical issues (China having monopoly on some lanthanide production) and (c) necessity to recover, recycle and reuse waste electrical and electronic equipment which incorporate amounts of lanthanides. Countercurrent chromatography (CCC) is a form of liquid-liquid chromatography adapted for the use of ionic liquids (ILs). Separations carried out by CCC have the following advantages: (a) more environmentally friendly, due to the low (or inexistent) vapour pressure of ILs and their ability to be easily recycled and also due to the fact that the separation is carried out in a close system (b) easy to scale up. However, the equipment is a prototype and its compatibility with ILs has yet to be established.

Objective of this work

The project is aimed to establish (a) an IL-based system able to perform lanthanide salt separation and (b) operating conditions for the CCC equipment

Progress to date

So far it was established that a PTFE coil of big volume (230 ml) is suitable for the separation of Er(NO3)3 and Nd(NO3)3 using as a solvent system $P_{66614}Cl$/ethyl acetate/H_2O (Fig. 1)

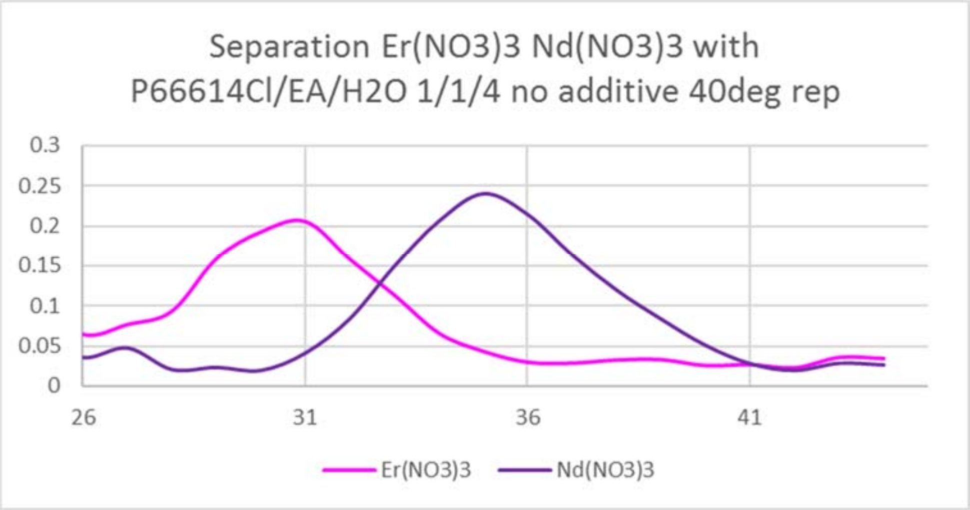

Figure 1 Separation of Er(NO3)3 and Nd(NO3)3 using $P_{66614}Cl$/ethyl acetate/H_2O at 40 °C on a PTFE coil

I have demonstrated previously that increasing the temperature the specificity of lanthanide salts separation increases. However, in an attempt to reach 50 °C, the PTFE coil ruptured.

In order to prove the effect of temperature upon the separation process, separations were carried out at 50 °C on stainless steel coils.

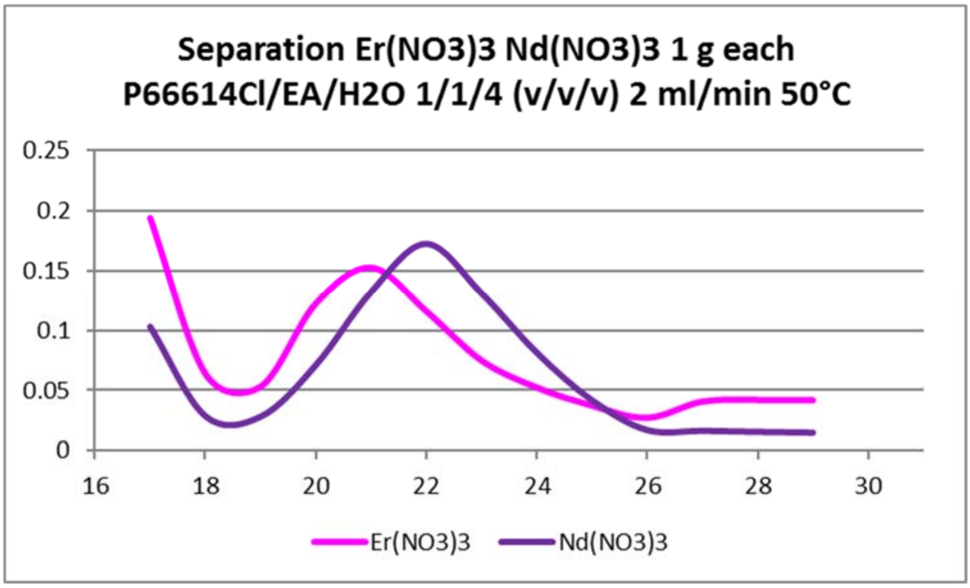

Figure 2 Separation of Er(NO3)3 and Nd(NO3)3 using P_{66614}Cl/ethyl acetate/H_2O at 50 °C on a stainless steel coil at 2 ml/min

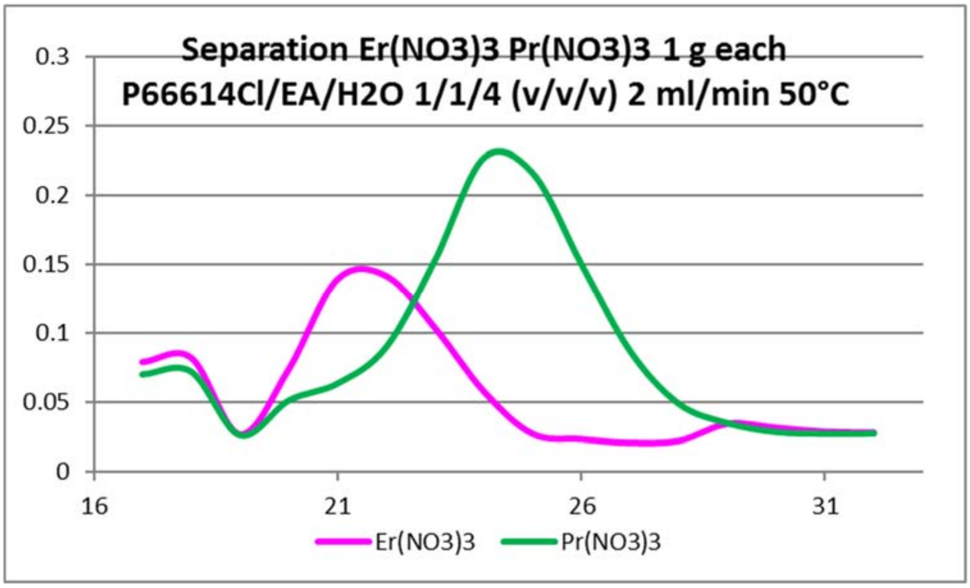

Figure 3 Separation of Er(NO3)3 and Pr(NO3)3 using P_{66614}Cl/ethyl acetate/H_2O at 50 °C on a stainless steel coil at 2 ml/min

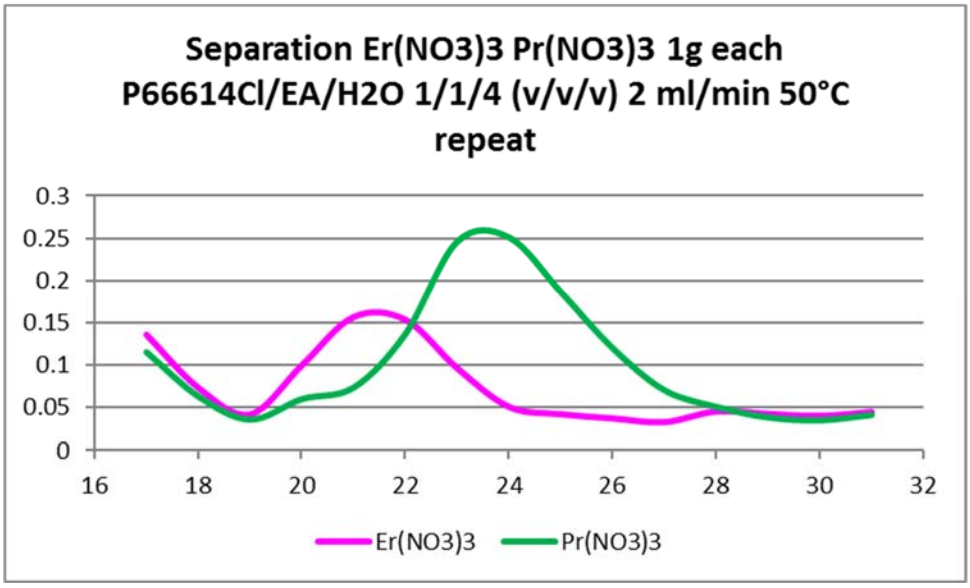

Figure 4 Separation of Er(NO3)3 and Pr(NO3)3 using P_{66614}Cl/ethyl acetate/H_2O at 50 °C on a stainless steel coil at 2 ml/min (repeat)

An attempt to increase the total volume of stainless steel coil by linking coils in series did not produce any separation, even at 50 °C.

The replacement of ethyl acetate with 3-pentanone (slightly more acidic) does not improve the system's performance too much, as seen in figure 5, but a decrease in the flow rate from 2 ml/min to 1.5 ml/min leads to a better separation, as seen in figure 6.

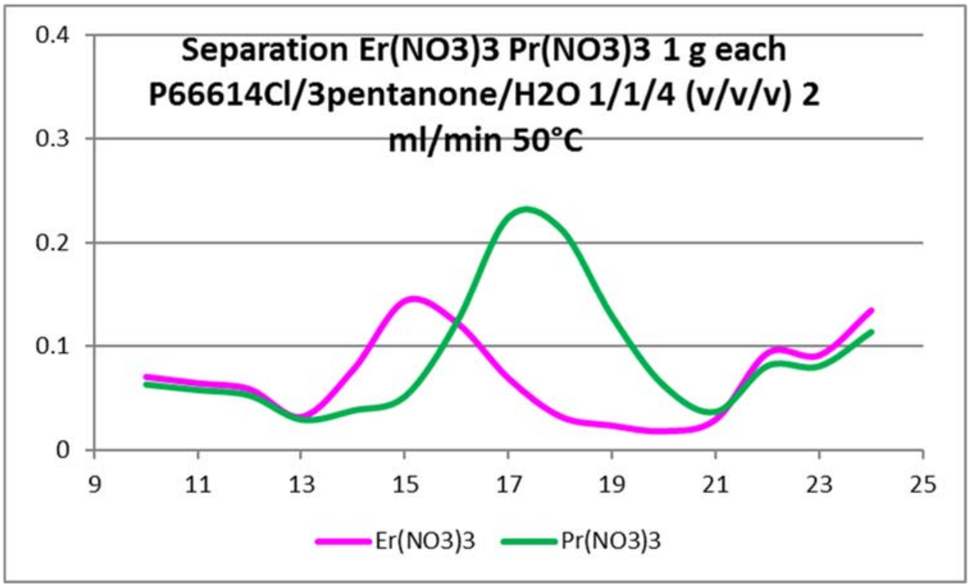

Figure 5 Separation of Er(NO3)3 and Pr(NO3)3 using P_{66614}Cl/3-pentanone/H_2O at 50 °C on a stainless steel coil at 2 ml/min

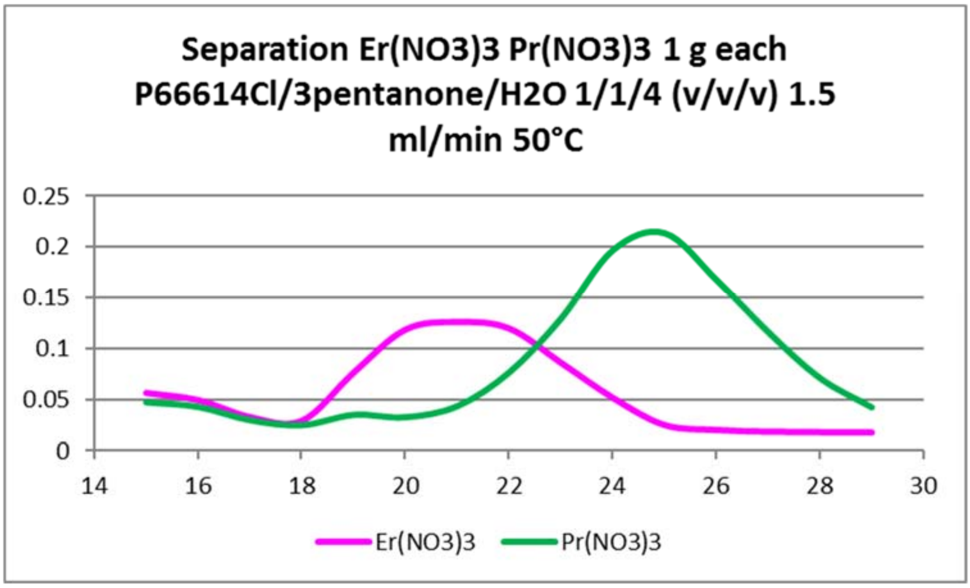

Figure 6 Separation of Er(NO3)3 and Pr(NO3)3 using $P_{66614}Cl$/3-pentanone/H_2O at 50 °C on a stainless steel coil at 1.5 ml/min

Conclusions and future work

It has been demonstrated so far that:

1) The PTFE coil is better to separate Er(NO3)3 and Nd(NO3)3 using $P_{66614}Cl$/ethyl acetate/H_2O
2) The stainless steel coil is better to separate Er(NO3)3 and Pr(NO3)3 using $P_{66614}Cl$/ethyl acetate/H_2O
3) Replacement of ethyl acetate by 3-pentanone has only a marginally better effect on separation of Er and Pr
4) A decrease in flow rate increases separation performances of Er and Pr

QUILL Quarterly Report

August - October 2018

Name:	**Martin Gillespie**		
Supervisor(s):	Dr P Nockemann, Dr Malgorzata Swadsba-Kwasny, Dr Stephen Glover		
Position:	PhD Student		
Start date:	01/10/2018	Anticipated end date:	30/09/21
Funding body:	DFE		

Hybrid Electrolytes for Solid-State Batteries in Electric Vehicles

Background

Petrol and diesel engines in vehicles are likely to soon become a thing of the past. Declining amounts of fossil fuels, rising atmospheric carbon dioxide levels, worsening air quality in cities and out of control climate change demand significant changes to global human behaviour. Transitioning from fossil fuels to electric vehicles (EVs) represents a huge step in the right direction. Electric vehicles provide transport without any of the noxious exhaust emissions from traditional combustion engines. Presently the build-up of combustion fumes in traffic dense areas causes a localised reduction in life quality, an increase in respiratory diseases, numerous deaths each year as well as adding to greenhouse gas levels globally. Noise pollution is reduced by using EVs, as are the number of consumable parts required for vehicles as there are significantly fewer moving parts in EVs. Much of the electricity needed to charge EVs will presently be generated from burning fossil fuels at existing power plants but this energy generation can be over ten times more efficient than within a combustion engine and of course electricity for EVs can be generated from renewable energy sources resulting in very little or no detrimental effects to the environment.

The electrolyte is a vital component in secondary batteries for EVs. A poor-quality electrolyte results in a poor-quality EV. The electrolyte facilitates the transport of metal cations between electrodes during charge/discharge cycles. A highly functioning electrolyte must display some vital characteristics, these are mentioned below and will be the focus of this work.

Objective of this work

To improve on the current state-of-the-art electrolytes with respect to ionic conductivity, ionic transference, electrode compatibility, stability (electrochemical, chemical and thermal), integrity under stress and environmental impact from non-intentional cell rupture. The goal is to optimise an electrolyte formulation which can be scaled up and used directly in the electric vehicle and possibly other energy storage sectors.

Progress to date

A study into the chemistry of secondary batteries and past research into the electrolytes used, particularly the work of several Japanese groups including Mandai and Yoshida into solvate ionic liquids. This promising avenue of electrolyte synthesis exploits the Lewis acid/base coordination chemistry between oxygen electron donors on oligoether species with a lithium cation from a dissociated bulky lithium salt. The formed solvate ionic liquids, particularly those comprising equimolar ratios display favourable electrochemical and thermal stability and have potential as high-quality electrolytes. To date I have synthesised three of these electrolytes under dry inert conditions and am presently in the process of carrying out a full characterisation on them. I have dried a substantial amount of lithium bistriflimide salt under high vacuum and temperature and a range of oligoethers have been dried over molecular sieves. These materials are now stored in an inert atmosphere for further work. I have been trained in the use of the glove box and in the running of Differential scanning calorimetry (DSC) and Thermogravimetric analysis (TGA) machinery. DSC and TGA analysis is currently underway on each electrolyte and linear sweep voltammetry (LSV) is to be carried out shortly along with Raman spectroscopy, and lithium NMR.

Due to being in the early stages of this work more equipment is still required for the project. I have researched the best equipment, contacted various suppliers, ordered an analytical balance and a hotplate stirrer with suitable attachments for use in the new glovebox, I await delivery. It's thought that counter anions play a very significant role in the outcome of all the electrolyte characteristics, crucially in the formation of the solid electrolyte interface and electrode stabilities over time, to this end I have requested alternative metal salts for my further investigations.

Conclusions and future work

After full characterisation on the synthesised electrolytes has been carried out any that show suitable promise will be built into a coin cell and its potential for use in a real-world setting will be evaluated. Data received from these battery tests will provide information on which characteristics require further modification and attention. Immediate future work into these solvate ionic liquids will comprise of electrolyte synthesis using variations of oligoether lengths, oligoether structural isomers, metal salt species and concentrations followed by the rigorous testing and analysis of each mixture.

QUILL Quarterly Report

August - October 2018

Name:	**Mark Gilmore**		
Supervisor(s):	Gosia Swadzba Kwasny/ John Holbrey		
Position:	PhD student		
Start date:	Dec 15	Anticipated end date:	Dec 18
Funding body:	QUILL		

Fundamental studies and urban mining applications of functionalized solvents

Background

This report focuses on explaining how the idea of eutectic formation was harnessed to produce previously unreported hydrophobic deep eutectic solvents based on trioctylphosphine oxide (TOPO) combined with phenol, providing one of the early examples of a eutectic system that forms a bi-phase with water. Full physical characterisation of the system was carried out including, phase analysis, density, viscosity, speciation and hydrophobicity studies. Two potential applications were then probed, using the system for extraction of uranium (vi) from aqueous acidic leaches, and removal of small natural products from aqueous streams which are produced as a by-product from the paper pulping industry amongst others.

Objective of this work

The objective of the work was to design new hydrophobic DESs which are currently under represented due to the inherent nature of DESs and their excellent ability to hydrogen bond which tends to lead to them being miscible with water. Producing hydrophobic DESs would lead to the possibility to perform biphasic extractions from a number of aqueous waste sources namely metal ions and natural product extraction from the waste streams. Once the hydrophobic DESs had been designed and produced, their ability to extract uranyl and phenol was measured using model systems.

Progress to date

Hydrophobic Deep Eutectic Solvents Incorporating Trioctylphosphine Oxide: Advanced Liquid Extractants

The first hydrophobic DES, reported by van Osch et al.[1] in 2015, combined a carboxylic acid (to provide H-bond donor functionality) with long chain quaternary ammonium salts to enhance hydrophobicity over more usual short chain ammonium or cholinium salts. Following this strategy, other hydrophobic DESs incorporating fatty acids and/or alcohols with organic salts have been described and their use for metal ion[2] and natural product[3,4] extractions demonstrated. However, in common with ionic liquids, the Coulombic interactions between the charge centres result in liquids with relatively high viscosity. This is compounded by the need to introduce large bulky alkyl substituents to impart hydrophobicity competing with the hydrophilic association of typically good hydrogen-bond acceptor anions present with water.

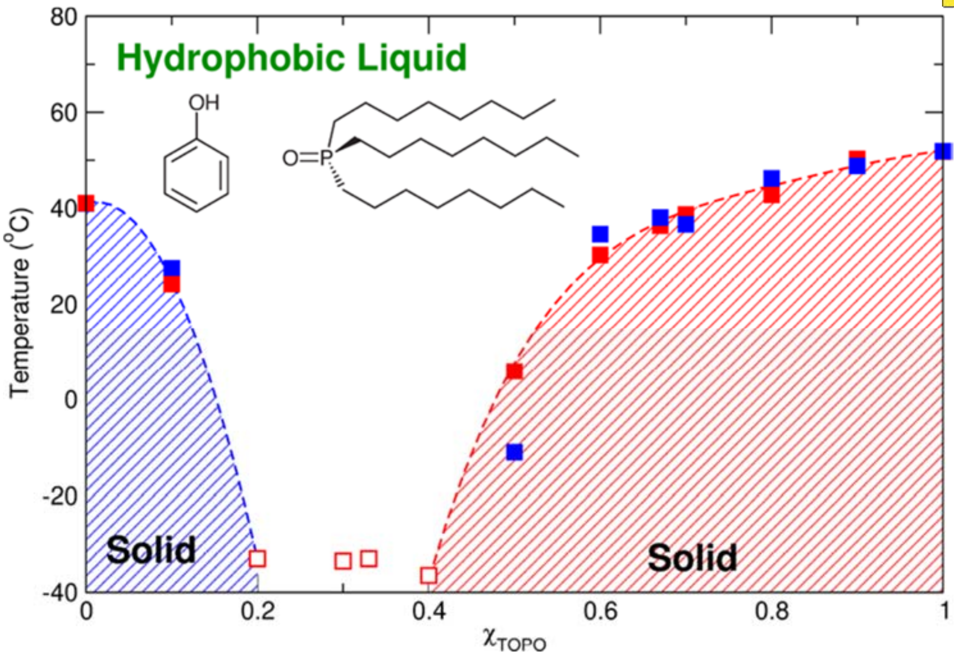

Figure 1: Phase diagram for TOPO:phenol mixture, constructed from observational solidification points (solid−liquid cell, red ■), DSC results (blue ■), and solid−liquid cell glass transitions (red □). Phenol (left) and TOPO (right) are also shown.

Moving away from ionic DESs, which include a salt (or an ionizable amine component[2]), Ribeiro et al.[5] have shown that hydrophobic eutectic solvents could be prepared from mixtures of DL-menthol with a range of carboxylic acids and used as extractive solvents for caffeine, tryptophan, isophthalic acid, and vanillin from water. Compared to the more usual ionic DES, these liquids have significantly lower viscosity as a result of eliminating the Coulombic charge interactions. The scope for formation of liquid eutectic solvents has subsequently been expanded to a range of terpenes with monocarboxylic acids[6] and, interestingly, also to make use of mixtures of carboxylic acids to access eutectic liquid compositions.[7]

Building on previous experience using trioctylphosphine oxide (TOPO) as a Lewis basic (hydrogen-bond accepting) ligand to generate liquid coordination complexes[8,9,10] with tuneable Lewis acid properties we were interested in studying whether trioctylphosphine oxide (TOPO) could be used as a hydrogen-bond-accepting component to produce DES and whether a liquid DES formed in this way could be used as an extractant phase containing high phosphine oxide concentrations. TOPO has many applications as a capping agent for the production of quantum confined nanomaterials,[11–15] and as an extractant[16] for metal ions, and organic acids[17–20] and phenolic compounds.[21,22,23] However, an issue with TOPO is its relatively low solubility in hydrocarbon solvents that are the choice for aqueous−organic liquid−liquid extraction processes. One approach to address this is the use of alternative phosphine oxide formulations, such as Cyanex 923[23,24]this is a mixture of trialkylphosphine oxides containing hexyl and octyl groups that is a liquid (mp −5 to 0 °C) and is completely miscible with common industrial diluents (such as kerosene) allowing higher concentrations of extractant to be achieved than with pure TOPO.

To our knowledge, TOPO has never been transformed into an ambient temperature DES, and we reasoned that a DES formed from TOPO containing a high phosphine oxide concentration would overcome some of the challenges faced by the choices of diluent, viz., limiting solubility in non-hazardous solvents such as odourless kerosene or high solubility in hazardous solvents such as dichloromethane or benzene. Here we report the formation of an ambient temperature hydrophobic eutectic liquid between TOPO and phenol, as a model hydrogen-bond donor, and the applicability of the system to metal extraction is demonstrated for the removal of uranyl ($[UO2]^{2+}$) ions from aqueous nitric acid.

Melting Point and Phase Composition.

A detailed investigation of the solid−liquid phase behaviour of the TOPO:phenol system was made using both visual observation from samples in a solid−liquid cell and by DSC (**Figure *1***). Across the intermediate composition range (χ_{TOPO} = 0.20−0.40), free-flowing liquids were obtained that became progressively more viscous on cooling, eventually forming glasses that could not be poured below around ca. −34 °C. The cooling and heating profiles in the DSC measurements at these compositions were essentially featureless; no crystallization of glass transition events were observable, either around the solidification points observed visually or scanning to −80 °C. In contrast, at χ_{TOPO} = 0.10 and from χ_{TOPO} = 0.50−1.00, solid samples were obtained from which melting was observable both visually and from first order transitions in the DSC at comparable temperatures in the two experiments.

Table 1: Thermal data [a] from DSC and observation

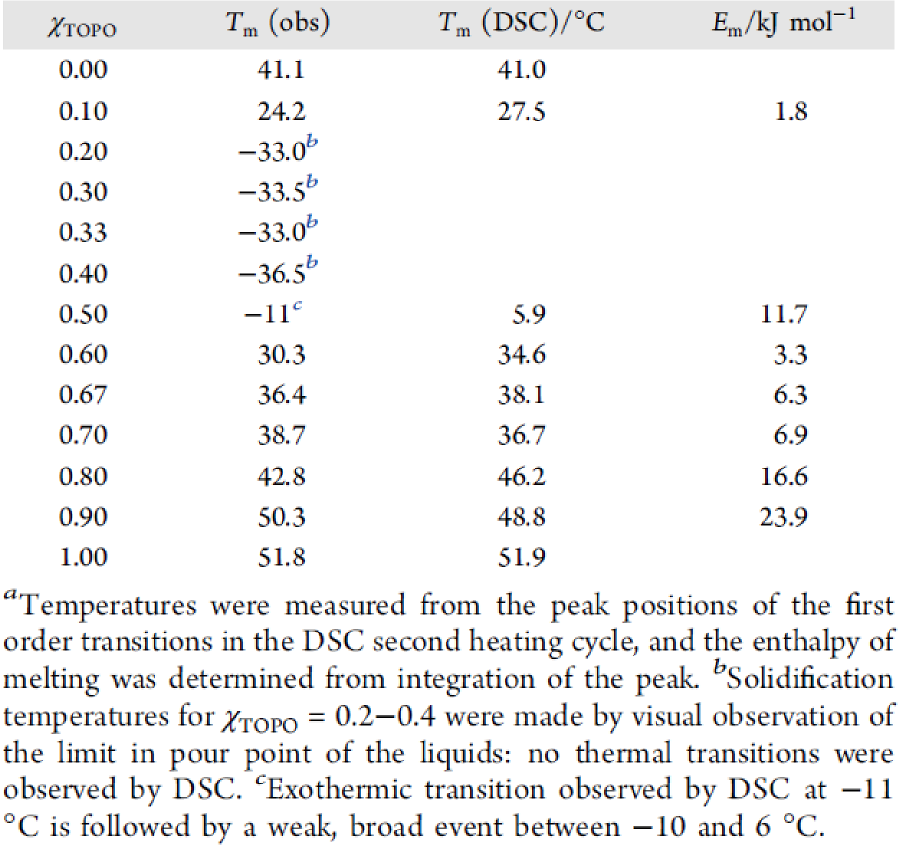

χ_{TOPO}	T_m (obs)	T_m (DSC)/°C	E_m/kJ mol^{-1}
0.00	41.1	41.0	
0.10	24.2	27.5	1.8
0.20	−33.0[b]		
0.30	−33.5[b]		
0.33	−33.0[b]		
0.40	−36.5[b]		
0.50	−11[c]	5.9	11.7
0.60	30.3	34.6	3.3
0.67	36.4	38.1	6.3
0.70	38.7	36.7	6.9
0.80	42.8	46.2	16.6
0.90	50.3	48.8	23.9
1.00	51.8	51.9	

[a] Temperatures were measured from the peak positions of the first order transitions in the DSC second heating cycle, and the enthalpy of melting was determined from integration of the peak. [b] Solidification temperatures for χ_{TOPO} = 0.2−0.4 were made by visual observation of the limit in pour point of the liquids: no thermal transitions were observed by DSC. [c] Exothermic transition observed by DSC at −11 °C is followed by a weak, broad event between −10 and 6 °C.

TOPO:phenol with χ_{TOPO} = 0.10 extensively supercools in the DSC, undergoing cold-crystallization on heating at ca. −50 °C and is then followed by melting at 27.5 °C. This pattern was repeated over three thermal cycles, and shows a small depression in melting of the χ_{TOPO} = 0.10 mixture compared to pure phenol (mp 41 °C). At χ_{TOPO} = 0.50, in the DSC, the samples supercooled and then, on heating, undergo cold-crystallization with an extremely broad (ca. 20 °C) endothermic transition cantered at −29 °C. This is followed by a sharp exotherm at −11 °C (ΔH = 11.7 kJ mol^{-1}), and a much weaker broad exotherm between −10 and 6 °C. In the solid−liquid cell, on heating slowly from −40 °C, the mixture was observed to melted to a slurry from ca. −10 °C, forming a single homogeneous clear liquid phase at 6 °C. Above $\chi_{TOPO} = 0.50$, reversible melting and freezing transitions are more readily observed in the TOPO:phenol mixtures, with all samples solidifying at temperatures above 0 °C in both the solid−liquid cell and DSC. Both the crystallization point on cooling and subsequent melting point on heating of the mixtures were systematically reduced by the introduction of phenol, and the melting transition in the DSC becomes increasingly broad, with a long trailing edge indicative of premelt disordering of the alkyl-chain regions as is often seen in plastic crystals, particularly from ionic liquid materials.[25,26,27]

The melting temperatures (and corresponding enthalpy) of the range of TOPO:phenol compositions are shown in **Error! Reference source not found.**, and the mole fraction TOPO:phenol temperature−composition phase diagram generated from this data is shown in **Figure *1***. In common with many ionic liquids and cholinium-based DES, the TOPO:phenol mixtures proved inherently difficult to crystallize forming glassy amorphous solids on cooling. The reduced melting points of the mixtures, coming from either high TOPO or high phenol composition, can be extrapolated to a eutectic point in the region of $\chi_{TOPO} = 0.33$ (1:2 TOPO:phenol) with an extensive liquid region down to ca. −34 °C between $\chi_{TOPO} = 0.2$ and 0.5, a reduction of 70 °C compared to the melting points of TOPO (mp 52 °C) and phenol (mp 42 °C).

Liquid−Liquid Extraction Studies

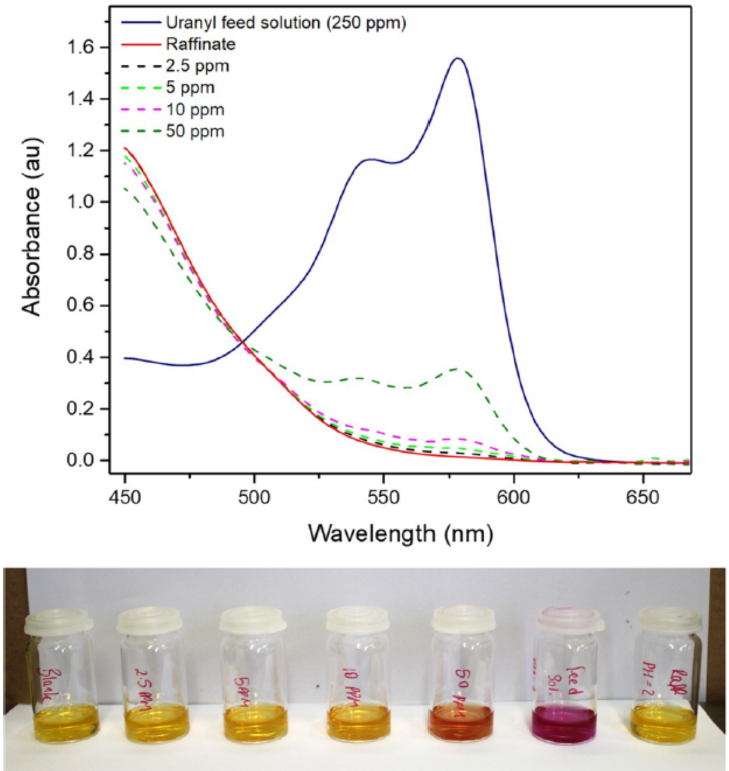

Figure 2: Transmission spectra (top) from the uranyl feed solution (250 ppm $[UO2]^{2+}$) containing Br-PADAP indicator (blue) and the raffinate after contact with TOPO:phenol (red). Standard solutions containing 5−50 ppm uranyl in nitric acid are shown as dashed lines for comparison.

Uranyl extraction was examined from acidic aqueous uranyl nitrate, contacting 1 cm^3 of TOPO:phenol ($\chi_{TOPO} = 0.50$, pre-equilibrated against the corresponding aqueous nitric acid solutions) with 1 cm^3 of uranyl-containing feeds (shaken, 10 min, ambient temperature) with uranyl nitrate concentrations of 250 and 2350 ppm in nitric acid (0.01−3.00 M). The final concentrations of U(VI) in the aqueous acid after extraction were determined by UV−vis spectroscopic analysis after addition of 2-(5-bromo-2-pyridylazo)-5-(diethylamino)phenol (Br-PADAP) as the spectroscopic probe.[28] UV−vis spectra of 5−50 ppm standards and the 250 ppm acidic uranyl nitrate stock solution before and after contact with the TOPO:phenol extractant are shown in Figure 2 along with a picture showing the appearance of each sample.

Analysis was based on the absorbance maxima at 545 and 578 nm in the UV−vis spectra of uranyl-containing samples spiked with Br- PADAP indicator (Figure 2) and the detection limit for U(VI) estimated to be 0.50 ppm. The distinctive deep purple of the U(VI)-complexed Br-PADAP indicator at 250 ppm uranyl concentration, corresponding to the intense maxima in the UV−vis spectrum at 578 nm, decreases markedly as the uranyl concentration in the solution decreases. Single contact mixing of uranyl solutions (250 ppm) in 0.01, 1.00, and 3.00 M nitric acid with the TOPO:phenol ($\chi_{TOPO} = 0.50$) liquid extractant resulted in reduction in uranyl concentrations in the raffinate phase to the detection limit for the measurements in the experiments (Table 2). The colour and UV−vis spectra of raffinate solutions (spiked with Br-PADAP) after contact with TOPO:phenol were comparable to those of the blank acidic Br-PADAP solution.

Table 2: Performance of TOPO:Phenol ($\chi_{TOPO} = 0.50$) as a liquid extractant for uranyl nitrate from nitric acid at different acid and uranyl concentration in the aqueous feed[a]

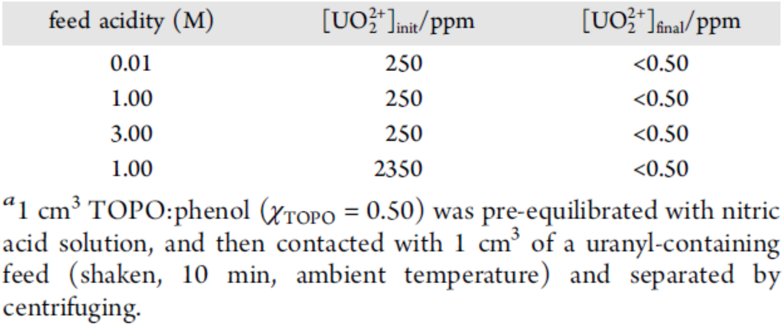

feed acidity (M)	$[UO_2^{2+}]_{init}$/ppm	$[UO_2^{2+}]_{final}$/ppm
0.01	250	<0.50
1.00	250	<0.50
3.00	250	<0.50
1.00	2350	<0.50

[a] 1 cm^3 TOPO:phenol ($\chi_{TOPO} = 0.50$) was pre-equilibrated with nitric acid solution, and then contacted with 1 cm^3 of a uranyl-containing feed (shaken, 10 min, ambient temperature) and separated by centrifuging.

When the uranyl concentration was increased 10-fold to 2350 ppm in 1.00 M HNO3 (the acidity at which TOPO has maximum efficiency) complete extraction of uranyl species was also observed demonstrating the excellent extraction potential of the TOPO:phenol system in comparison to conventional TOPO-based extraction systems.[29,30,31] Distribution ratios could be estimated from the initial and final $[UO2]^{2+}$ concentrations in the aqueous phase; however, because the final values are all around the limit of detection the results are unreliable. D was estimated to be at least 500 from the 250 ppm uranyl solutions, and from the 2350 ppm solution the corresponding value is ca. 5000. This efficient extraction and the estimated distribution ratios are similar to values of 1×10^3 reported for uranium partitioning in the TRPO extraction process[32] from high salt and nitric acid solutions using a 30 wt % mixture of trialkylphosphine oxides in kerosene. In the TRPO process and here, the origin of the high uranyl extraction efficiencies is the high concentration of phosphine oxide in the extracting phase (30 wt % for TRPO and ca. 80 wt % in the TOPO:phenol ($\chi_{TOPO} = 0.50$) system here, which is between 10 and 20 times greater than that usually used in kerosene.[31]

The work described is an excerpt from a recent publication in ACS Sustainable Chemistry & Chemical engineering, for more information about the work please see: Mark Gilmore, Éadaoin N.

McCourt, Francis Connolly, Peter Nockemann, Małgorzata Swadźba-Kwaśny* , and John D. Holbrey*, Hydrophobic Deep Eutectic Solvents Incorporating Trioctylphosphine Oxide: Advanced Liquid Extractants, ACS Sustainable Chem. Eng., Advance online publication., DOI: 10.1021/acssuschemeng.8b04843

1 D. J. G. P. van Osch, L. F. Zubeir, A. van den Bruinhorst, M. A. A. Rocha and M. C. Kroon, *Green Chem.*, 2015, **17**, 4518.

2 D. J. G. P. van Osch, D. Paramentier, C. H. J. . Dietz, A. van den Bruinhorst, R. Tuiner and Kroon, *Chem. Commun.*, 2016, **52**, 11987.

3 J. Cao, M. Yang, F. Cao, J. Wang and E. Su, *ACS Sustain. Chem. Eng.*, 2017, **5**, 3270.

4 J. Cao, L. Chen, M. Li, F. Cao, L. Zhao and E. Su, *Green Chem.*, 2018, **20**, 1879.

5 B. D. Ribeiro, C. Florindo, L. C. Iff, M. A. Z. Coelho and I. M. Marrucho, *ACS Sustain. Chem. Eng.*, 2015, **3**, 2469.

6 A. R. Martins, E. A. Crespo, P. V. A. Pontes, L. P. Silva, M. Bu, G. J. Maximo, E. A. C. Batista and C. Held, *ACS Sustain. Chem. Eng.*, 2018, **6**, 8836.

7 C. Florindo, L. Romero, I. Rintoul, C. Branco and I. M. Marrucho, *ACS Sustain. Chem. Eng.*, 2018, **6**, 3888.

8 J. M. Hogg, F. Coleman, A. Ferrer-Ugalde, M. P. Atkins and M. Swadźba-Kwaśny, *Green Chem.*, 2015, **17**, 1831.

9 J. M. Hogg, L. C. Brown, K. Matuszek, P. Latos, A. Chrobok and M. Swadźba-kwaśny, *Dalt. Trans.*, 2017, **46**, 11561.

10 F. Coleman, G. Srinivasan and M. Swadz, *Angew. Chemie*, 2013, **52**, 12582–12586.

11 I. Mekis, D. V Talapin, A. Kornowski, M. Haase and H. Weller, *J. Phys. Chem.*, 2003, **107**, 7454.

12 A. A. Guzelian, J. E. B. Katari, A. V Kadavanich, U. Banin, K. Hamad, E. Juban, A. P. Alivisatos, R. H. Wolters, C. C. Arnold and J. R. Heath, *J. Phys. Chem.*, 1996, **100**, 7212.

13 T. Trindade and P. O. Brien, *Chem. Mater.*, 1997, **9**, 523.

14 T. Cassagneau, T. E. Mallouk, J. H. Fendler, V. Uni, U. V Park, V. Pennsyl, V. Ad, M. Processing, C. U. V, P. O. Box and N. York, *J. Am. Chem. Soc.*, 1998, **120**, 7848.

15 F. V Mikulec, M. Kuno, M. Bennati, D. A. Hall, R. G. Griffin and M. G. Bawendi, *J. Am. Ceram. Soc.*, 2000, **122**, 2532.

16 E. K. Watson and W. A. Rickelton, *Solvent Extr. Ion Exch.*, 1992, **10**, 37.

17 S. Uenoyama, T. Hano, M. Hirata and S. Miura, *J. Chem. Technol. Biotechnol.*, 1996, **67**, 260.

18 P. O. Saboe, L. P. Manker, W. E. Michener, D. J. Peterson, D. G. Brandner, S. P. Deutch, M. Kumar, R. M. Cywar, G. T. Beckham and E. M. Karp, *Green Chem.*, 2018, **20**, 1791.

19 T. Brouwer, M. Blahusiak, K. Babic and B. Schuur, *Sep. Purif. Technol.*, 2017, **185**, 186.

20 G. Kim, S. Park and B. Um, *Ind. Crop. Prod.*, 2016, **89**, 34.

21 P. Praveen and K. Loh, *J. Memb. Sci.*, 2013, **437**, 1.

22 P. Praveen and K. Loh, *Chemosphere*, 2016, **153**, 405.

23 E. K. Watson, W. A. Rickelton, A. J. Robertson and T. J. Brown, *Solvent Extr. Ion Exch.*, 1988, **6**, 207.

24 CYANEX 923 Extractant-Solvent Extraction Reagent. https://www.cytec.com/sites/default/files/datasheets/SPT-032-D.pdf.

25 S. Forsyth, J. Golding, D. R. Macfarlane and M. Forsyth, *Electrochim. Acta*, 2001, **46**, 1753.

26 J. D. Holbrey, W. M. Reichert, R. P. Swatloski, G. A. Broker, W. R. Pitner, K. R. Seddon and R. D. Rogers, *Green Chem.*, 2002, **4**, 407.

27 C. Patrick, R. Douglas, M. Jennifer, D. R. Macfarlane and J. M. Pringle, *J. Mater. Chem.*, 2011, **21**, 7640.

28 S. Biswas, P. N. Pathak and S. B. Roy, *Spectrochim. Acta - Part A Mol. Biomol. Spectrosc.*, 2012,

91, 222.
29 F. T. Bunus, V. C. Domocoş and P. Dumitrescu, *J. Inorg. Nucl. Chem.*, 1978, **40**, 117.
30 T. Sato, T. Nishida and M. Yamatake, *J. Appl. Chem. Biotechnol.*, 1973, **23**, 909.
31 R. Babecki, A. W. . Platt and J. C. Tebby John, *Polyhedron*, 1989, **8**, 1357.
32 W. Jianchen and S. Chongli, *Solvent Extr. Ion Exch.*, 2001, **19**, 231.

QUILL Quarterly Report

August- October 2018

Name:	**Peter McNeice**		
Supervisor(s):	Dr Andrew Marr, Dr Patricia Marr		
Position:	PhD student		
Start date:	October 2016	Anticipated end date:	July 2020
Funding body:	QUILL IAB		

Base Stable and Basic Ionic Liquids

Background

The imidazolium cation is the most common cation in ionic liquids due to its acid stability, thermal stability and oxidative stability.[1] Unfortunately, it can be extremely sensitive to base. The most acidic position is the C2 proton which deprotonates to form a carbene (Figure 1). The instability of the C2 position in base was demonstrated in 1964 with heavy water buffers causing deuteration at the C2 position.[2] The acidity of this proton limits the use in base catalysed reactions. This has been investigated by Aggarwal *et. al.*[3] who found that [BMIM][Cl] was deprotonated to form a carbene which went on to attack the aldehyde component of a Baylis-Hillman reaction, reducing the yield. They found that bases with pK_a as low as 8 or 9 could generate a carbene.

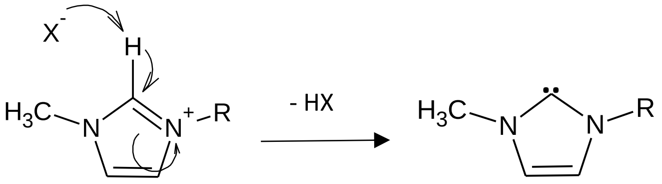

Figure 1: Deprotonation of an imidazolium cation to form a carbene. X^- can be the anion or a base.

When an ionic liquid is able to catalyse a reaction, it is called a functionalised ionic liquid (FIL), previously known as task specific ionic liquids (TSIL).[4] These materials can be created due to the tuneable properties of ionic liquids and have the potential to cut down on auxiliary stoichiometric catalysts and prevent the formation of salts.

Ionic liquids can be basic due to the presence of a Brønsted basic (proton accepting) anion. Examples include ionic liquids with OH^-,[5] imidazolate ($[Im]^-$),[6] carboxylate,[7,8] amino acids[9] and dicyanamide ($[DCA]^-$)[10] as anions (Figure 2).

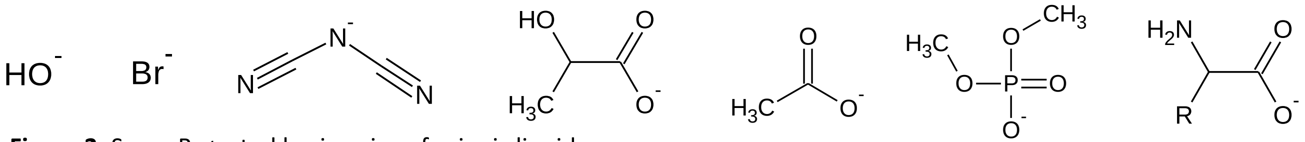

Figure 2: Some Brønsted basic anions for ionic liquids.

Ionic liquids with basic anions often suffer from instability. The anion is able to attack the cation to form two neutral species as shown in Figure 1. Strong bases such as halide ions and OH^- in particular suffer from this effect.

Heterogensing ionic liquids can increase their stability and allows for simple separation of the ionic liquid catalyst from the reaction mixture. Supported ionic liquid phase (SILP) catalyst systems have recently become common in reactions.[11,12,13] In SILPs, the ionic liquid is immobilised onto a porous solid with high surface area (Figure 3). The catalyst layer often has high activity as the surface area available is greatly increased relative to the volume of ionic liquid. This means less catalyst and a lower volume of ionic liquid can be utilised which is in keeping with the Principles of Green Chemistry.

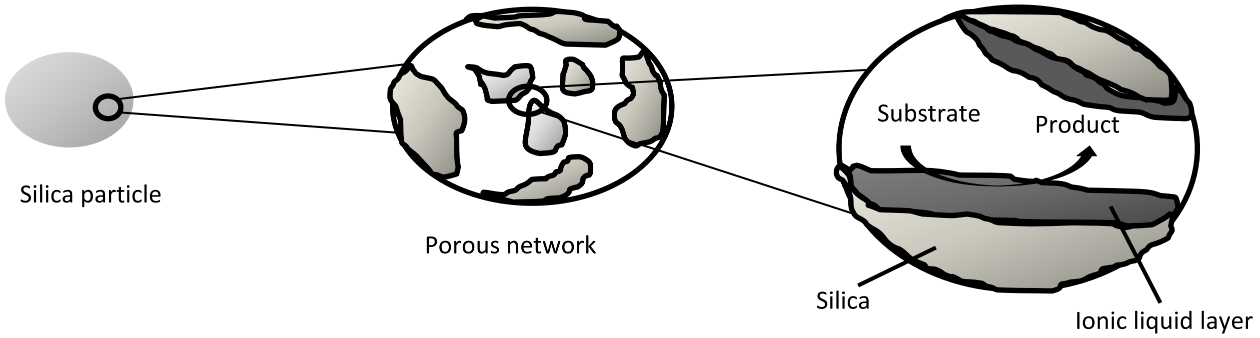

Figure 3: A representation of the structure of a supported phase ionic liquid.

Objective of this work

The overall aim of this project is to synthesise functionalised ionic liquids which are base stable and basic. Basic ionic liquids will be able to act as both solvent and catalyst for reactions, which will eliminate waste. Stability is key for catalysis as well as recovery of the ionic liquid.

Progress to date

A previous report discussed Knoevenagel and Aldol condensations catalysed by binary alkoxide ionic liquids.[14]

The previous report discussed applying the ionic liquids to a wider range of substrates for Aldol condensations. Under the same reaction conditions as the previously reported Aldol reactions, the substrates used for the Aldol condensation were varied (Table 1).

Table 1: Aldol condensation reactions between various aldehydes and ketones catalysed by $[\mathrm{Pyrr}_{14}][\mathrm{NTf}_2]_{0.57}[\mathrm{O}^i\mathrm{Pr}]_{0.43}$.

Entry	Aldehyde	Ketone	Products (Yield/%)[a]
1	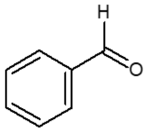	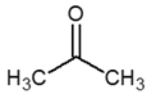	**A** 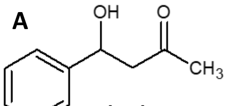 **(15)** **B** 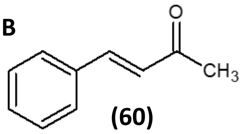 **(60)** **Total Yield = 75 %**
2	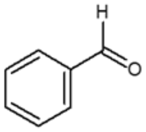	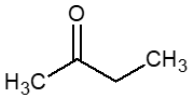	**C** 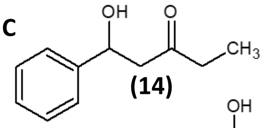 **(14)** **D** 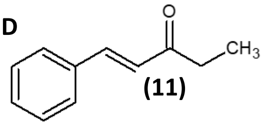 **(11)** 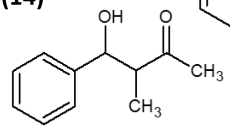 **E/F** **(syn: 7/ anti: 10)** **Total Yield = 42 %**

3	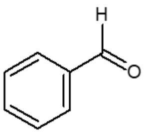	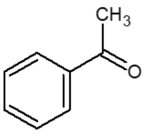	**G** 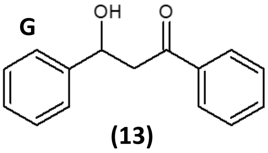 **(13)** **H** 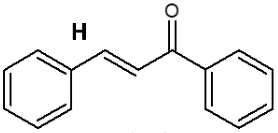 **(29)** **I** 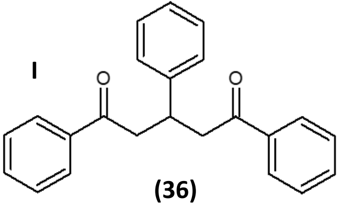 **(36)** **Total Yield = 78 %**
4	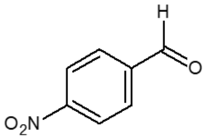	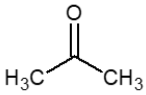	**J** 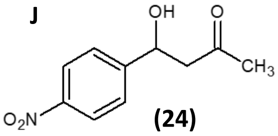 **(24)** **K** 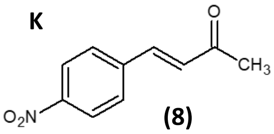 **(8)** **Total Yield = 32 %**
5[b]	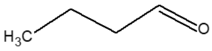	NA	**L** 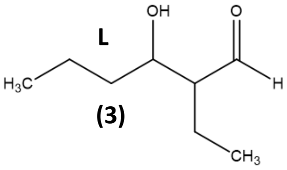 **(3)** **M** 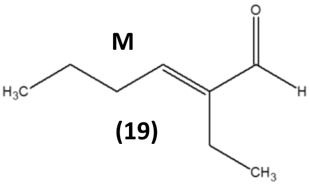 **(19)** **Total Yield = 22 %**

Conditions: Aldehyde (0.22 mmol, 1 eq.), ketone (2.20 mmol, 10 eq.), $[Pyrr_{14}][NTf_2]_{0.57}[O^iPr]_{0.43}$ (0.083 g, 0.20 mmol 1 eq.), sulfolane (0.501 g, 4.17 mmol, 1 mL/0.5 mmol IL), (25 °C, stir rate 500 RPM). [a] Obtained from ^1H NMR of extracted organics against a known mass of ethyl trifluoroacetate. [b] 0.5 eq $[Pyrr_{14}][NTf_2]_x[O^iPr]_{1-x}$ used.

The initial system tested, the reaction between acetone and benzaldehyde produced a total yield of 75 % (Table 1, entry 1). When acetone was replaced by the bulkier butanone the total yield decreased to 42 % and there were four products present due to the two reactive sites on butanone (Table 1, entry 2).

Replacing benzaldehyde with 4-nitrobenzaldehyde (Table 1, entry 4) reduced the total yield to 32 % which is consistent with Climent *et. al.*[15] who found that substituted rings had lower reactivity than benzaldehyde. The selectivity of this reaction is towards hydroxy ketone **J** whereas the reaction between benzaldehyde and acetone is more selective for ketone **K**. This is due to the electron withdrawing nature of the nitro group which disfavours the dehydration step. The reaction between 4-nitrobenzaldehyde and acetone is often seen to stop at the hydroxyketone.[16] The fact that dehydration occurs in the system reported here is possibly as a result of the high basicity of $[Pyrr_{14}][NTf_2]_{0.57}[O^iPr]_{0.43}$.

For the self-Aldol of butanal, only 0.5 equivalents of $[Pyrr_{14}][NTf_2]_{0.57}[O^iPr]_{0.43}$ were used (Table 1, entry 5). The total yield is low, 23 %. This ispartly be due to the lower base loading but also due to the lower reactivity of the non-activated aliphatic aldehyde. This reaction shows greater selectivity for the ketone product **K** compared to the other Aldol reactions. A longer reaction time may improve the yield and convert any remaining hydroxy ketone **J** to ketone **K**.

Interestingly, the reaction between benzaldehyde and acetophenone (Table 1, entry 4) produces hydroxy ketone **G**, ketone **H**, and the Michael addition product **I**. This was also found by Takahashi *et. al.*[17] who attributed this reactivity to the presence of *iso*-propoxide in their system. Following the dehydration of **G** to **H** a further molecule of acetophenone adds to the double bond of **H** to form product **I**. This is as a result of excess acetophenone in the system. Longer reactions times and higher temperatures are likely to increase selectivity for the Michael addition product. Using a smaller excess of acetophenone is likely to increase selectivity for Aldol products **G** and **H**.

The above results show that the binary alkoxide ionic liquid catalysts can act on a range of substrates in the Aldol condensation. This compares favourably to a system using guanidinium based ionic liquids (30 mol. %) which catalysed the reaction between 4-nitrobenzaldehyde and various ketones.[18] Using non-bulky ketones produced moderate to high yields, 50-96 %. The hydroxyketone was the sole product. However the reaction times ranged from 2-120 hours compared to the 1.5 hours used in this system. It was also found that the guanidinium ionic liquids could not catalyse the Aldol reaction when benzaldehyde or aliphatic aldehydes were used whereas the binary ionic liquids in this report successfully catalysed reactions with these substrates. The above Aldol results are not optimised and with further work individual products could be produced in higher yield and selectivity.

Recovery and reuse of the binary ionic liquids from the homogeneous reaction mixtures has not been possible. This may be due to their deactivation during the reaction or during the recovery process (extraction or evaporation of the products). Heterogenising the ionic liquids is likely to increase their stability during the reaction and will allow for a milder separation process, making their reuse achievable.
To this end, both $[Pyrr_{14}][NTf_2]_x[O^iPr]_{1-x}$ and $[Pyrr_{14}][NTf_2]_x[OH]_{1-x}$ physisorbed SILPs have been prepared. Thermogravimetric analysis (TGA) showed the SILP to be roughly 10 wt. % ionic liquid, calculated by subtracting the final mass from the initial mass. TGA showed the $[Pyrr_{14}][NTf_2]_x[O^iPr]_{1-x}$ SILPs begin decomposing at a temperature roughly 40 °C higher than in liquid form (Table 2). However $[Pyrr_{14}][NTf_2]_x[OH]_{1-x}$ SILPs are found to be less thermally stable than in the liquid form (Table 2). This could be due to decomposition of the ionic liquid layer or chemically induced decomposition of the silica support upon reacting with the basic ionic liquid. The thermal stability of $[Pyrr_{14}][NTf_2]_x[O^iPr]_{1-x}$ as determined by TGA increases as the proportion of $[O^iPr]^-$ decreases but there is no trend observed for $[Pyrr_{14}][NTf_2]_x[OH]_{1-x}$ SILPs. In a previous report[19] $[Pyrr_{14}][NTf_2]_x[O^iPr]_{1-x}$ ionic liquids were found to be stable whereas the anion of $[Pyrr_{14}][NTf_2]_x[OH]_{1-x}$ ionic liquids were unstable which is potentially a reason for the lower thermal stability of $[Pyrr_{14}][NTf_2]_x[OH]_{1-x}$ SILPs.

Table 2: TGA decomposition data of binary ionic liquids and equivalent binary SILPs.

Entry	Liquid (T_{onset}, °C)[a]	SILP (T_{onset}, °C)[a]
1	$[Pyrr_{14}][NTf_2]_{0.95}[O^iPr]_{0.05}$ (232.75)	$[Pyrr_{14}][NTf_2]_{0.92}[O^iPr]_{0.08}$ (274.79)
2	$[Pyrr_{14}][NTf_2]_{0.85}[O^iPr]_{0.15}$ (241.79)	$[Pyrr_{14}][NTf_2]_{0.82}[O^iPr]_{0.18}$ (271.04)
3	$[Pyrr_{14}][NTf_2]_{0.58}[O^iPr]_{0.42}$ (229.90)	$[Pyrr_{14}][NTf_2]_{0.57}[O^iPr]_{0.43}$ (267.37)
4	NA	$[Pyrr_{14}][OH]$ (219.92)
5	$[Pyrr_{14}][NTf_2]_{0.51}[OH]_{0.49}$ (243.93)	$[Pyrr_{14}][NTf_2]_{0.50}[OH]_{0.50}$ (232.11)
6	$[Pyrr_{14}][NTf_2]_{0.75}[OH]_{0.25}$ (245.29)	$[Pyrr_{14}][NTf_2]_{0.67}[OH]_{033}$ (225.13)

[a] Determined by thermogravimetric analysis.

As an initial test of their activity, the SILPs were applied to the Knoevenagel condensation between Malononitrile and Benzaldehyde (Figure 4,

Table 3). The SILPs were more active with a greater proportion of basic anion in the SILP. This is consistent with liquid phase reactions.[14]The reaction yields of the best performing catalysts are above 90 % (

Table 3, entries 3, 5, 6 The results of the SILP catalysed reactions show that the binary ionic liquids are still active catalysts when immobilised on silica.

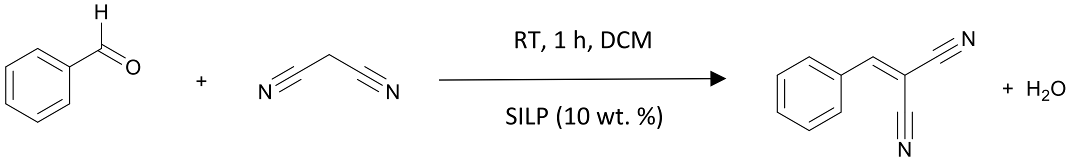

Figure 4: Knoevenagel Condensation between malononitrile and benzaldehyde.

Table 3: Yield of Knoevenagel condensation between Malononitrile and Benzaldehyde catalysed by 10 wt. % SILP.

Entry	SILP (10 wt. %)	Contained Yield (%)[a]
1	$[Pyrr_{14}][NTf_2]_{0.92}[O^iPr]_{0.08}$	32
2	$[Pyrr_{14}][NTf_2]_{0.82}[O^iPr]_{0.18}$	58
3	$[Pyrr_{14}][NTf_2]_{0.57}[O^iPr]_{0.43}$	93
4	$[Pyrr_{14}][NTf_2]_{0.67}[OH]_{033}$	79
5	$[Pyrr_{14}][NTf_2]_{0.50}[OH]_{0.50}$	92
6	$[Pyrr_{14}][OH]$	95

Conditions: Malononitrile (0.037 g, 0.57 mmol), benzaldehyde (0.073 g, 0.69 mmol), SILP (0.0075, 10 wt. %), DCM (0.114, 1:1 wt/wt DCM:Reagents), (RT, stir rate 500 RPM and time 24 h). [a]Obtained from ^1H NMR against a known mass of ethyl trifluoroacetate.

Following the reaction, ^{19}F NMR spectroscopy was used to calculate the approximate wt. % of ionic liquid that had leached from the SILP. 30-50 wt. % of the ionic liquid leached from each SILP. This shows that physisorbed SILPs are not an appropriate support for the recovery of the binary ionic liquids and alternate methods of heterogenising the ionic liquids must be attempted.

Conclusions and future work

Binary alkoxide ionic liquids have shown good activity and substrate scope for Aldol condensation reactions. Substrates including bulky ketones and aliphatic aldehydes, with yields comparing favourably to literature systems. The ionic liquids were also found to catalyse the tandem Aldol condensation - Michael addition of acetophenone and benzaldehyde to produce a 1,5-diketone. However the ionic liquids have not been successfully reused following homogeneous reactions. The ionic liquids must therefore be heterogenised to increase their stability and allow for potential reuse.

Physisorbed SILPs of binary alkoxide and hydroxide ionic liquids have been prepared. The alkoxide SILPs show greater thermal stability than the hydroxide SILPs which mirrors the stability of the liquid systems. The SILPs were found to catalyse the Knoevenagel condensation between malononitrile and benzaldehyde but leached from the silica surface.

It has been found that physisorption of the ionic liquids onto silica is not an appropriate method for their heterogenisation. Attempts will now be made to heterogenise the ionic liquid by creating polymeric ionic liquids and also intercalating the ionic liquids into ionic clay materials such as hydrotalcite. This will allow for a stronger interaction between the support and the ionic liquid (covalent and Coulombic) which may help prevent leaching.

Publication

Work from QUILL report May-July 2018 (reference 14) was published:
P. McNeice, A. C. Marr, P. C. Marr, M. J. Earle, K. R. Seddon, Binary Alkoxide Ionic Liquids, *ACS Sustainable Chem. Eng*, 2018*,* **6**, 13676-13680, DOI: 10.1021/acssuschemeng.8b04299.

References

---

[1] S. T. Handy, *Curr. Org. Chem.*, 2005, **9**, 959-988.

[2] R. A. Olofson, W. R. Thompson, J. S. Michelman, *J. Am. Chem. Soc.*, 1964, **86**, 1865-1866.

[3] V. K. Aggarwal, I. Emme, A. Mereu, *Chem. Commun.*, 2002, 1612-1613.

[4] A. C. Cole, J. L. Jensen, I. Ntai, K. Loan, T. Tran, J. K. Weaver, D. C. Forbes, J. H. J. Davis, *J. Am. Chem. Soc.*, 2002, **124**, 5962-5963.

[5] J.-M. Xu, Q. Wu, Q.-Y. Zhang, F. Zhang, X.-F. Lin, *Eur. J. Org. Chem.*, 2007, 1798-1802.

[6] H. Luo, Z. Zhai, W. Fan, W. Cui, G. Nan, Z. Li, *Ind. Eng. Chem. Res.*, 2015, **54**, 4923-4928.

[7] Y. Liu, Y. Huang, P.-O. Boamah, L. Cao, Q. Zhang, Z. Lu, H. Li, *J. Appl. Polym. Sci.*, 2015, **132**, 41727.

[8] A. Cieniecka-Rosłiewicz, K. Kita, A. Fojutowski, J. Nawrot, K. Materna, J. Pernak, *Chem. Eur. J.*, 2008, **14**, 9305-9311.

[9] H. Peng, Y. Zhou, J. Liu, H. Zhang, C. Xia, X. Zhou, *RSC Adv.*, 2013, **3**, 6859-6864.

[10] D. R. MacFarlane, S. A. Forsyth, J. Golding, G. B. Deacon, *Green Chem.*, 2002, **4**, 444-448.

[11] A. Riisager, R. Fehrmann, M. Haumann, P. Wasserscheid, *Top. Catal.*, 2006, **40**, 91-102.

[12] K. L. Luska, A. Bordet, S. Tricard, I. Sinev, W. Grünert, B. Chaudret, W. Leitner, *ACS Catal*, 2016, **6**, 3719-3726.

[13] A. Weiß, M. Giese, M. Lijewski, R. Franke, P. Wasserscheid, M. Haumann, *Catal. Sci. Technol.*, 2017, **7**, 5562-5571.

[14] P. McNeice, *Base Stable and Basic Ionic Liquids*, QUILL Quarterly Report May-July 2018, Unpublished, August 2018.

[15] M. J. Climent, A. Corma, S. Iborra, J. Primo, *J. Catal.*, 1995, **151**, 60-66.

[16] M. Stiles, D. Wolf, G. V. Hudson, *J. Am. Chem. Soc.*, 1959, **81**, 628-631.

[17] H. Takahashi, T. Arai, A. Yanagisawa, *Synlett*, 2006, **17**, 2833–2835.

[18] A. Zhu, T. Jiang, B. Han, J. Huang, J. Zhang, X. Ma, *New J. Chem.*, 2006, **30**, 736-740.

[19] P. McNeice, *Base Stable and Basic Ionic Liquids*, QUILL Quarterly Report December-March 2018, Unpublished, August 2018.

QUILL Quarterly Report

August - October 2018

Name:	**Keith Moore**		
Supervisor(s):	Gosia Swadźba-Kwaśny		
Position:	Research Assistant		
Start date:	July 2018	Anticipated end date:	Jan 2019
Funding body:	Research Centre in Sustainable Energy / QUILL		

Grant Proposal Writing and Website Management

Objective of this work

To continue research of advanced liquid materials in QUILL, it is crucial to maintain funding streams from grant awarding bodies. The role focuses on collating the research and policy information, and working in collaboration with PIs to produce successful grant proposals. Additionally, the QUILL website is maintained to ensure it is up to date, and a valuable resource for promotion and dissemination.

Progress to date

A first draft of an EPSRC proposal on ionic liquid and semi-solid electrolytes for metal ion batteries was produced. This principally involved research into conventional lithium ion technology, electric vehicles and current research into advanced battery technology. Attendance at an advanced battery workshop hosted by HORIBA-MIRA also influenced the content fed into the proposal draft. Insight into the current state of the field was also developed at a summer school on the applications of x-ray methods to energy materials hosted by NECEM and the University of Newcastle.
Work also commenced amending and updating a proposal that was submitted unsuccessfully to the European Commission Horizon 2020 Program for a MSCA European Training Network in 2018. This has principally involved identifying weaknesses in the prior submission, with input from the QUB Research & Enterprise office. This ITN focuses on training early career researchers in the field of ionic liquids and other advanced liquid materials, while also conducting fundamental research into ILs and their applications in biofuels, energy capture and energy storage.

Research was also started for a possible proposal on the topic of 3D printing and smart inks using IL precursors, with a principal interest in incorporating advanced printing methods into the fabrication of photovoltaic devices.

The QUILL website, now hosted as a subsite of the QUB main site, has undergone substantial development. Initial work introduced substantial ease of access and presentational developments, along with producing graphic content to promote the work of QUILL researchers. The site is now typically updated weekly to ensure up to date content.

Future work

Continued maintenance of the website, along with planned implementation of a secure access section for dissemination of materials to members of the Industrial Advisory Board and senior academics. Completion of a final draft of the EPSRC proposal and submission is intended. Redrafting of the MSCA ETN for Jan 2019 submission is also intended.

QUILL Quarterly Report

August - October 2018

Name:	Gareth Nelson		
Supervisor(s):	Dr John Holbrey, Dr Małgorzata Swadźba-Kwaśny		
Position:	PhD student		
Start date:	13/09/16	Anticipated end date:	13/09/19
Funding body:	DEL		

Ionic Liquid Catalysts for the Glycolysis of PET

Background

There are 4 broad types of PET recycling, primary recycling is pre-consumer scrap recycling. Secondary recycling is physical recycling, this approach first grinds the PET, then melts it before reforming it. The heat and force exerted in this process degrades the polymer leaving it unsuitable for many uses. Tertiary recycling is chemical recycling, the PET is recycled through chemical action, generally through depolymerisation of PET into constituent monomers. These monomers are re-polymerised to regenerate virgin PET. Quaternary recycling is the recovery of energy from the material, this is usually through incineration. This project focuses on chemical recycling of PET as it gives high quality polymers as a product. There are several methods for the depolymerisation of PET, these methods attack the ester linkage to break down the polymer. The use of alcohols (alcoholysis), amines (aminolysis), glycols (glycolysis), or water (hydrolysis) have previously been successful in the depolymerisation of PET. The focus of this project is glycolysis; this occurs through a transesterification reaction between PET and ethylene glycol (EG), commonly catalysed by a metal acetate, carbonate or sulfate. This reaction is attractive because the product, bis(2-hydroxyethyl)terephthalate (BHET), requires no additional processing before being converted to PET thus is easy to incorporate into PET production. Work utilising ionic liquids as a catalysts was investigated by H, Wang et al.[1,2] Initially their work utilised imidazolium halide and several acidic ionic liquids, poor yields were achieved but this showed a new approach to the glycolysis reaction.[2] Q, Wang also utilised ionic liquids as catalysts, previously H, Wang had performed this reaction using [bmim][$FeCl_4$], the logical extension of this was to test other transition metal salt containing ionic liquids.[3,4] Q, Wang found that while [bmim][$FeCl_4$] was effective, $[bmim]_2[ZnCl_4]$ and $[bmim]_2[CoCl_4]$ were more effective, achieving similar conversion of PET (almost 100%) but greater yields of BHET with an increase of almost 20% over [bmim][$FeCl_4$] for both ionic liquids. Work in literature had previously used acetate ionic liquids, however the results reported were lower and required higher temperatures and more catalyst than those reported by H, Wang using halometallate ionic liquids.[5]

1. H. Wang, Y. Lui, Z. Li, X. Zhang, S. Zhang, and Y. Zhang, Eur. Polym. J., 2009, **45**, 1535–1544
2. H. Wang, Z. Li, Y. Liu, X. Zhang, and S. Zhang, Green Chem., 2009, **11**, 1568-1575.
3. H. Wang, R. Yan, Z. Li, X. Zhang, and S. Zhang, Catal. Commun., 2010, **11**, 763–767.
4. Q. Wang, Y. Geng, X. Lu, and S. Zhang, ACS Sustain. Chem. Eng. 2015, **3**, 340−348
5. A.M. Al-Sabagh, F.Z. Yehia, A.M.M.F. Eissa, M.E. Moustafa, G. Eshaq, A.R.M. Rabie, and A.E. El-Metwally Ind. Eng. Chem. Res., 2014, **53**, 18443−18451

Objective of this work

The objective of this work is the production of bis(2-hydroxyethyl)terephthalate (BHET), a monomeric intermediate in PET production, from the glycolysis of waste PET. To achieve this, the applications of novel ionic liquids as catalysts for the glycolysis of PET in particular halometallate ionic liquids and acetate containing ionic liquids.

Progress to date

A range of ionic liquids were tested in the glycolysis reaction, these were repeated and the results were averaged. Some of these are repeats from previous experiments however there has been some doubt raised on the accuracy of the reaction temperature previously recorded. As such the temperatures of the oil bath the reaction was performed in was monitored using a thermocouple. The conversion is the percentage mass loss of PET through the reaction, the yield was found through HPLC analysis and calculated through a calibration curve. As can be seen from the graph below the yields were far lower than would have been expected, to ensure that these results are accurate the calibration curve will be remade and all the catalysts used will be repeated once more. If the yield is found to be very different the entire set of experiments will be repeated.

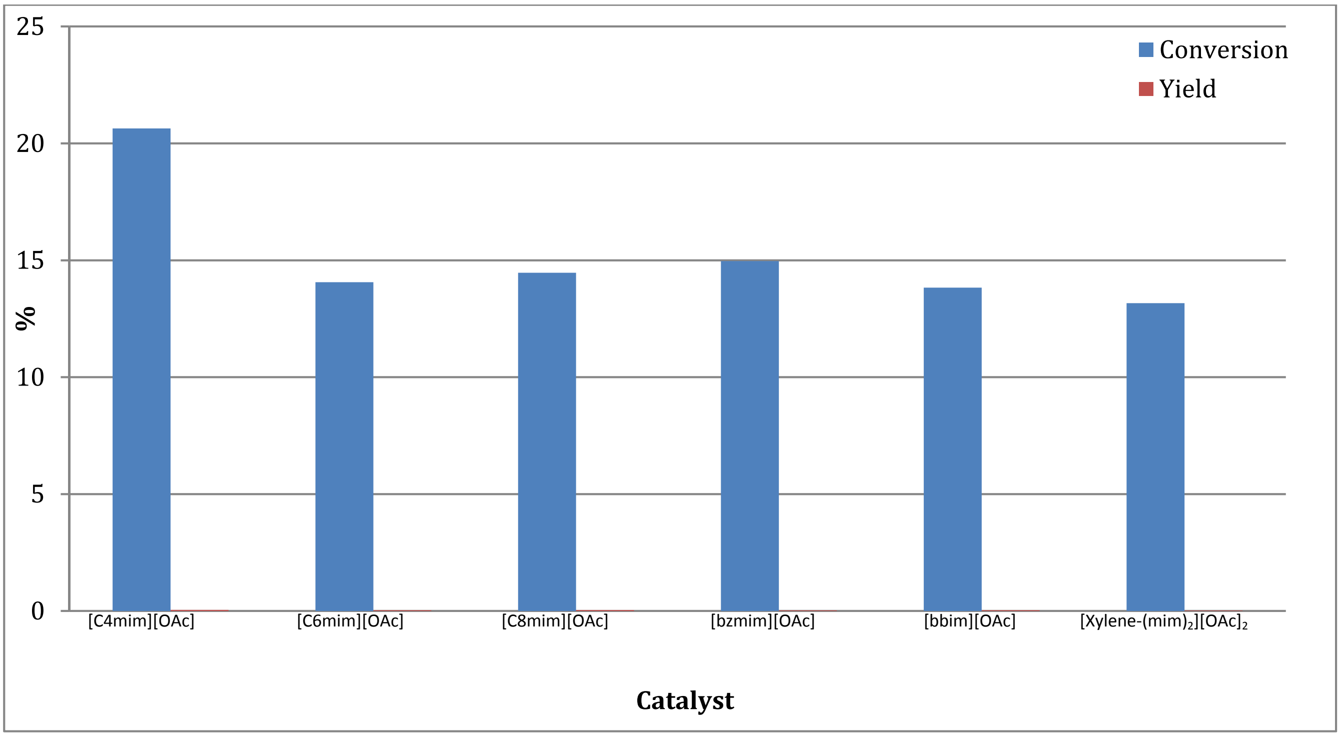

Fig. 1 Graph to compare conversion and yield for ionic liquid catalysts in the glycolysis of PET, reaction time 3 hours, temperature 180 °C, 0.01 mol catalyst (0.005 mol for [Xylene-(mim)$_2$][OAc]$_2$), 2 g PET and 20 g ethylene glycol.

The activity about the C2 position is of great interest, previously I have shown that with the halometallate ionic liquids having a methyl group in the C2 position rather than a proton reduced the conversion and yield to 0%. It was found that the capping the C2 position does not show any impact on the conversion, however these experiments also suffered from the errors seen in yield calculations so the impact may be seen more in the selectivity rather than the yield. A likely explanation is that the acetate anion is a sufficiently strong base to catalyse the reaction while the carbene formation reaction actually occurs at a higher temperature so the impact of the cation on the reaction is reduced. This is partially supported by figure 3, which shows that at 190 °C there is a very evident difference in catalytic activity between the catalysts.

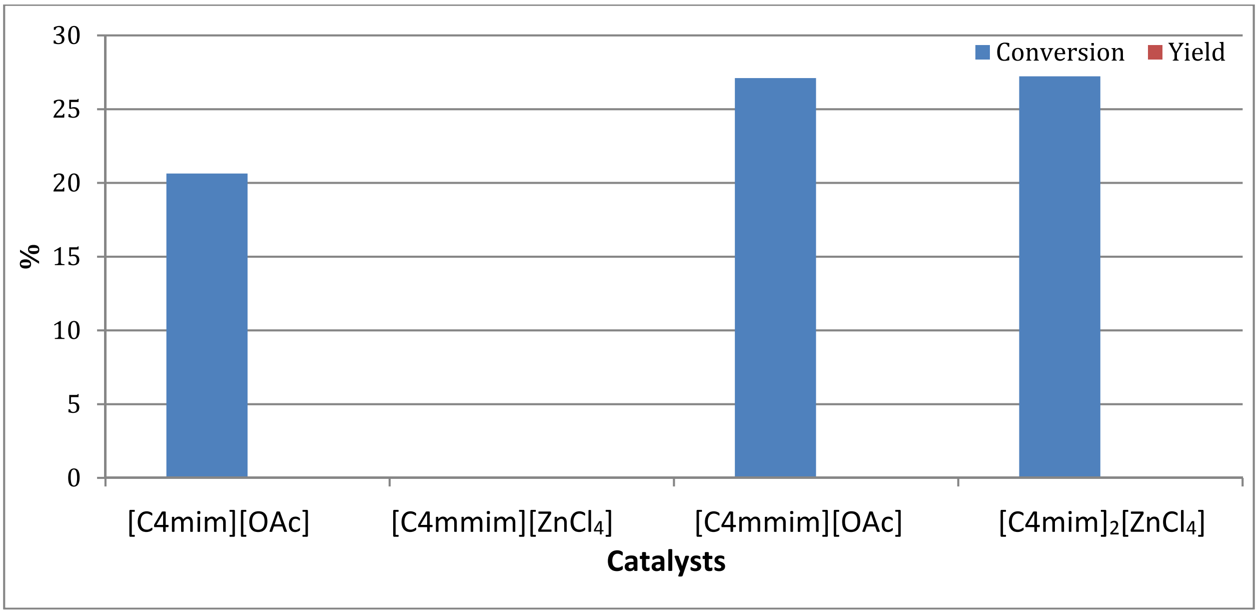

Fig. 2 Graph to compare conversion and yield for ionic liquid catalysts in the glycolysis of PET, reaction time 3 hours, temperature 180 °C, 0.01 mol catalyst, 2 g PET and 20 g ethylene glycol.

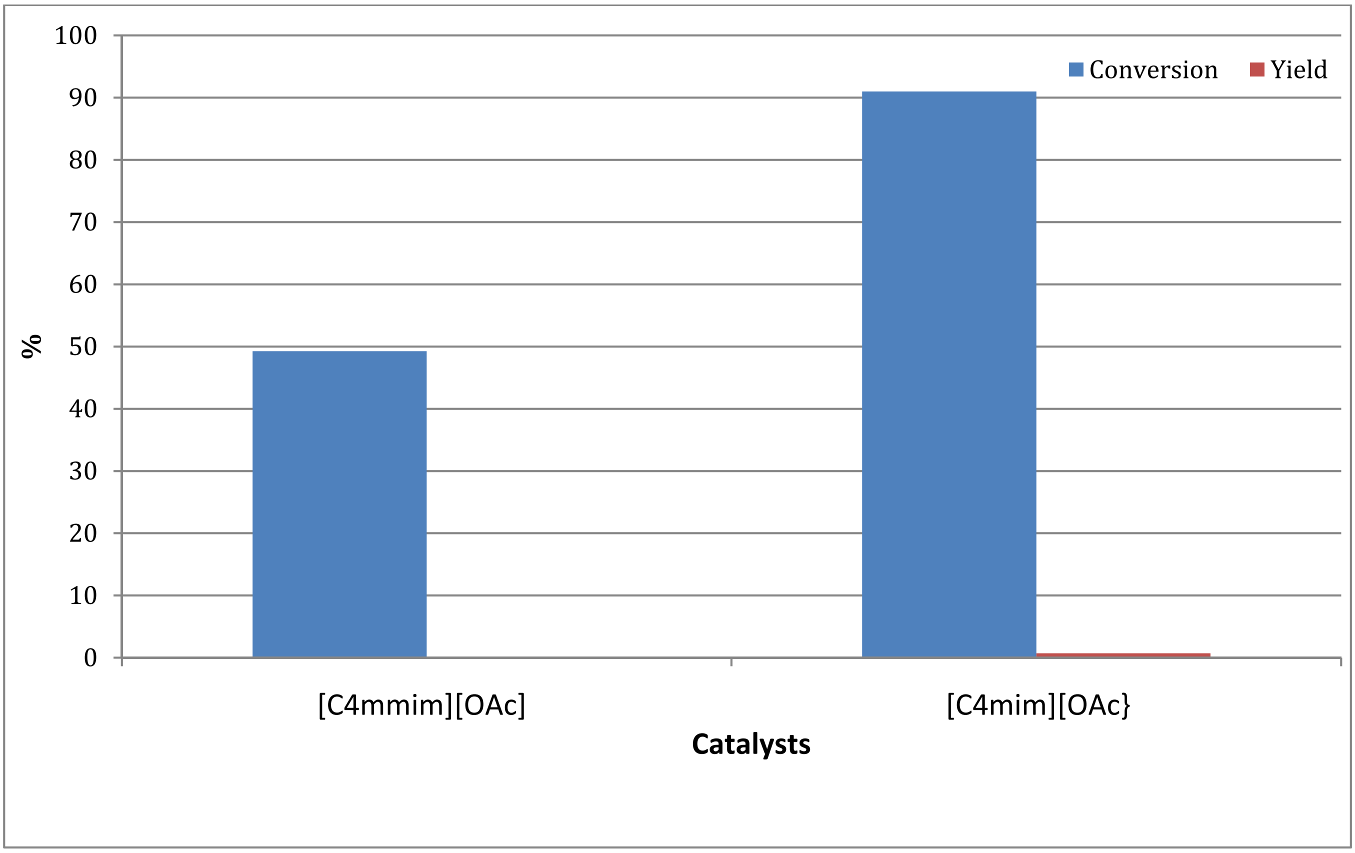

Fig. 3 Graph to compare conversion and yield for ionic liquid catalysts in the glycolysis of PET, reaction time 3 hours, temperature 190 °C, 0.01 mol catalyst, 2 g PET and 20 g ethylene glycol.

A set of experiments were performed in which [bmim][OAc] was used as a catalyst while the temperature was varied. From this it can be seen that increasing the temperature correlates to an increase in conversion. The conversion increases in an almost exponential manner, however the 195 °C result is much lower than the result at 190 °C and would be more suggestive of a linear relationship. Both these experiments are currently being repeated in order to confirm a exponential or a linear relationship.

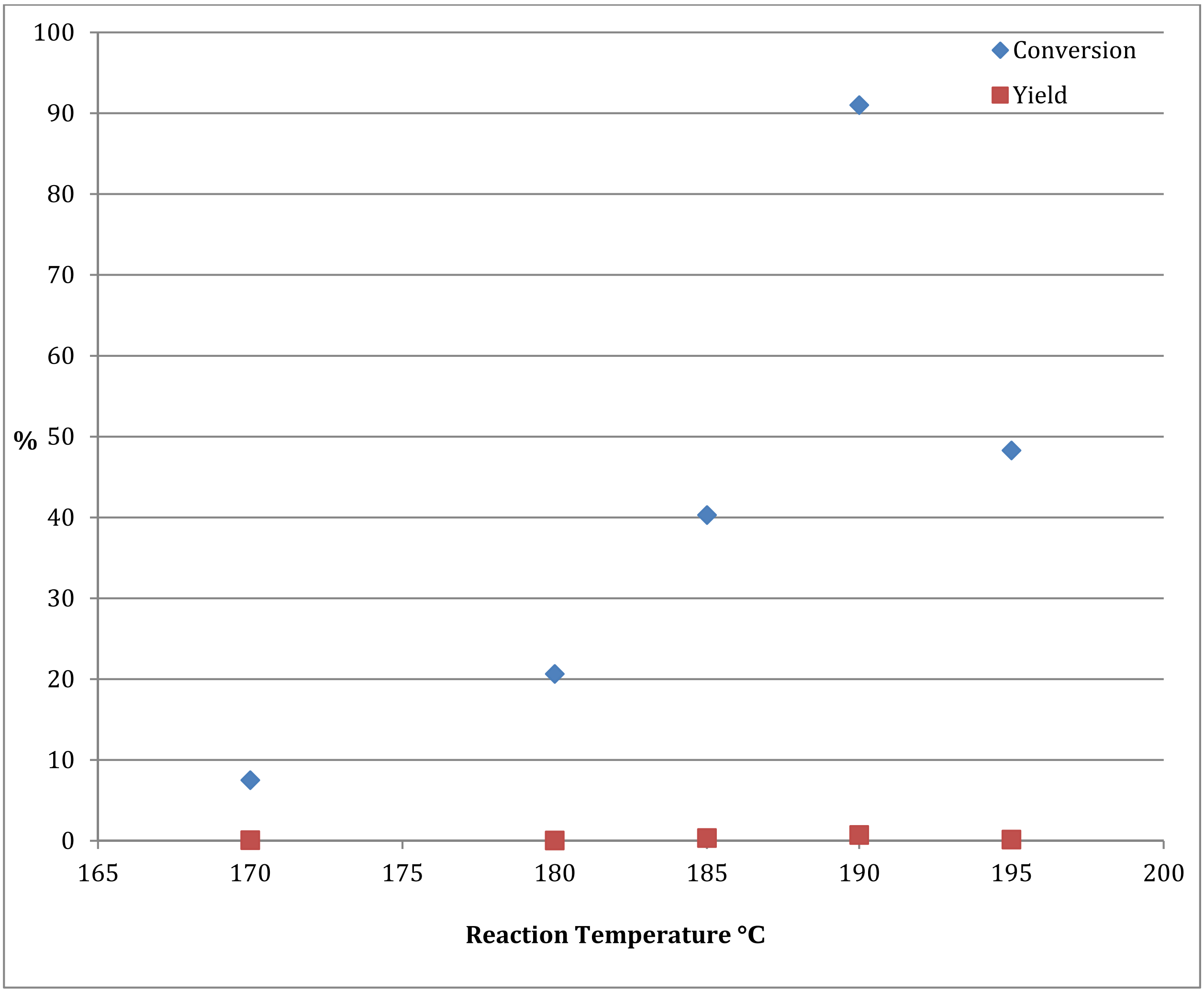

Fig. 4 Graph to compare conversion and yield for [bmim][OAc] as a catalyst in the glycolysis of PET, reaction time 3 hours, 0.01 mol [bmim][OAc], 2 g PET and 20 g ethylene glycol.

Using the neutron source at ISIS I investigated the solvation structure and interactions between a cholinium phosphate ionic liquid and the key components of the PET glycolysis reaction, namely BHET and EG in order to more fully understand the role of the ionic liquid as both a solvent and a catalyst for the glycolysis of PET. Cholinium phosphate was synthesised from choline chloride by reacting it with phosphoric acid and the evolution of HCl which was removed by a vacuum induced by a water aspirator. Due to concerns about the melting point of the ionic liquid and the potential handling of radioactive solids the ionic liquid was combined with EG in a ratio of 1:6. We had hoped to use both hydrogenous and deuterated cholinium phosphate, however we were unable to get the appropriate starting materials for the deuterated cholinium phosphate on time. As such we were only able to study hydrogenous cholinium phosphate with hydrogenous, deuterated and a 1:1 hydrogenous to deuterated mixture of EG as solvents for three isotopomers of BHET (all deuterated, all protiated and ring-deuterated). Fully deuterated BHET was synthesised by the ISIS Deuteration Facility from deuterated para-xylene by oxidation to terephthalic acid followed by controlled esterification with deuterated ethylene glycol. Partially (ring) deuterated BHET was prepared in a corresponding manner from deuterated terephthalic acid with hydrogenous glycerol.

Conclusions and future work

Unfortunately most of the work performed in this time period has errors in the analysis of the yield, this is being corrected currently. The data acquired at ISIS is currently being modelled and the samples used are being tested to determine accurate composition information and the density at 90 °C to aid in the modelling process. Additional time at ISIS at some point early next year is incredibly likely and will round out the raw data by providing an additional contrast using deuterated cholinium phosphate, which will improve the modelling. Work is continuing on the production and testing of 4,5-dichloro-1,3-dibutylimidazolium acetate, 4,5-dichloro-1,3-dimethylimidazolium acetate and 4,5-dichloro-1-butyl-3-methylimidazolium acetate as catalysts for the glycolysis of PET. Additional 'gemini' ionic liquids have been or are being created, methylimidazolium ionic liquids using pentyl, ethyl and a xylene linkers have been made, the use of dichloroimidazoles and alkylimidazoles are being considered at this time, these decisions will be made based on the results from the dialkyldichloroimidazolium acetate ionic liquid experiments. A longer term aim is the testing of other PET sources and the use of coloured PET.

QUILL Quarterly Report

May - October 2018

Name:	**Dr. Natalia V. Plechkova**		
Supervisor(s):	Dr. Peter Nockemann + Dr. Gosia Swadźba-Kwaśny + Dr. John Holbrey + Dr. Stephen Glover		
Position:	PDRA		
Start date:	1st June 2018	End date:	31st October 2018
Funding body:	CASE + Wrightbus + Horiba Mira Ltd		

Evaluation of Solid State Battery Electrolytes for Stationary Energy Storage and Electric Vehicles

Background

The constantly increasing demand for advanced energy storage devices in portable electronics, electric vehicles and large scale power grids has plummeted research on lithium and sodium batteries over the past decade. In order to improve their electrochemical performance and enhance the service safety, the development of advanced electrode, electrolyte, and auxiliary materials is essential. Ionic liquids are characterised by many unique properties such as ultralow volatility, high ionic conductivity, good thermal stability, low flammability, a wide electrochemical window, and tunable polarity and basicity/acidity. These properties create the possibilities of designing batteries with excellent safety, high energy/power density and long-term stability, and also provide better ways to synthesise known materials. Ionic liquid-derived materials, such as poly(ionic liquids), ionogels and ionic liquid-tethered nanoparticles, retain most of the characteristics of ionic liquids while being endowed with other favourable features, and thus they have received a great deal of attention as well. Their unique characteristics enable them to serve as advanced resources, medium, or ingredient for almost all the components of batteries, including electrodes, liquid electrolytes, solid electrolytes, artificial solid–electrolyte interphases and current collectors.

An ideal electrolyte would display the following characteristics:
Low Cost
Non-toxic
Non-flammable
Non-reactivity with other cell components
Wide electrochemical stability window, 0 to > 5 V
Wide temperature stability range, -20 + 50 °C
Excellent ionic conductivity to enable rapid ion transport
Negligible electronic conductivity to minimise self-discharge
Stability over several year battery life

Objective of this work

The objective of this project is to develop novel electrolytes and electrolyte additives for Na batteries with the particular focus on solid-state electrolytes in order to enable high safety and high performance batteries

Progress to date

Two directions were pursued during this project:

1) Preparation of electrolytes based on derivatives of glycerol. Glycerol is generally obtained from plant and animal sources where it occurs as triglycerides. Triglycerides are esters of glycerol with long-chain carboxylic acids. The hydrolysis, saponification, or transesterification of these triglycerides produces both glycerol and the fatty acid derivative, therefore, glycerol is a side product of biodiesel production. Glycerol from triglycerides is produced on a large scale, but the crude product is of variable quality, with a low selling price of as low as 2-5 US cents per kilogram in 2011.[1] It can be purified, but the process is expensive. Some glycerol is burned for energy, but its heat value is low. Crude glycerol from the hydrolysis of triglycerides can be purified by treatment with activated carbon to remove organic impurities, alkali to remove unreacted glycerol esters, and ion exchange to remove salts. High purity glycerol (> 99.5%) is obtained by multi-step distillation; vacuum is helpful due to the high boiling point of glycerol (290 °C).

   Glycerol is a colourless and odourless liquid that is sweet-tasting and non-toxic.

   The issue with glycerol itself is that it is viscous and easily oxidising (unstable). Therefore, it was decided to modify its structure.

   By using the procedure suggested by Lemaire and coworkers,[2] 1,2,3-trimethoxypropane (trimethoxy-derivative of glycerol with the viscosity similar to water and boiling point of 90 °C under moderate vacuum) was prepared and characterised by ^{1}H NMR spectroscopy:

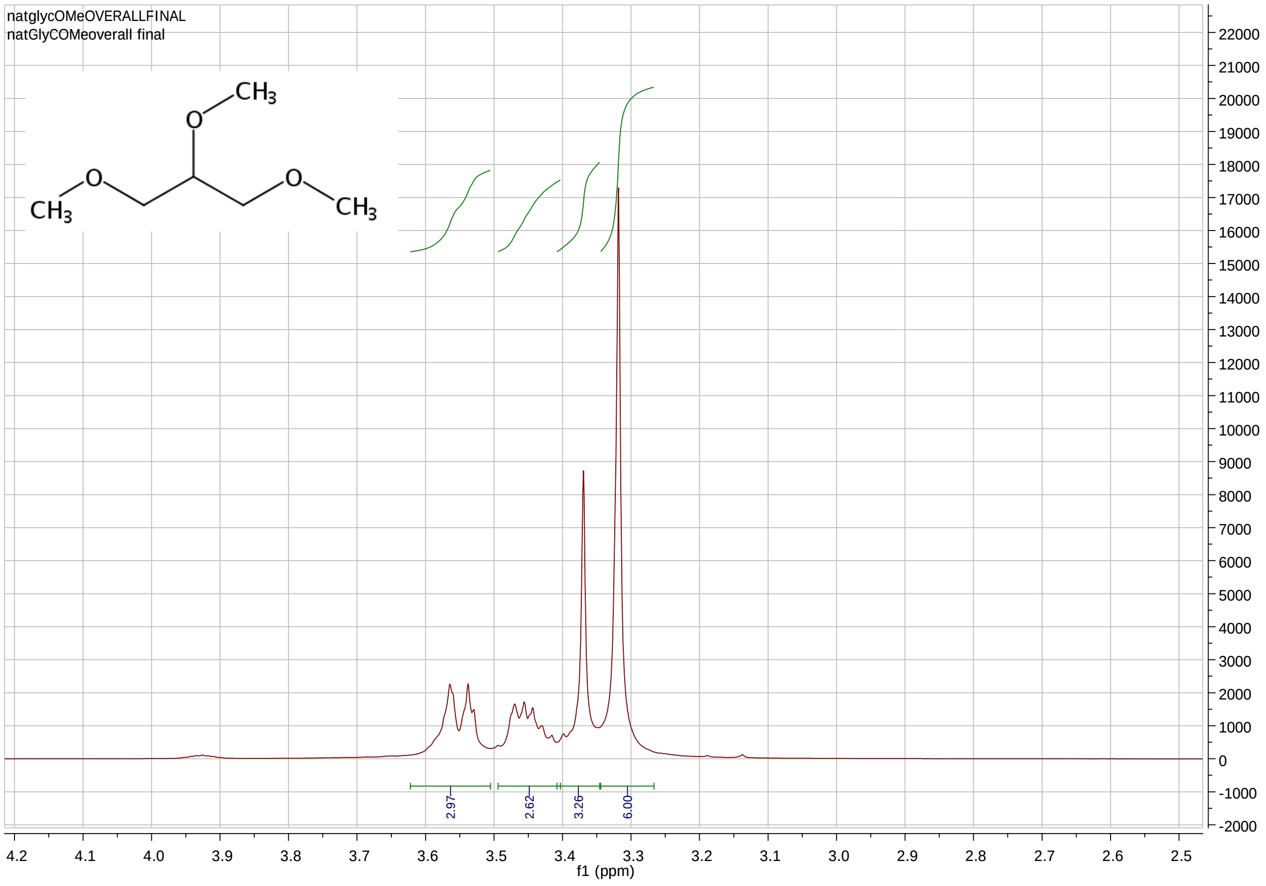

1) Preparation of chloroethoxy-precursors from commercially available glycol ethers to be used as alkylating agents for various bases in order to prepare ionic liquids with low viscosity, as it is well known that the presence of ethoxy groups in the alkyl chain(s) of ionic liquids leads to the reduction of viscosities.[3]

For instance, 2-(2-methoxyethoxy)ethanol was prepared and characterised by ^{1}H NMR and ^{13}C NMR spectroscopy:

Synthesis of 1-chloro-2-(2-methoxyethoxy)ethane (adapted from Dr. Ferrero Vallana's Thesis)

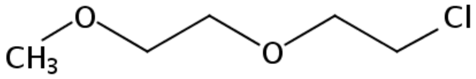

A solution of 2-(2-methoxyethoxy)ethanol (50.00g, 0.416 mol) and pyridine (32.92g, 0.416 mol) in dichloromethane (200 cm^{3}) was added to a three-necked round-bottom flask fitted with a condenser under a dinitrogen flush. A solution of thionyl chloride (49.51g, 0.416 mol) in dichloromethane (30 cm^{3}) was then added dropwise over a period of 2 h to the stirred mixture via a pressure equalising funnel at room temperature. Once the addition was complete, the reaction was heated under reflux for 12 h. The reaction mixture was then cooled to room temperature and washed with saturated aqueous sodium hydrogencarbonate (200cm^{3}), and then magnesium sulfate (5 g) was added to the organic phase. This mixture was then filtered and the filtrate was concentrated using a rotavaporator *in vacuo* at 40 °C to leave a pale yellow liquid. A Kugelrohr distillation of the product at 100 °C *in vacuo* produced a colourless liquid (54.86 g; 95% yield), which was used immediately for the preparation of ethoxy-functionalised ionic liquids.

Similarly, 1-(2-chloroethoxy)-2-(2-methoxyethoxy)ethane

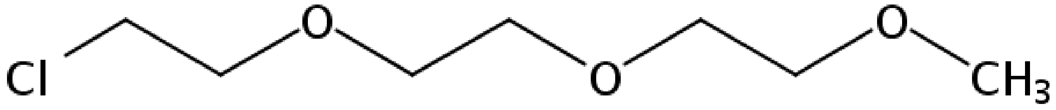

and

13-chloro-2,5,8,11-Tetraoxatridecane

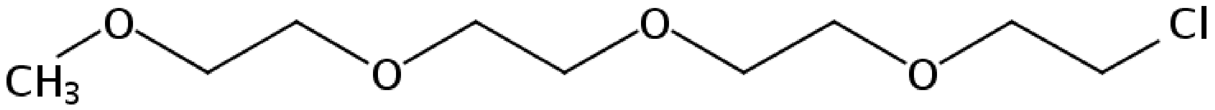

Were prepared.

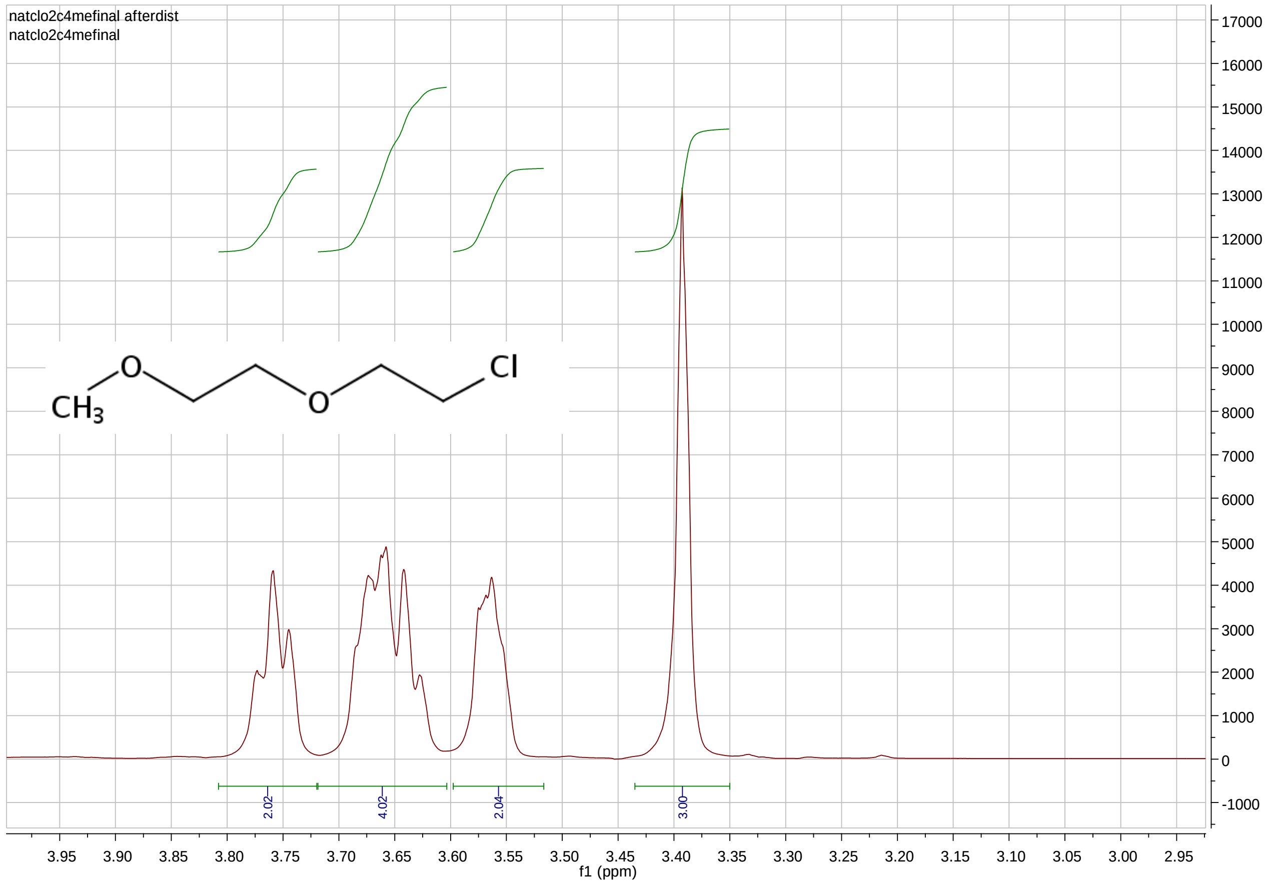
natclo2c4mefinal afterdist
natclo2c4mefinal
CH3
O
O
Cl
2.02
4.02
2.04
3.00
17000
16000
15000
14000
13000
12000
11000
10000
9000
8000
7000
6000
5000
4000
3000
2000
1000
0
-1000
3.95 3.90 3.85 3.80 3.75 3.70 3.65 3.60 3.55 3.50 3.45 3.40 3.35 3.30 3.25 3.20 3.15 3.10 3.05 3.00 2.95
f1 (ppm)

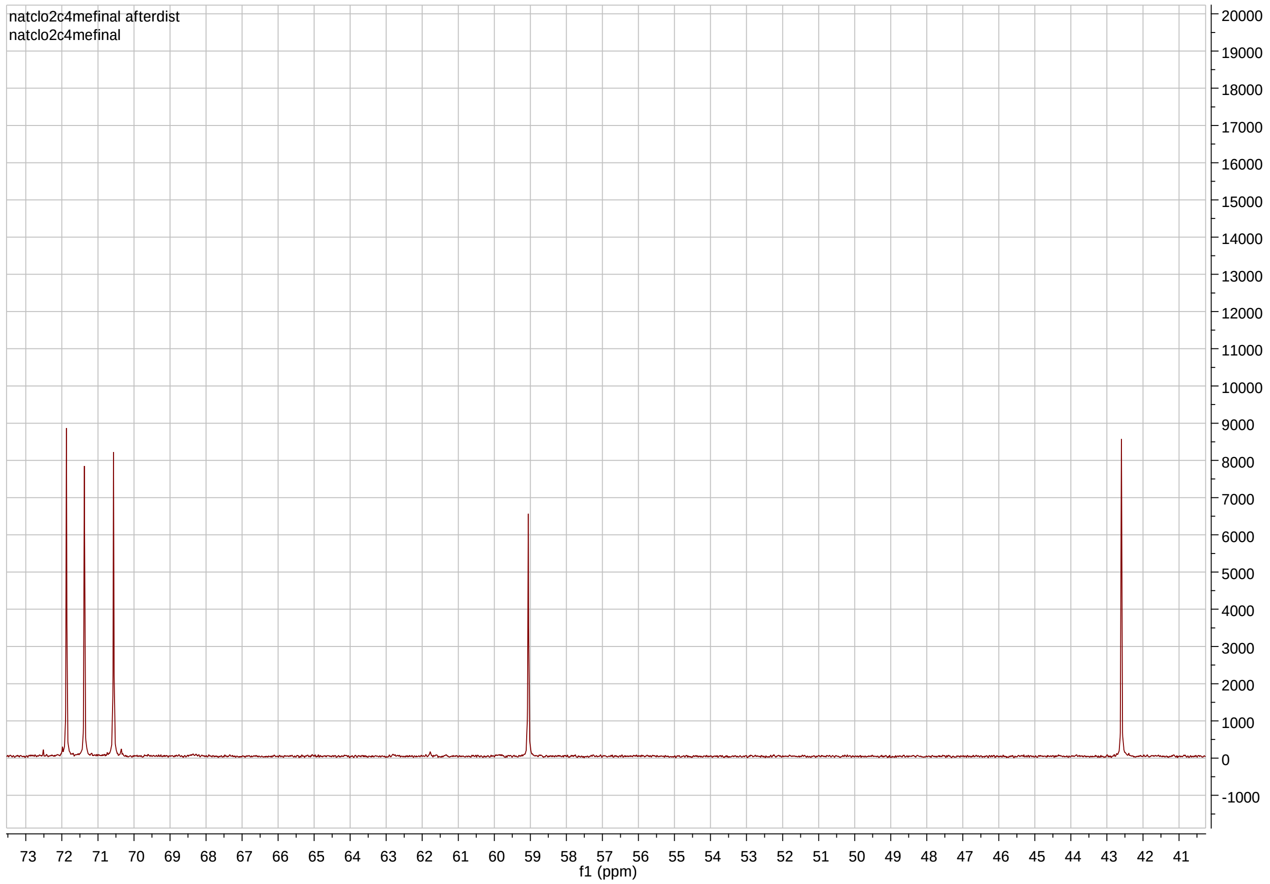
natclo2c4mefinal afterdist
natclo2c4mefinal
20000
19000
18000
17000
16000
15000
14000
13000
12000
11000
10000
9000
8000
7000
6000
5000
4000
3000
2000
1000
0
-1000
73 72 71 70 69 68 67 66 65 64 63 62 61 60 59 58 57 56 55 54 53 52 51 50 49 48 47 46 45 44 43 42 41
f1 (ppm)

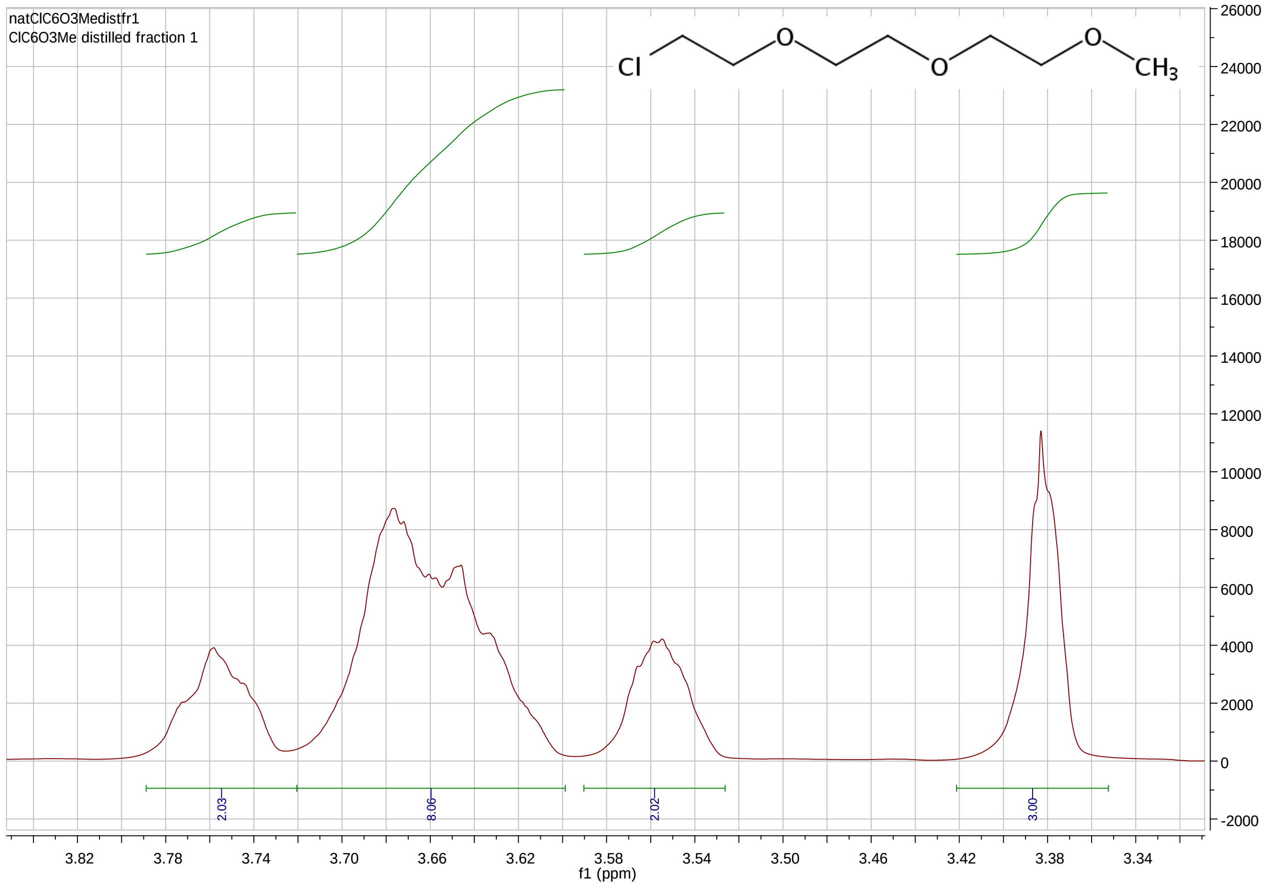

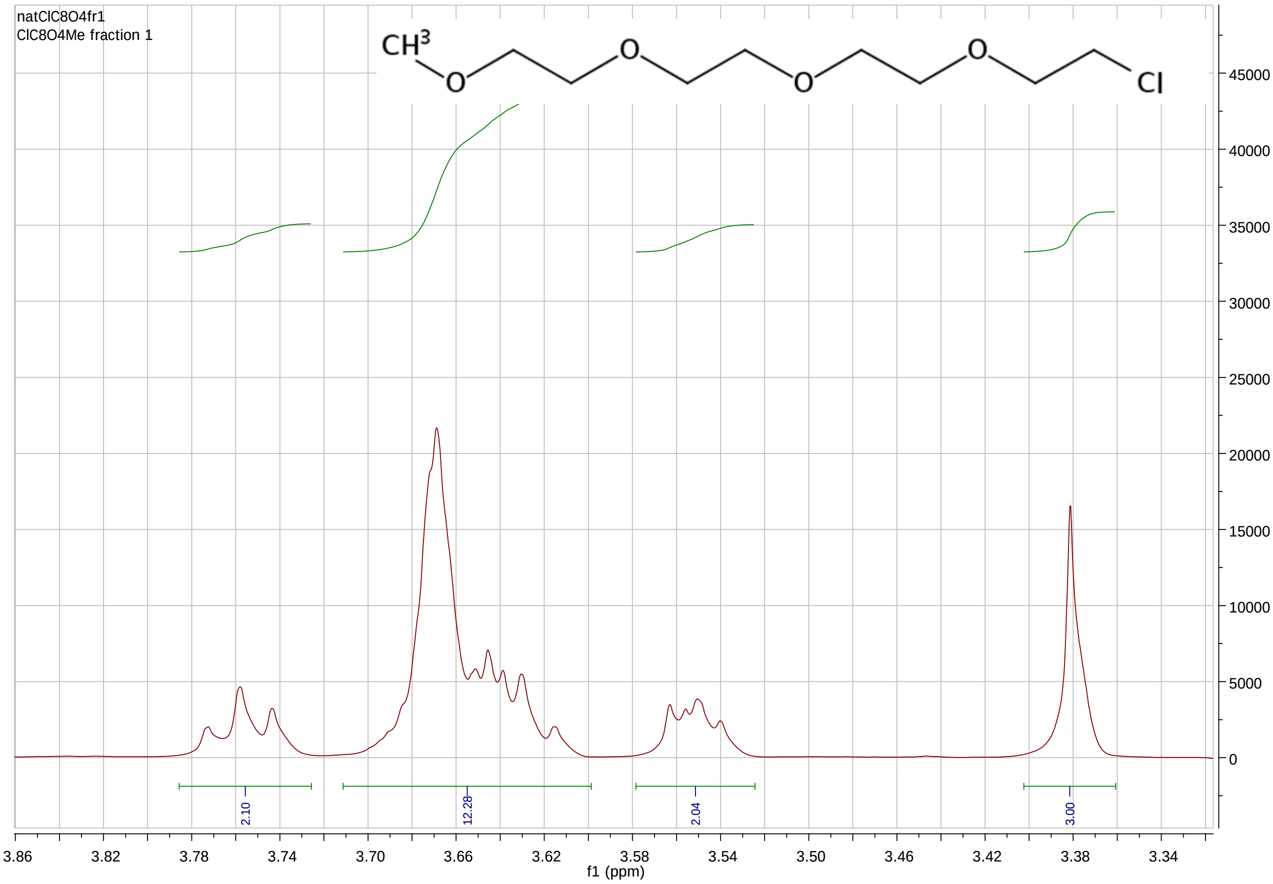

For electrochemical applications, information on physical/electrochemical properties of ILs, such as viscosity, conductivity, electrochemical stability, and the diffusion coefficient of electroactive species in ionic liquids is important.[4,5] As a means of increasing ionic conductivity, imidazolium-based ionic liquids have been well studied because of their superior electrochemical properties, for instance wide electrochemical window and high conductivity.[6] However, the efforts to use these ILs as electrolytes for electrochemistry were unsuccessful due to their low cathodic stability caused by the presence of acidic C-2 hydrogen atom as well as to the migration of imidazolium cations along with activated metal ions. Some improvement on the electrochemical stability was achieved by substituting C-2 hydrogen with an alkyl group.[7] The cathodic stability of the ionic liquids can be enhanced by replacing imidazolium-based cations with pyrrolidinium or piperidinium-based cations .[8] Additionally, considerable interest has been revived in the ILs based on the ether- or hydroxyl functionalized oniums (*e.g.* ammonium[9] and phosphonium[10]) with various anions. The possibility of introducing an ether group into one of the side alkyl chains (e.g. $CH_3OCH_2CH_2$ or CH_3OCH_2) of onium has been widely used to realize low-melting, and low viscosity ionic liquids.[9] The structure effects on their various properties are needed to be understood for potential applications in electrolyte materials.

Preparation of methylpyrrolidinium epoxy- chloride ionic liquids

$[C_{CH2CH2OCH2CH2OMe}\ m]pyrr\ Cl = [C_{20201}mpyrr]Cl$

N-methylpyrrolidine was mixed with 1 equivalent of the ethoxy chloride at 60 °C in acetonitrile. $[C_{CH2CH2OCH2CH2OMe}\ mpyrr]Cl$, (yield 96%). This mixture was stirred for 1 week. Light yellow viscous liquids were prepared. These liquids were washed with diethyl ether 3 times to remove any unreacted media.

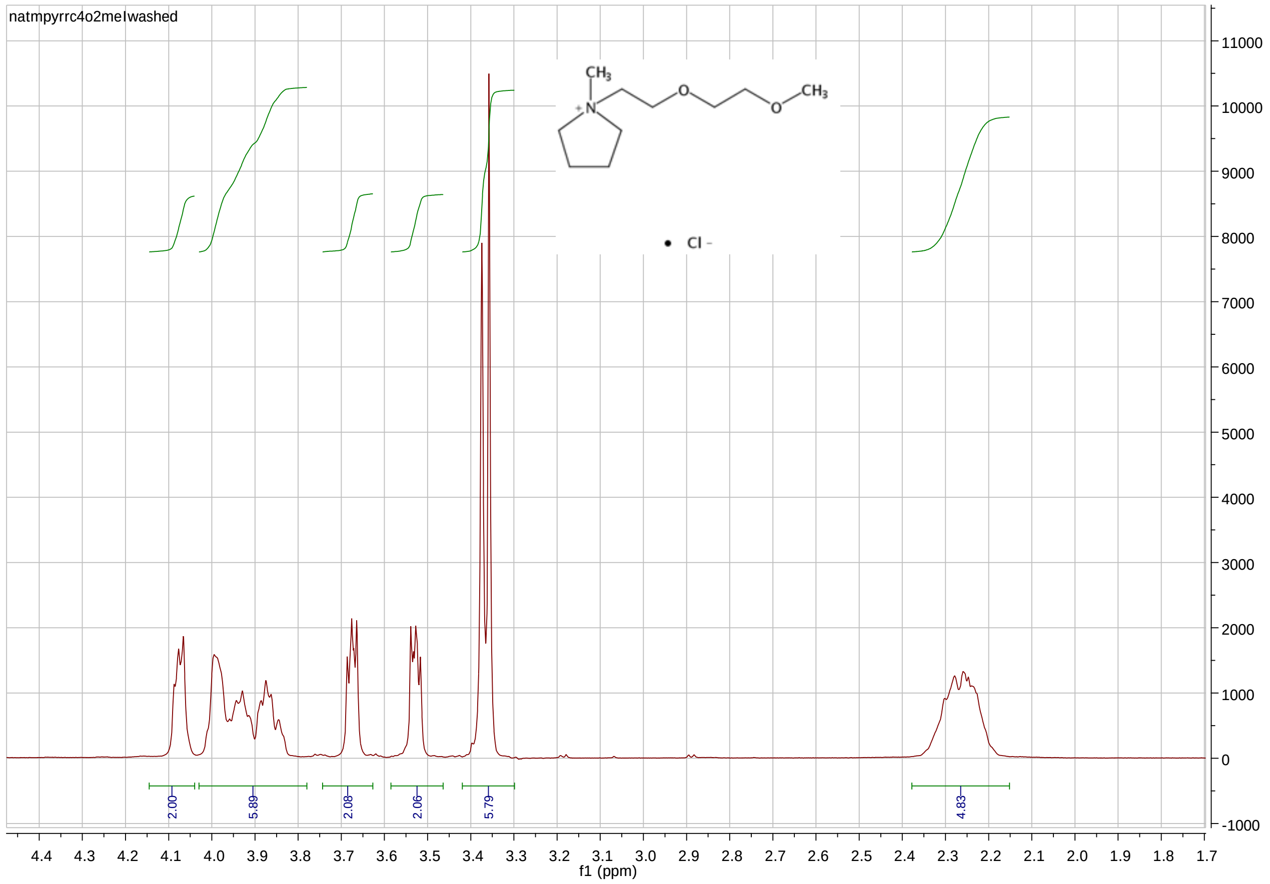

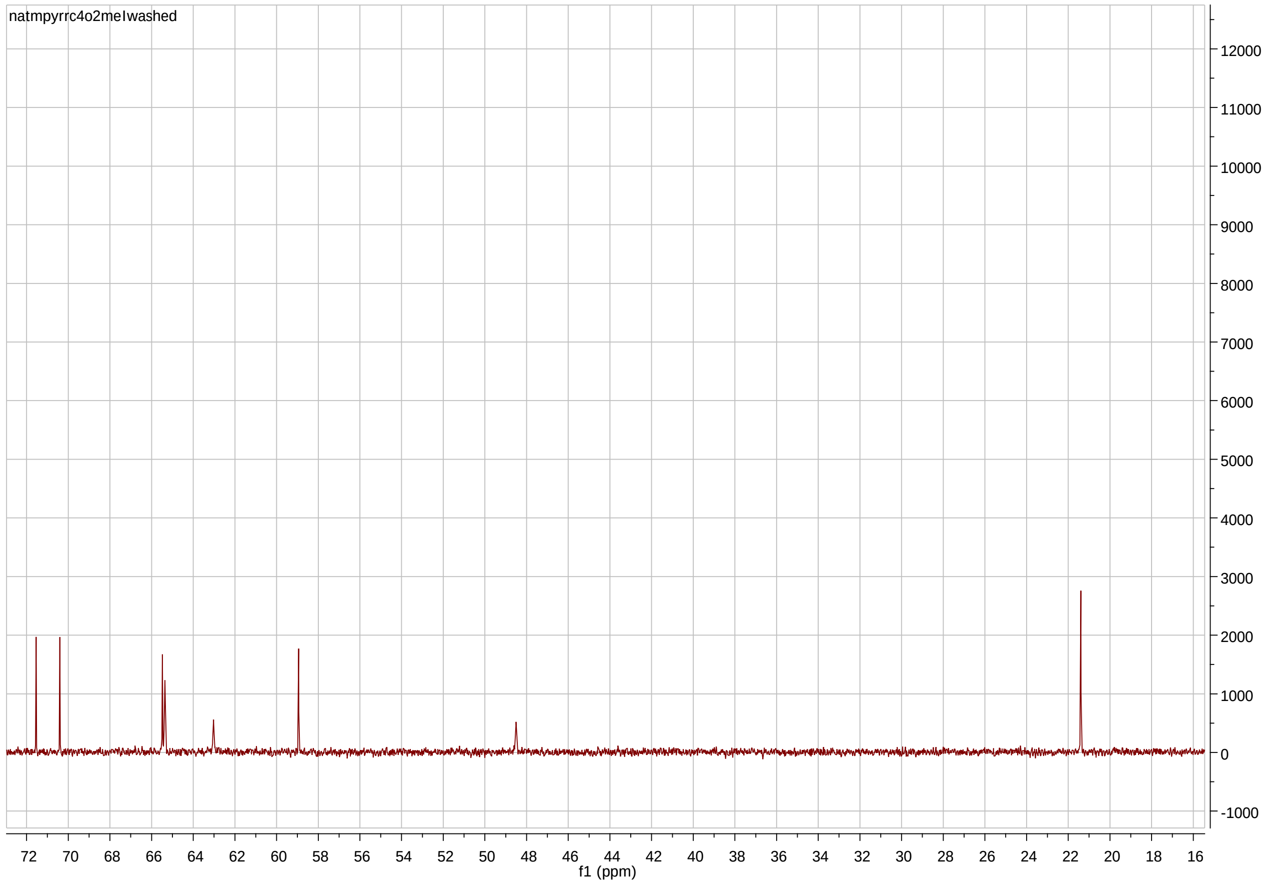

Preparation of phosphonium epoxy- halide ionic liquids.

There was a dilemma in the preparation of phosphonium $[P_{6\,6\,6\,x}]^+$ ionic liquids. From one side, high temperatures (over 100 °C) are needed to ensure completion of reaction; from the other side, when high temperatures are applied, several alkylation products are formed (for instance, ^{31}P NMR spectrum displays that). Therefore, it was not possible to synthesise ethoxy chloride ionic liquids using trihexylphosphine and ethoxy chlorides. As iodides are more reactive than chlorides, ethoxy chlorides were converted to ethoxy iodides (classic Finkelstein reaction).

Synthesis of 1-iodo-2-(2-methoxyethoxy)ethane

1-chloro-2-(2-methoxyethoxy)ethane (1mol) was reacted with sodium iodide (1.05mol) with 20 ml dry acetone (dried with $MgSO_4$ overnight) in a screw capped tube overnight at 60 °C and stirring. Next morning, a precipitate of NaCl was formed when the reaction was stopped stirring. This precipitate was removed by filtration. Acetone was removed by evaporation on a rotavaporator. Dichloromethane was added to the product and more NaCl precipitated which was removed by filtration. Dichloromethane was removed by filtration and the formed yellow liquid was dried *in vacuo* at 70 °C.

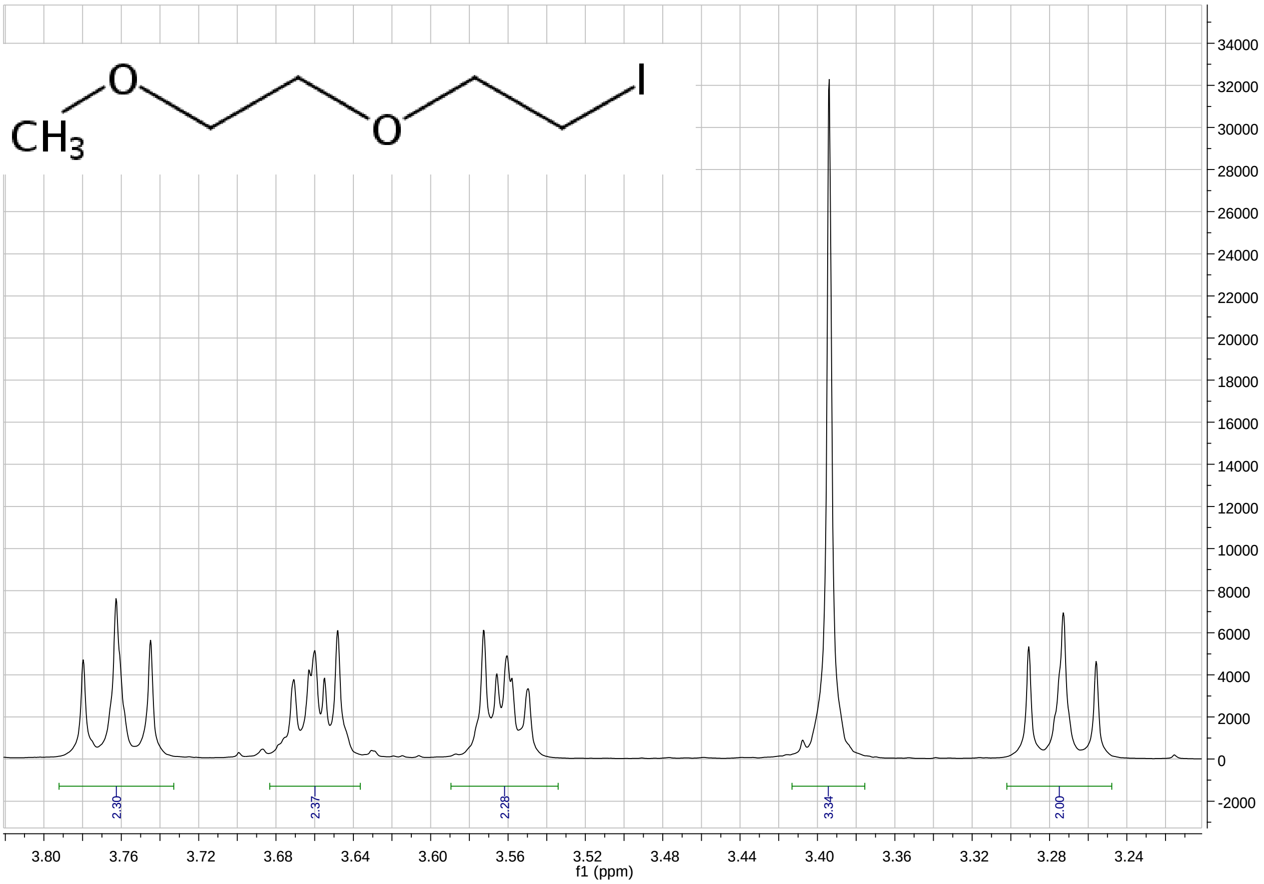
CH3
O
O
I
34000
32000
30000
28000
26000
24000
22000
20000
18000
16000
14000
12000
10000
8000
6000
4000
2000
0
-2000
2.30
2.37
2.28
3.34
2.00
3.80
3.76
3.72
3.68
3.64
3.60
3.56
3.52
3.48
3.44
3.40
3.36
3.32
3.28
3.24
f1 (ppm)

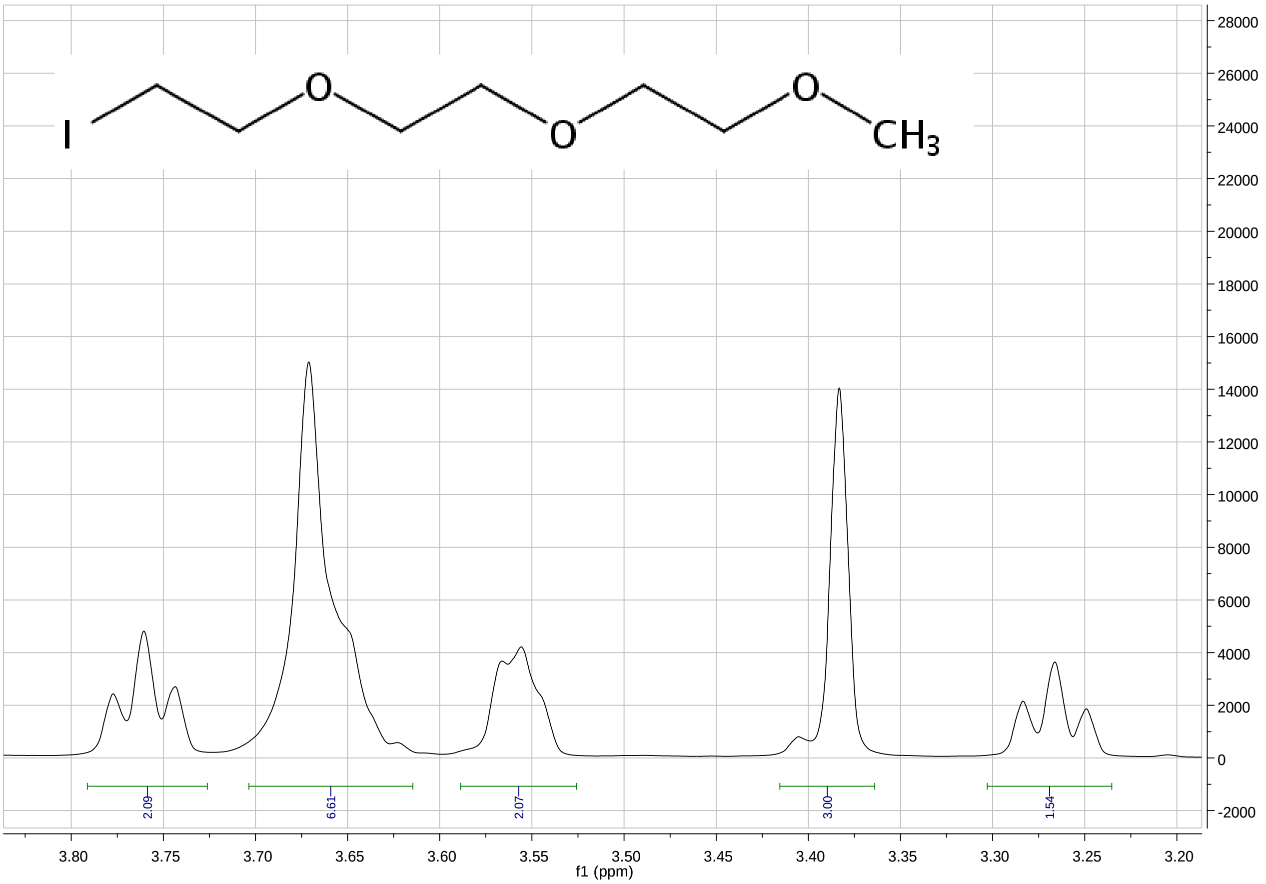
I
O
O
O
CH3
2.09
6.61
2.07
3.00
1.54
28000
26000
24000
22000
20000
18000
16000
14000
12000
10000
8000
6000
4000
2000
0
-2000
3.80
3.75
3.70
3.65
3.60
3.55
3.50
3.45
3.40
3.35
3.30
3.25
3.20
f1 (ppm)

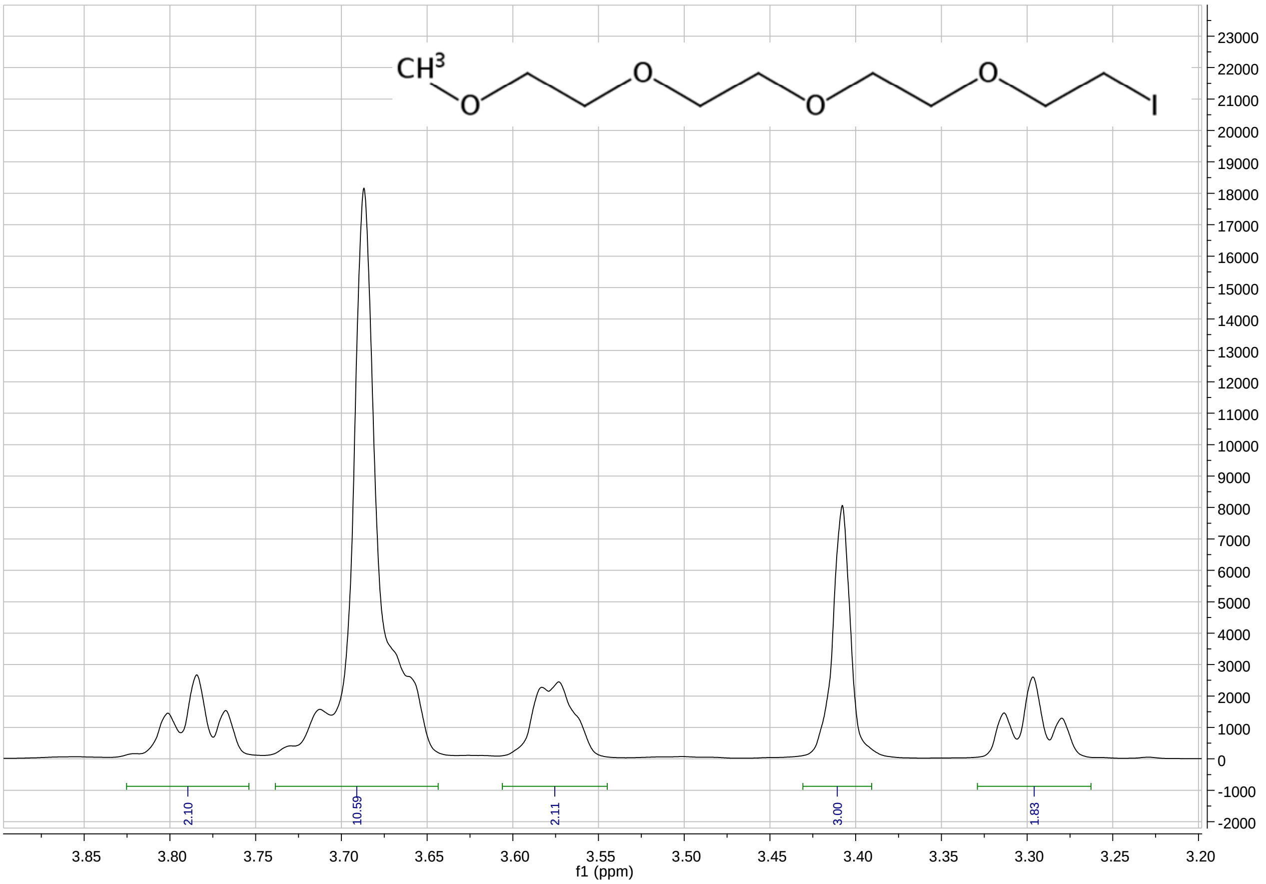
CH3
O
O
O
O
I
2.10
10.59
2.11
3.00
1.83
23000
22000
21000
20000
19000
18000
17000
16000
15000
14000
13000
12000
11000
10000
9000
8000
7000
6000
5000
4000
3000
2000
1000
0
-1000
-2000
3.85
3.80
3.75
3.70
3.65
3.60
3.55
3.50
3.45
3.40
3.35
3.30
3.25
3.20
f1 (ppm)

Synthesis of $[P_{6\ 6\ 6\ CH2CH2OCH2CH2OMe}]I = [P_{6\ 6\ 6\ 20201}]I$

Trihexylphosphine (1.0747g) was reacted with 1-iodo-2-(2-methoxyethoxy)ethane (0.863g) in dry acetonitrile at 70 °C for 1 week. After the reaction, acetonitrile was removed using was removed by evaporation on a rotavaporator. To remove the residues of both the phosphine and ethoxy iodide, the compound was washed with diethyl ether 3 times. The product was dried by evaporation on a rotavaporator and *in vacuo* to produce a viscous yellow liquid.

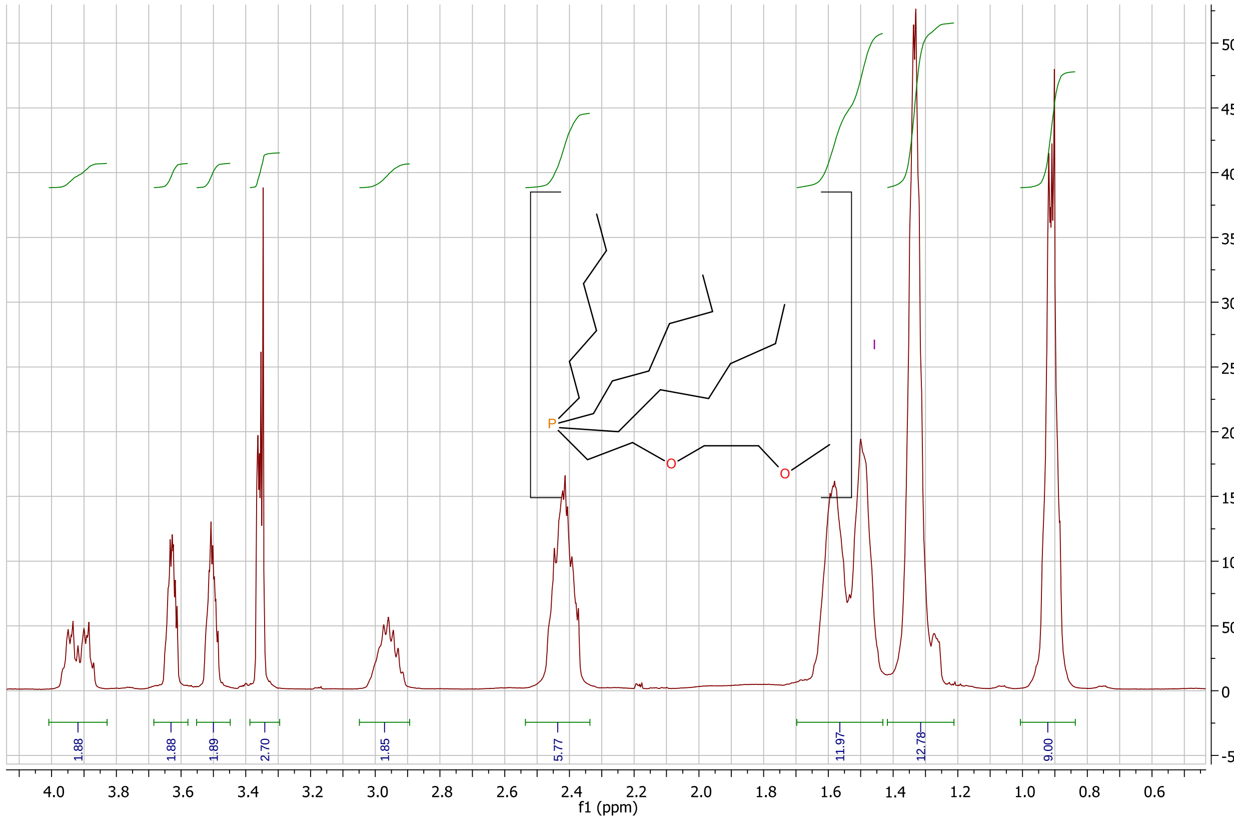

P
O
O
O
I

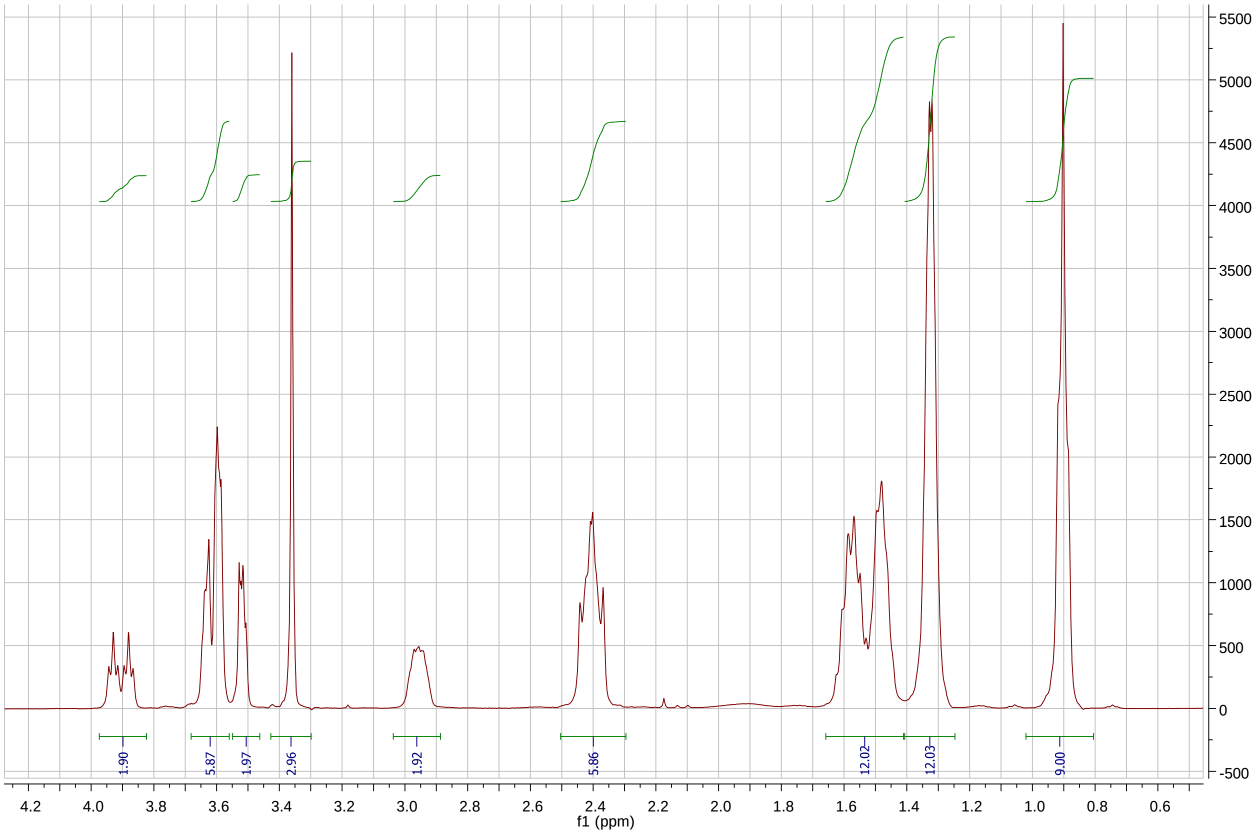

1.90
5.87
1.97
2.96
1.92
5.86
12.02
12.03
9.00
4.2
4.0
3.8
3.6
3.4
3.2
3.0
2.8
2.6
2.4
2.2
2.0
1.8
1.6
1.4
1.2
1.0
0.8
0.6
f1 (ppm)
5500
5000
4500
4000
3500
3000
2500
2000
1500
1000
500
0
-500

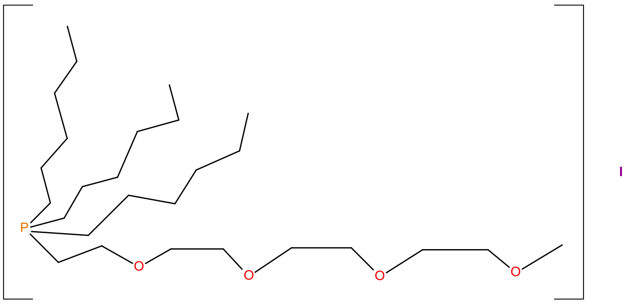

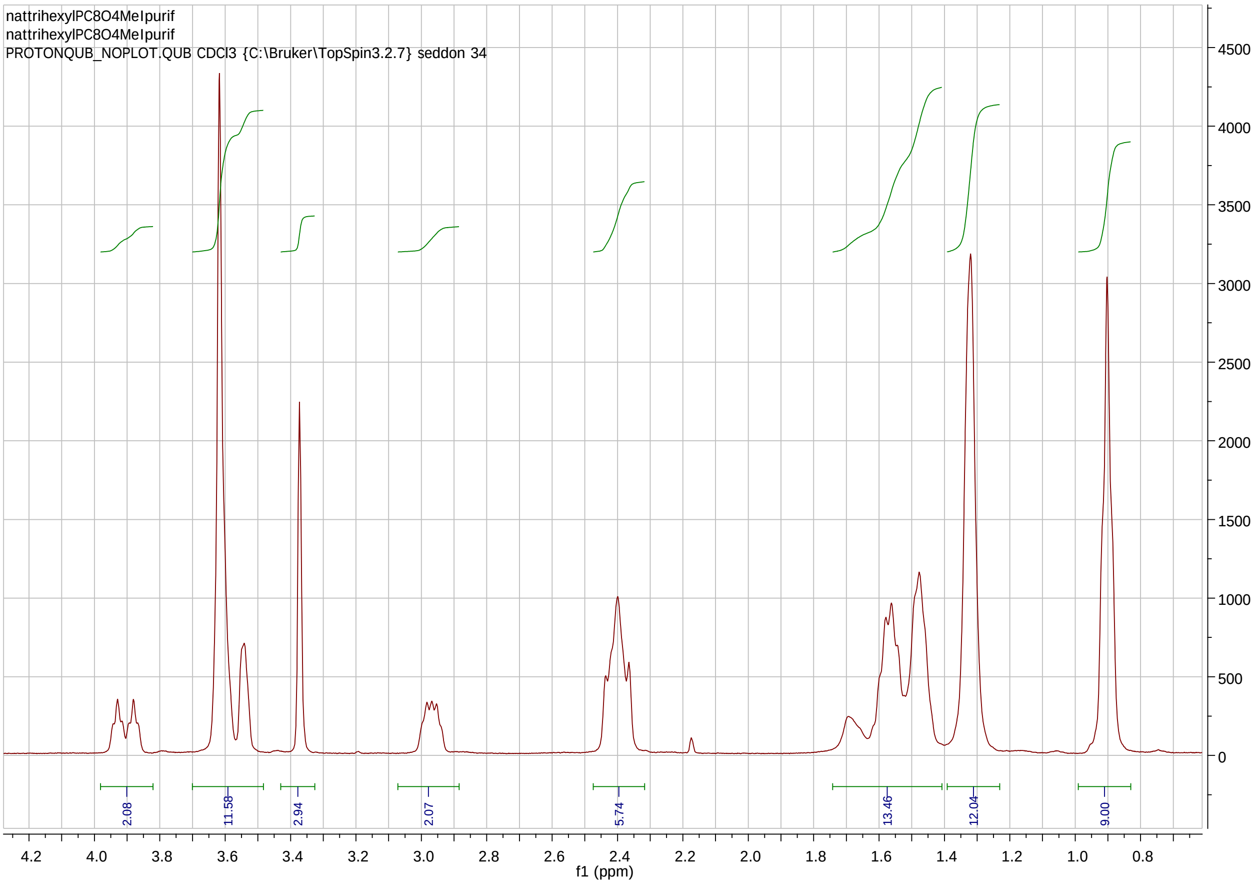

These can be applied as liquid low-viscosity electrolytes or polymerised into solid-state electrolytes.

Conclusions and future work

Ionic liquids and related materials will be especially advantageous in processes where their unique characteristics are essential, such as the operation of batteries at high temperatures, high voltages, or in open systems. More stable, less viscous and less expensive ionic liquids are in great need of development, and further attention should be directed to the science of the effect of ionic liquid-based materials on the battery performance. On the other hand, in order to improve the economic feasibility and overcome some drawbacks of ionic liquids, the hybrids of ionic liquid-based materials with conventional ‘cheap’ materials are more promising than the pure materials. The ionic liquid–molecular solvent hybrid electrolytes, the ionogels, and the ionic liquid-derived carbon coatings on support materials are all important strategies to further improve ionic liquid usage. The next step of this project is to prepare ionic liquid with fluorinated anions and also to characterise and prepare glycerol-derived electrolytes. Additionally, several epoxy chains can be incorporated in ionic liquid structures, as opposed to one, to give extra decrease in viscosities and for structural comparison.

References

(1) Kong, P. S.; Aroua, M. K.; Daud, W. Conversion of crude and pure glycerol into derivatives: A feasibility evaluation. *Renewable & Sustainable Energy Reviews* **2016,** *63*, 533.

(2) Sutter, M.; Pehlivan, L.; Lafon, R.; Dayoub, W.; Raoul, Y.; Metay, E.; Lemaire, M. 1,2,3-Trimethoxypropane, a glycerol-based solvent with low toxicity: new utilization for the reduction of nitrile, nitro, ester, and acid functional groups with TMDS and a metal catalyst. *Green Chemistry* **2013,** *15* (11), 3020.

(3) Harris, K. R.; Makino, T.; Kanakubo, M. Viscosity scaling of the self-diffusion and velocity cross-correlation coefficients of two functionalised ionic liquids and of their non-functionalized analogues. *Phys. Chem. Chem. Phys.* **2014,** *16* (19), 9161.

(4) Simka, W.; Puszczyk, D.; Nawrat, G. Electrodeposition of metals from non-aqueous solutions. *Electrochimica Acta* **2009,** *54* (23), 5307.

(5) Vorotyntsev, M. A.; Zinovyeva, V. A.; Picquet, M. Diffusional transport in ionic liquids: Stokes-Einstein relation or "sliding sphere" model? Ferrocene (Fc) in imidazolium liquids. *Electrochimica Acta* **2010,** *55* (18), 5063.

(6) Liu, K.; Zhou, Y. X.; Han, H. B.; Zhou, S. S.; Feng, W. F.; Nie, J.; Li, H.; Huang, X. J.; Armand, M.; Zhou, Z. B. Ionic liquids based on (fluorosulfonyl)(pentafluoroethanesulfonyl)imide with various oniums. *Electrochimica Acta* **2010,** *55* (23), 7145.

(7) Nguyen, D. Q.; Hwang, J.; Lee, J. S.; Kim, H.; Lee, H.; Cheong, M.; Lee, B.; Kim, H. S. Multi-functional zwitterionic compounds as additives for lithium battery electrolytes. *Electrochemistry Communications* **2007,** *9* (1), 109.

(8) Wu, T. Y.; Su, S. G.; Gung, S. T.; Lin, M. W.; Lin, Y. C.; Lai, C. A.; Sun, I. W. Ionic liquids containing an alkyl sulfate group as potential electrolytes. *Electrochimica Acta* **2010,** *55* (15), 4475.

(9) Han, H. B.; Liu, K.; Feng, S. W.; Zhou, S. S.; Feng, W. F.; Nie, J.; Li, H.; Huang, X. J.; Matsumoto, H.; Armand, M.et al. Ionic liquid electrolytes based on multi-methoxyethyl substituted ammoniums and perfluorinated sulfonimides: Preparation, characterization, and properties. *Electrochimica Acta* **2010,** *55* (23), 7134.

(10) Tsunashima, K.; Kodama, S.; Sugiya, M.; Kunugi, Y. Physical and electrochemical properties of room-temperature dicyanamide ionic liquids based on quaternary phosphonium cations. *Electrochimica Acta* **2010,** *56* (2), 762.

QUILL Quarterly Report

August - October 2018

Name:	**Kathryn Ralphs**		
Supervisor(s):	Nancy Artioli and Gosia Swadźba-Kwaśny		
Position:	PDRA		
Start date:	01/06/2018	Anticipated end date:	30/11/2018
Funding body:	CASE		

Renewable methanol from biogas for a low carbon economy in Northern Ireland

Background

Methanol is gaining increasing importance as a precursor to alternative fuels, fuel cells, DME and LPG. However, currently the UK methanol market accounts for only 4% of the European market, resulting in reliance on importation of methanol. Most methanol synthesized worldwide is from syngas (200 °C, up to 100 bar) obtained from natural gas (fossil fuels).
In this project we are investigating the direct hydrogenation of CO_2 to methanol. The hydrogen used will be obtained from water electrolysis from energy obtained from a curtailed wind farm. CO_2 is a waste product from anaerobic digestor plants. (In the UK there are 640 AD plants and 270 curtailed wind farms).

The direct hydrogenation of CO_2 to methanol recycles CO_2 (major cause of global warming) into a fuel and can provide a source of hydrocarbons. The process is exothermic and hence favours low temperatures and high pressures. However high temperatures are required to achieve a sufficient rate of reaction. At high temperatures the RWGS reaction dominates, reducing selectivity to methanol. In commercial processes the process is operated at low one pass conversions and relies on recycling unconverted reactants to attain high conversions.

In this project we aim to design and synthesize an optimized catalyst to improve methanol selectivity. We are currently investigating SCILL catalysts as it is thought that an ionic liquid layer on the commercial $CuZnO/Al_2O_3$ catalyst will increase the concentration of the CO_2 near the active site. In the literature the positive effects of ionic liquids on CO_2 hydrogenation to *e.g.* formic acid has been described e.g. stabilization of transition states. At a later stage of the project a novel type of microchannel fixed bed reactor will be developed. This configuration will allow for simultaneous increase in the reaction temperature, pressure and space velocity, resulting in shifting of the equilibrium conversion per pass of CO_2 and boosting catalytic activity.

Objective of this work

The objective of the project is to hydrogenate CO_2 to methanol in high yield and selectivity. This will be achieved by the development of a SCILL based on $CuZnO/Al_2O_3$ and an ionic liquid that will increase the concentration of CO_2 next to catalyst active sites and increase the selectivity towards methanol product.

Progress to date

We have investigated and prepared two classes of ionic liquids, ionic liquids with high thermal stability and those with lower thermal stability.

IL with high thermal stability:

[PPh_4][NTf_2]
[PPh4][Bu^FSO_3]

IL with lower thermal stability:

[BMIM][OAc]
[HMIM][FAP]

The ionic liquids have been characterised.

Solid catalysts with an ionic liquid layer (SCILL) have been prepared with the above mentioned ionic liquids and CuZnO/Al_2O_3 catalyst. Some of the SCILL's have been characterized by TPR, XRD, SEM and EDX. The following SCILL's have underwent catalytic testing in the direct hydrogenation of CO_2 to methanol.

[BMIM][OAc]
[PPh_4][NTf_2]

Due to the success of the [PPh_4][NTf_2] we have now prepared SCILL's with a IL loading of 10-50% which will be tested and fully characterised in the near future. Due to the high thermal stability required we have also investigated transition metal carbides using ionic liquids as precursors. These include:

Mo-TMC
Cu-ZnO-TMC

Characterization

TPR

Catalysts prepared are initially analysed by temperature programmed reduction (TPR) as an estimate of activity. Generally, the lower the reduction temperature the more active the catalyst. Fig 1 shows the TPR data for the conventional catalyst and the two SCILL's prepared with ionic liquids with lower thermal stability. The reduction temperature for the CuZnO/Al_2O_3 catalyst is approx. 440 K. The reduction temperature for CuZnO/Al_2O_3 [BMIM][OAc] SCILL is very similar. This could mean the catalyst should show comparable activity to the CuZnO/Al_2O_3 catalyst or it is possible that the ionic liquid has simply decomposed on the surface of the catalyst and we are analysing TPR for CuZnO/Al_2O_3 rather than the SCILL. This is more than likely possible as during initial preparations we did not investigate the thermal stability of the ionic liquid. The reduction temperature for the CuZnO/Al_2O_3 [HMIM][FAP] SCILL is around 430 K, however it has shifted to the right and is more difficult to reduce indicating a reduced activity.

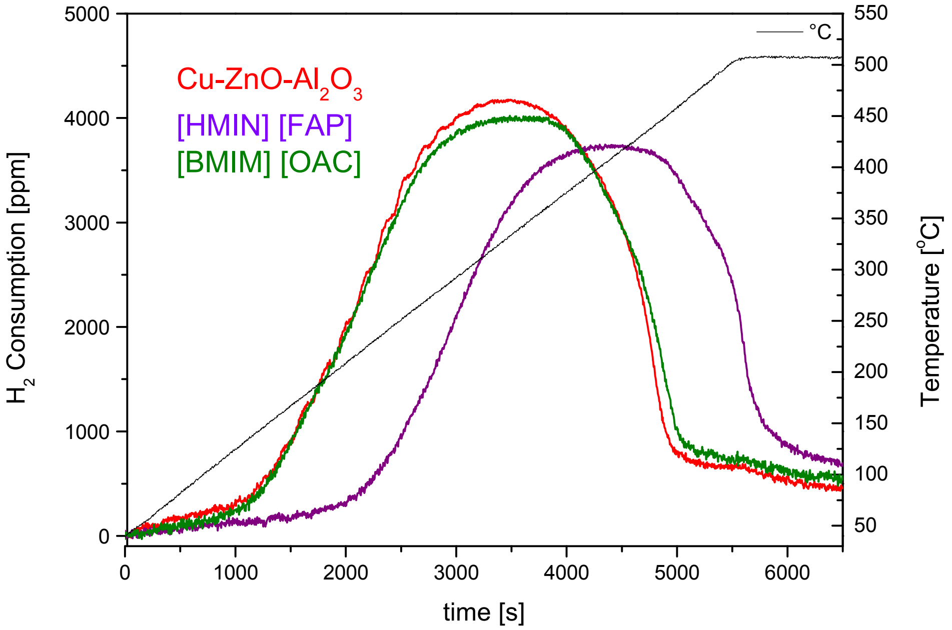

Figure 1: TPR of catalysts and SCILL's with low thermal stability

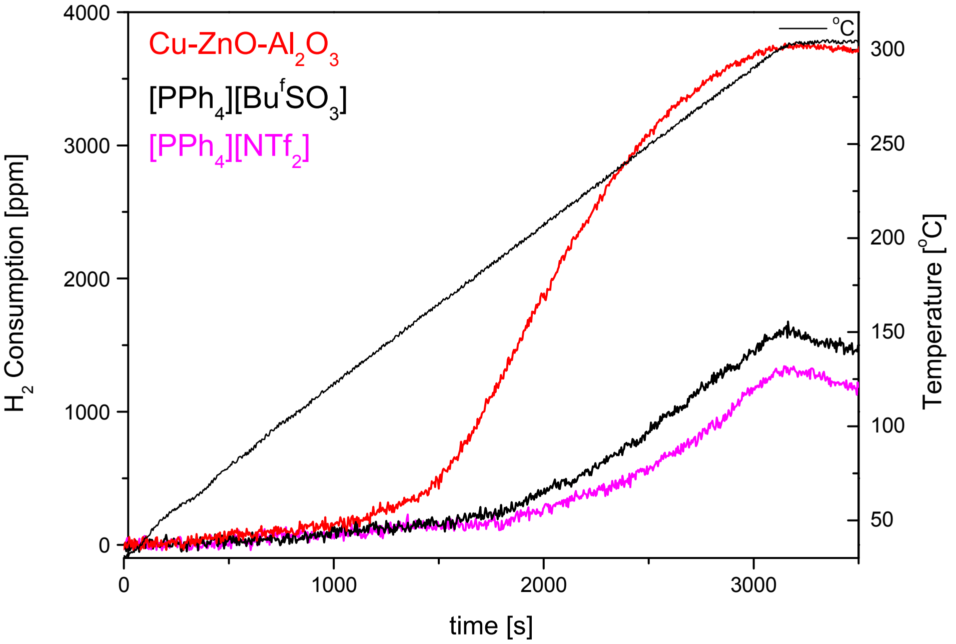

Figure 2: TPR of catalysts and SCILL's with high thermal stability

Figure 2 shows the TPR data for the two SCILL's with the high thermal stability ionic liquid. The TPR's for both catalysts indicated they are difficult to reduce and therefore catalytic activity is likely to be poor. However, catalytic testing revealed that the [PPh4][NTf$_2$] based SCILL is very selective to methanol product (75%) and displays similar conversions as the commercial heterogenous CuZnO/Al_2O_3 catalyst.

XRD

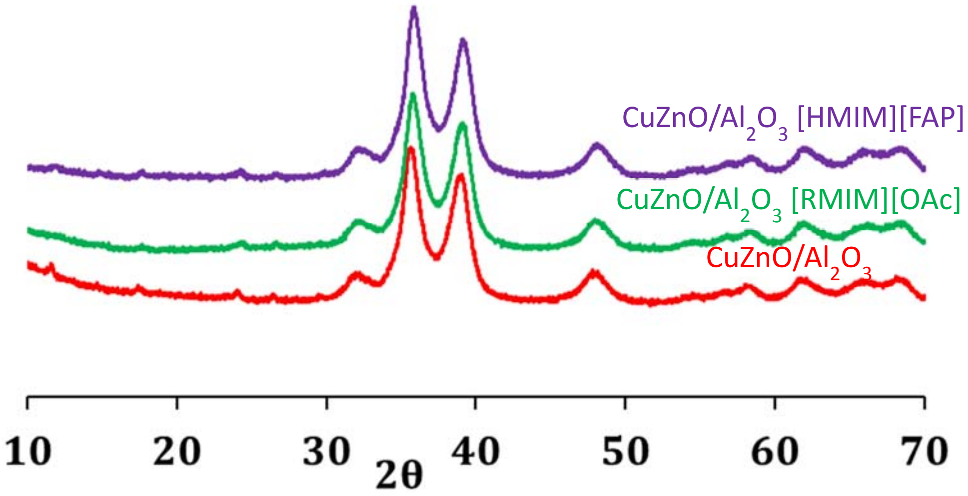

Figure 3: XRD patterns for SCILL's with lower thermally stable ionic liquids

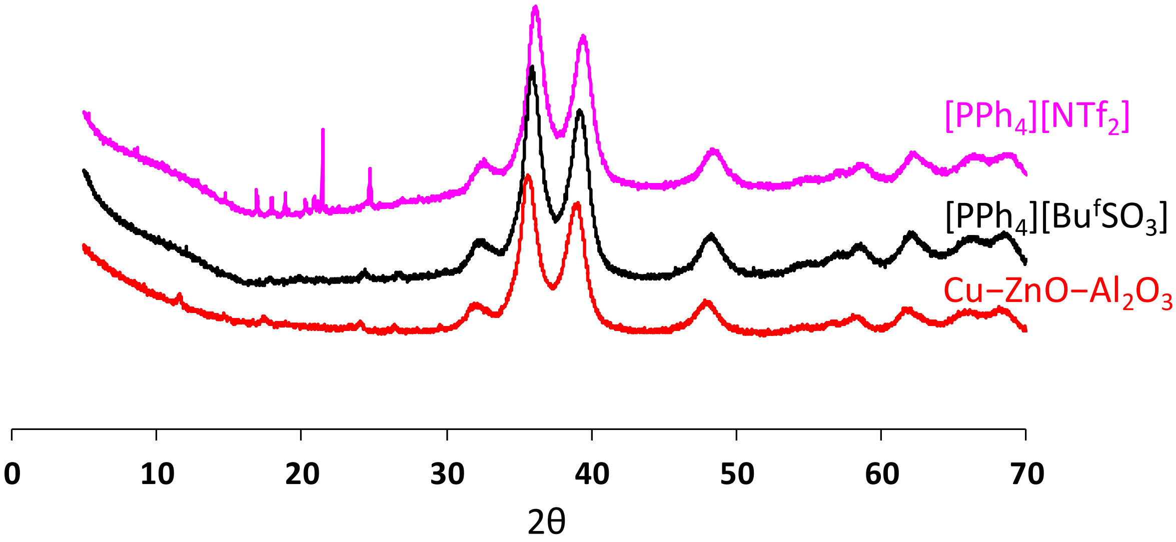

Figure 4: XRD patterns for SCILL's with ionic liquids with high thermal stability.

Figure 3 and 4 shows the XRD patterns of the CuZnO/Al$_2$O$_3$ catalyst and the CuZnO/Al$_2$O$_3$ based SCILL's. From the XRD pattern there appears to be very little change in the XRD between the catalysts which indicated no change in morphology or crystallinity of the catalyst.

SEM and EDX

SEM and EDX analysis can be seen in fig 5. SEM images show no notable difference in appearance of the catalyst and the SCILL's. EDX analysis for the catalyst and [BMIM][OAc] based SCILL are very similar, however the EDX analysis for [HMIM][FAP] SCILL is quite different. The percentage of copper in the [HMIM][FAP] SCILL is higher at 53.4% compared to 46-47% for the catalyst and [BMIM][OAc]

SCILL. The percentage of oxygen is considerably reduced in the [HMIM][FAP] SCILL and the presence of P and F has been detected.

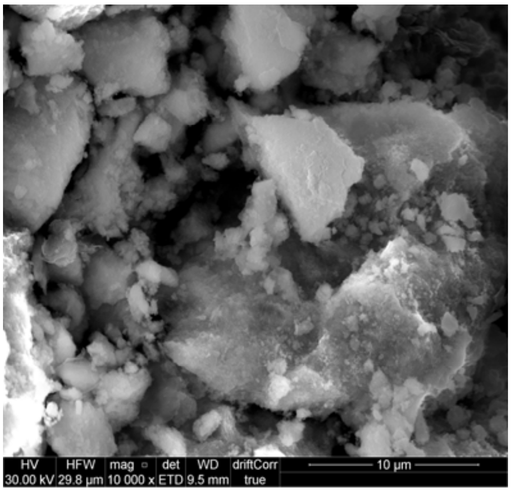

metal	% composition
Cu	46
O	32
Zn	15
Al	7

CuZnO/Al$_2$

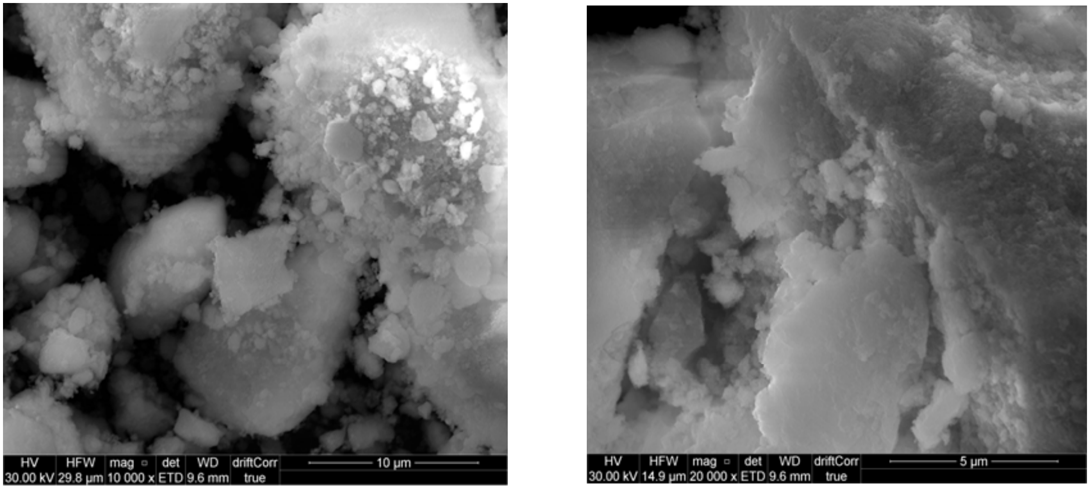

CuZnO/Al$_2$O$_3$

metal	% composition
Cu	47
O	31
Zn	15
Al	7

CuZnO/Al$_2$O$_3$

metal	% composition
Cu	53.4
O	21.1
Zn	16.1
Al	5
F	4
P	0.4

Figure 5: SEM and EDX of SCILL's

Catalytic testing

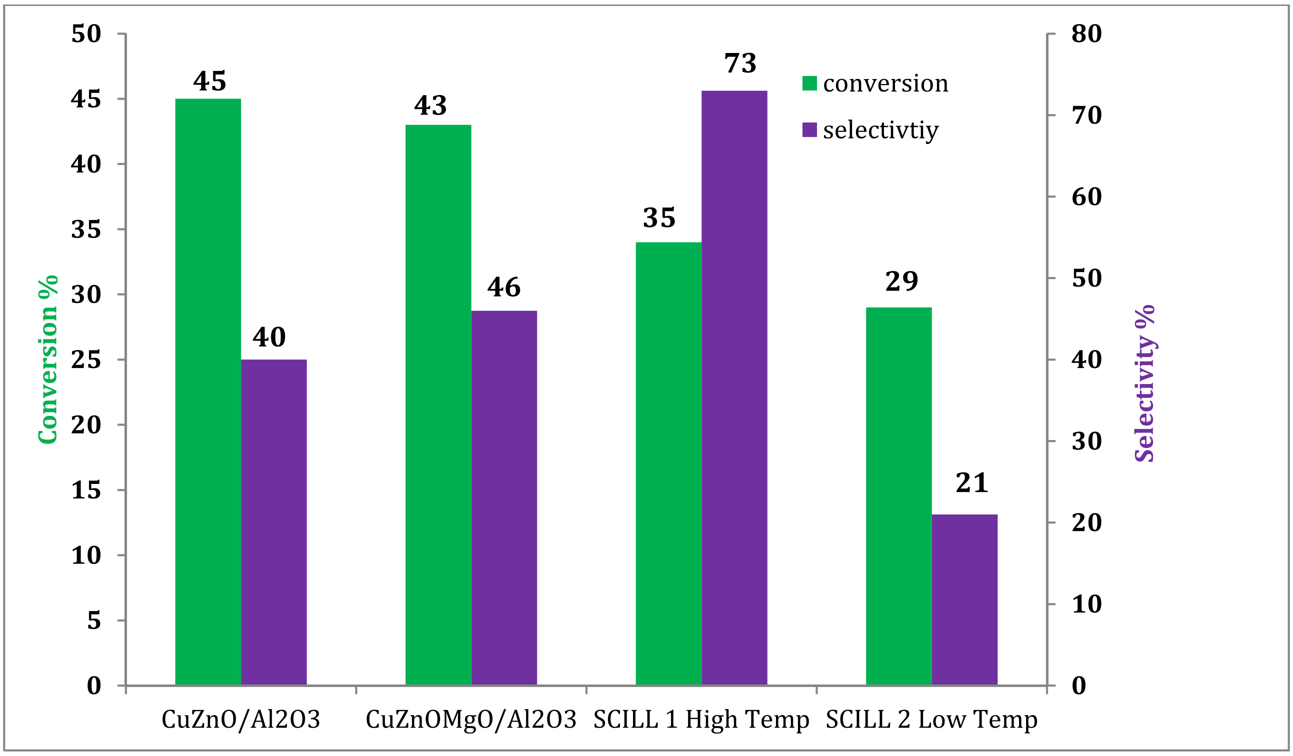

Figure 6 Catalytic activity results after 10 h

Catalytic activity results are given in figure 6. Two heterogenous catalysts were tested and two SCILL's based on a $CuZnO/Al_2O_3$ catalysts. The two heterogenous catalysts gave a conversion of 43-45 % and a selectivity of 40-46% to methanol. $[PPh_4][NTf_2]$ SCILL (SCILL 1) showed a slight drop in conversion when compared to $CuZnO/Al_2O_3$ catalysts, however, the selectivity to methanol has been significantly enhanced to 73%. This means we are getting more methanol per pass which is very significant as this reaction is thermodynamically limited to 40%. [BMIM][OAc] SCILL gave reduced conversion and selectivity.

Future work

Due to the significant enhancement of selectivity using $[PPh_4][NTf_2]$ SCILL we plan to test this catalyst with different loadings of ionic liquids. We also plan to test the other SCILL's and TMC's prepared. The catalysts will also be fully characterized. Once the catalyst design has been optimized the reactor design and reaction parameters will be optimized.

QUILL Quarterly Report

August - October 2018

Name:	**Lei Wang (40197808)**		
Supervisor(s):	John Holbrey		
Position:	[✓ PhD student]/Summer student/PDRA		
Start date:	01/10/2017	Anticipated end date:	13/12/2018
Funding body:	No funding		

Chemical recycling of polymer wastes using novel zwitterionic catalysts

Background

Poly (ethylene terephthalate) (PET) is one of polyester, which has become the most favourable packaging material with excellent tensile strength, chemical resistance, processability and thermal stability. Nowadays, PET is used for soft drink bottles, high strength fibres, tape recorders and videos owing to its excellent physical and chemical properties. For a long time, however, the recycling of post-consumer PET packing materials was not possible. PET recollection as well as recycling processes have made a huge progress in the last 20 years due to increasing trend of using plastic bottle and packages as a worldwide phenomenon that naturally leads to the entry of used PET bottles into the waste stream. Among the various methods of PET recycling, only chemical recycling conforms to the principles of sustainable development because it leads to the formation of the raw materials from which PET is originally made, so PET decomposition and its conversion into reusable chemical products becomes one of the important recycling strategies for this material. So, in this project, PET from an industrial manufacturer was depolymerized by new zwitterionic imidazolium-2-carboxylate salts as catalysts (or catalyst-precursors) which compared with corresponding ionic liquid as catalyst in the presence of ethylene glycol via glycolysis to give bis(hydroxyethyl)terephthalate [BHET]. The effects of reaction temperature, glycolysis time, the amount of ethylene glycol, and the amount of zwitterionic catalysts on the glycolysis reaction were investigated.

Objective of this work

Investigate that novel zwitterionic catalyst imidazolium-2-carboxylate salts in the glycolysis of PET and the effect of different conditions such as reaction temperature, reaction time, the amount of ethylene glycol, and the amount of zwitterionic catalyst which were compared with ionic liquid as catalyst in the glycolysis of PET.

Progress to date

1. Effect of reaction conditions

--1,3-dimethylimidazolium-2-carboxylate as catalyst

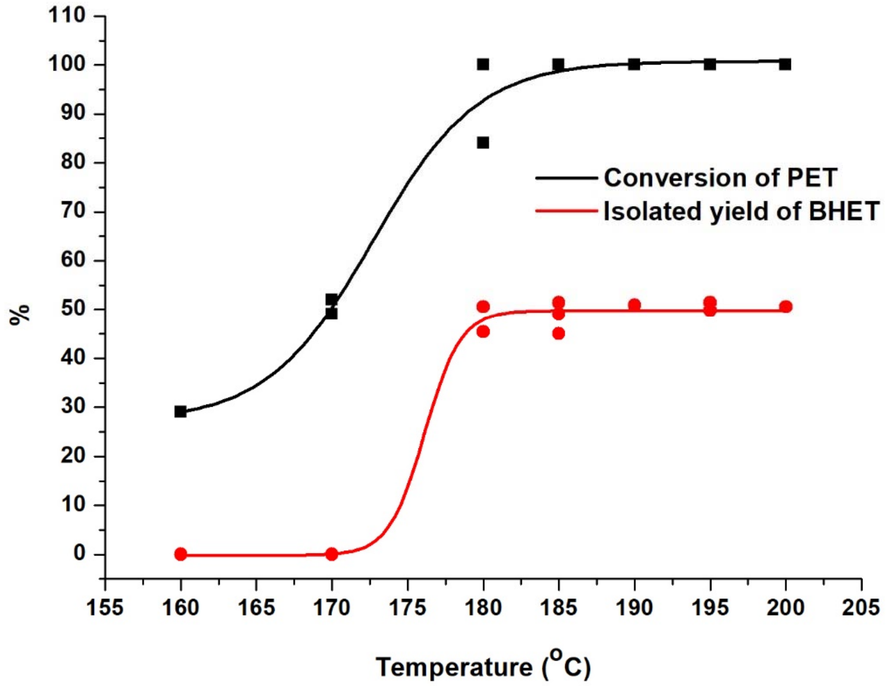

Reaction conditions: 1 atm, 1.0 g PET, 10.0 g EG, 0.2 g catalyst, 255 rpm, 1 h.

Fig. 1.1 Effect of reaction temperature on the yield of BHET, the conversion of PET.

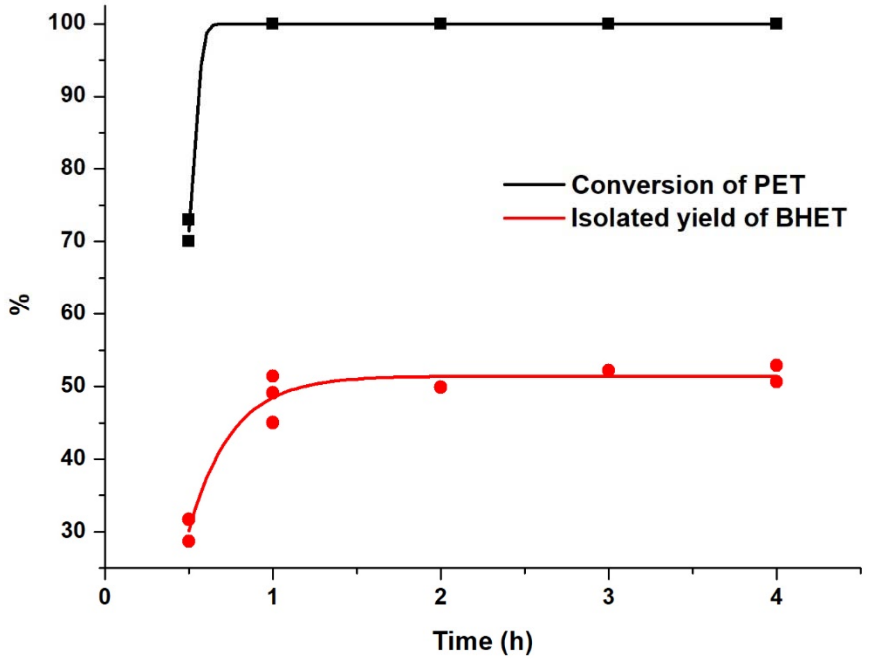

Reaction conditions: 1 atm, 185℃, 1.0 g PET, 10.0 g EG, 0.2 g catalyst, 255 rpm.

Fig. 1.2 Effect of reaction time on the yield of BHET, the conversion of PET.

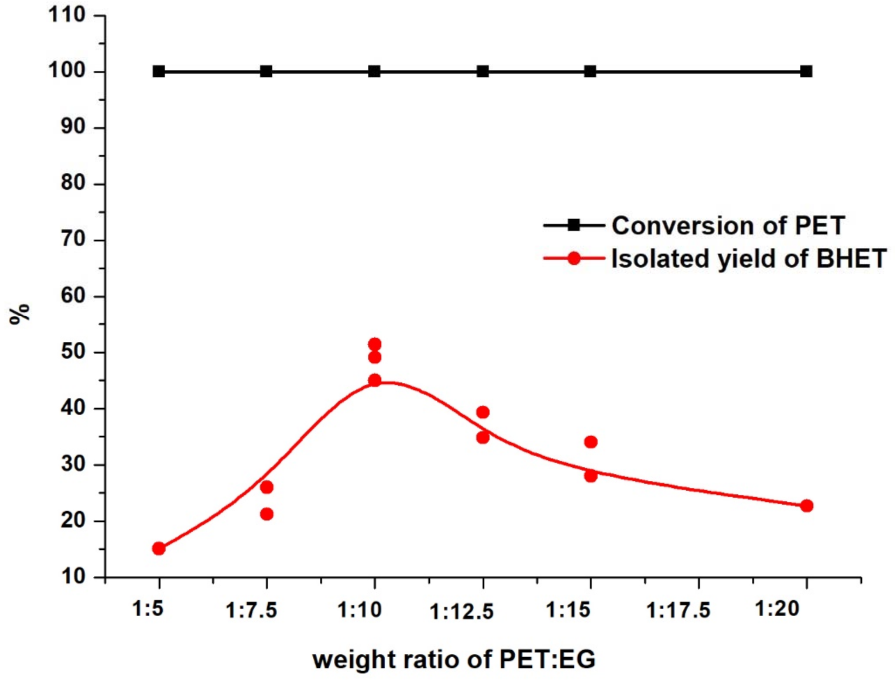

Reaction conditions: 1 atm, 185℃, 1.0 g PET, 1 h, 0.2 g catalyst, 255 rpm.

Fig. 1.3 Effect of weight ratio of PET:EG on the yield of BHET, the conversion of PET.

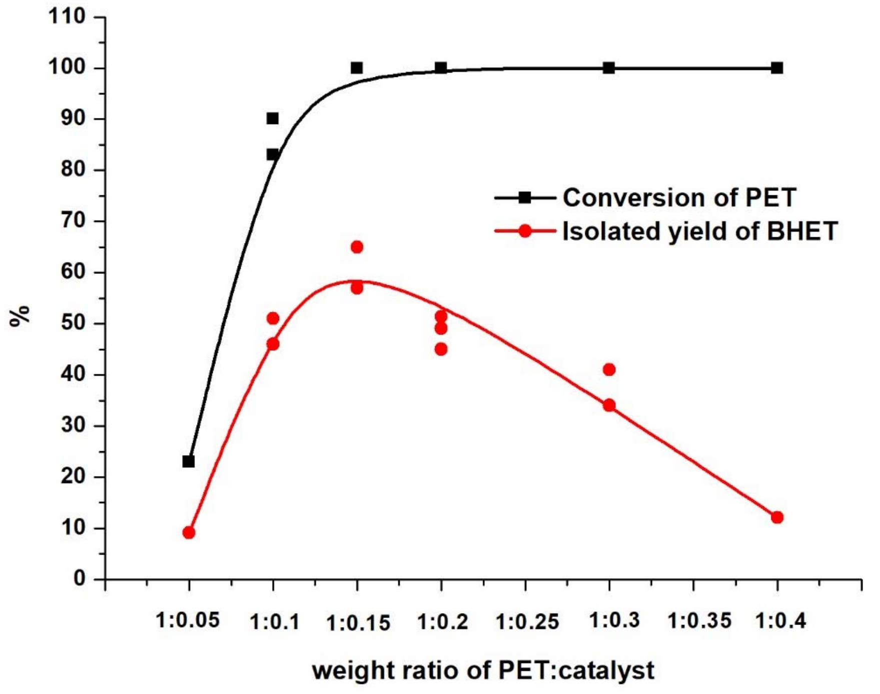

Reaction conditions: 1 atm, 185℃, 1.0 g PET, 10.0 g EG, 1 h, 255 rpm.

Fig. 1.4 Effect of weight ratio of PET: catalyst on the yield of BHET, the conversion of PET.

2. Effect of reaction conditions

--1,3-dimethylizolium acetate as catalyst

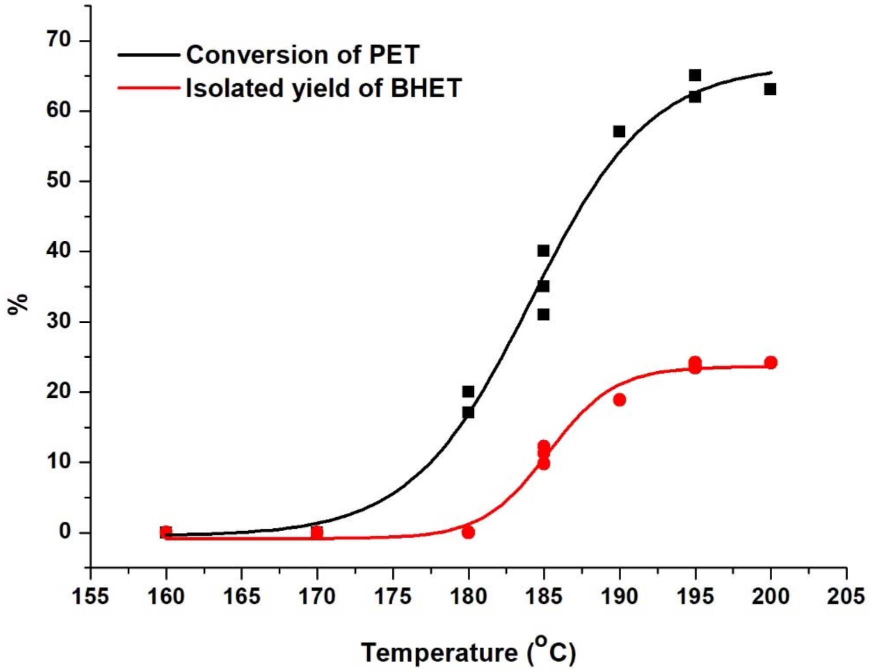

Reaction conditions: 1 atm, 1.0 g PET, 10.0 g EG, 0.2 g catalyst, 255 rpm, 1 h.

Fig. 2.1 Effect of reaction temperature on the yield of BHET, the conversion of PET.

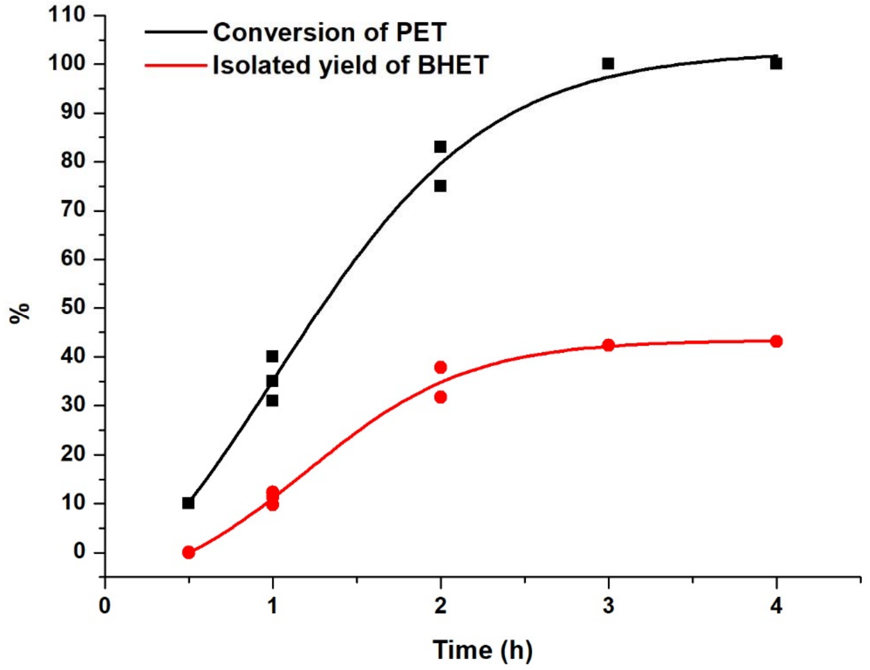

Reaction conditions: 1 atm, 185℃, 1.0 g PET, 10.0 g EG, 0.2 g catalyst, 255 rpm.

Fig. 2.2 Effect of reaction time on the yield of BHET, the conversion of PET.

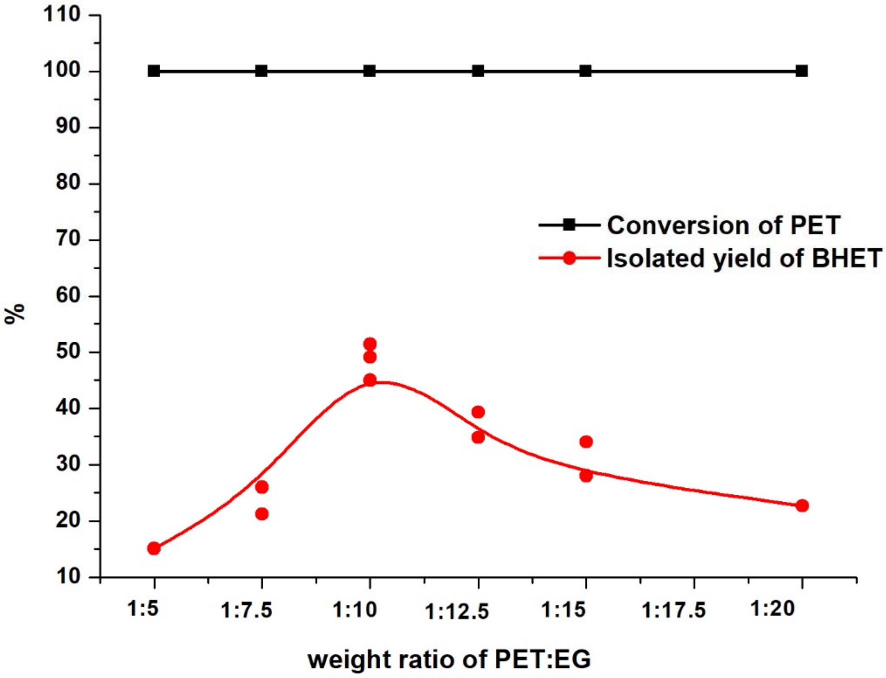

Reaction conditions: 1 atm, 185℃, 1.0 g PET, 1 h, 0.2 g catalyst, 255 rpm.

Fig. 2.3 Effect of weight ratio of PET:EG on the yield of BHET, the conversion of PET.

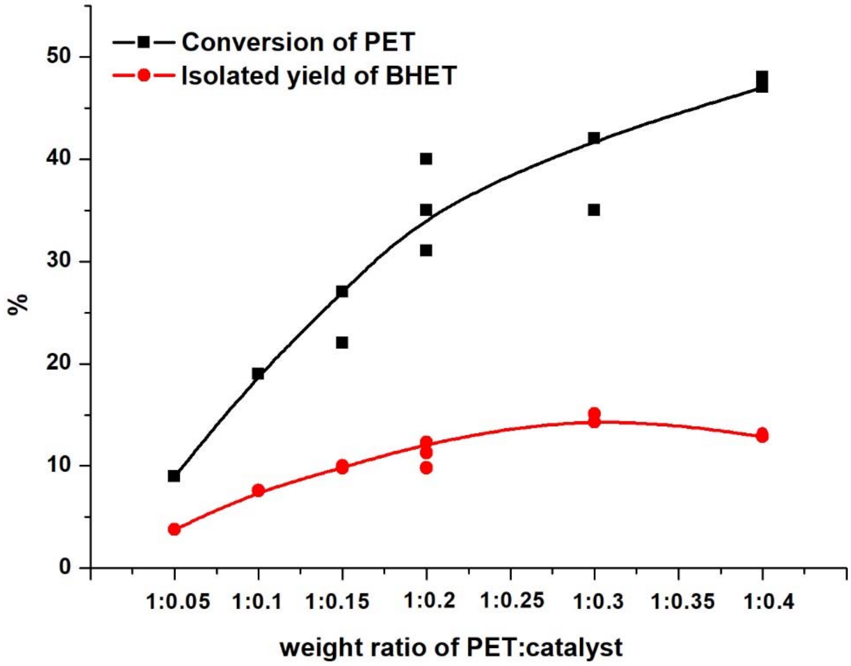

Reaction conditions: 1 atm, 185℃, 1.0 g PET, 10.0 g EG, 1 h, 255 rpm.

Fig. 2.4 Effect of weight ratio of PET: catalyst on the yield of BHET, the conversion of PET.

Conclusions and Future Work

This is the first time that the imidazolium-carboxylate has been used as a catalyst (or catalyst precursor) for the glycolysis of PET. The catalyst 1,3-dimethylimidazolium-2-carboxylate was synthesized easily from the reaction of DMC with 1-methylimidazolium, and it is stable to store and use. In the glycolysis, the main product from the depolymerization catalyzed by carboxylate was monomer BHET. The results showed that reaction parameters, such as reaction temperature, glycolysis time, the ethylene glycol dosage and the amount of catalyst can effect the glycolysis of PET on the yield of BHET, the conversion of PET, and the selectivity of BHET. When the 1,3-dimethylimidazolium-2-carboxylate was used in the glycolysis, complete PET degradation (100% PET conversion) was obtained at 180 ^{o}C, 1 h, with 10 wt% load of catalyst and at 1:5 ratio PET:EG. Using 1.0 g PET, 10.0 g ethylene glycol, 0.15 g catalyst at 185 ^{o}C under nitrogen for 1 h can give the maximum BHET yield (61%), 100% PET conversion, and the higher BHET selectivity. When the ionic liquid was used as the catalyst in the glycolysis, it would require longer time (3 h), higher temperature (195 ^{o}C), more catalyst (0.3 g) and the relative ethylene glycol to get > 60% BHET yield, 100% PET conversion. By contrast, it is demonstrated that 1,3-dimethylidazolium-2-carboxylate can behave as a more efficient catalyst than ionic liquids and metal salts for the glycolysis in the presence of ethylene glycol. In addition, the carboxylate catalyst was recycled in the glycolysis which conforms to the principles of sustainable development and performs valuable to study. As the separation BHET from reaction mixture was not all BHET formed in the glycolysis, so the further work needs to be done to explore isolation of BHET and separate the BHET from the remaining reaction mixture to achieve maximum recycling of BHET.